

TRANSLATIONAL CONTROL IN NUTRIENT RESPONSE
AND AGING

by
Michael S. Harris

A dissertation submitted to Johns Hopkins University in conformity with
the requirements for the degree of Doctor of Philosophy

Baltimore, Maryland

May, 2016

© 2016 Michael S. Harris
All Rights Reserved

Abstract

Translation is a major step in the production of functional protein from coding regions, and as such is subject to extensive regulation. Here, I describe translational profiling of physiological responses in living mammals. First, ribosome profiling has been adapted for use in whole tissues and a ribosome affinity purification system has been developed. This affinity purification system has been used here to provide physical evidence of translation in non-coding regions, but in mice could also be used for ribosome profiling of small cell populations. In collaboration, I have combined ribosome profiling with RNA-Seq and proteomics to study changes in protein production in aging. This study revealed many tissue-specific differences between young and old animals, and established a correlation between change in translation and change in protein level in aging. Changes in alternative splicing were also seen for several transcripts. Lastly, I have applied ribosome profiling to study translational changes in mouse liver resulting from high-fat diet and glucose. While the changes present in these two responses are similar, they differ greatly in magnitude. Furthermore, in high-fat fed animals, the normal response to glucose is dramatically reduced.

Readers:

Nicholas Ingolia (advisor)
Assistant Professor, UC Berkeley Molecular and Cell Biology Dept.

Chen-Ming Fan
Adjunct Professor, Johns Hopkins University Dept. of Biology
Staff Member, Carnegie Institute of Washington Dept. of Embryology

Acknowledgements

I would like to thank my family, especially my parents, Bob and Joanne Harris. First, for encouraging my curiosity and interest in science and second, for their support throughout my academic career.

I would also like to thank my advisor, Nick Ingolia. The freedom he has given me to work in my own way, combined with his patient and supporting guidance, has undoubtedly improved my graduate school experience.

Next, I would like to thank the members of the Ingolia and Lareau labs, past and present, for their support and input. I would particularly like to thank Anna McGeachy, my labmate from joining through defending, for her support and for reminding me of more important deadlines than I can remember.

Lastly, I would like to thank the Biology Department and CMDB program at Johns Hopkins University, the Carnegie Institution of Washington Department of Embryology especially my committee members, Steve Farber and Chen-Ming Fan, and the MCB department at UC Berkeley for providing a welcoming scientific community at various points along my graduate school career.

Table of contents

TITLE PAGE	i
ABSTRACT	ii
ACKNOWLEDGEMENTS.....	iii
TABLE OF CONTENTS	iv
LIST OF FIGURES	vi
CHAPTER 1: INTRODUCTION	1
CHAPTER 2: RIBOSOME PROFILING IN WHOLE TISSUES AND RIBOSOME AFFINITY PURIFICATION - Results.....	10
Ribosome Profiling Reveals Pervasive Translation Outside of Annotated Protein-Coding Genes	19
Discussion	26
CHAPTER 3: TRANSLATIONAL REGULATION IN AGING.....	28
Identification of Long-Lived Proteins Reveals Exceptional Stability of Essential Cellular Structures - Results	29
Discussion	33
Integrated Transcriptome and Proteome Analyses Reveal Organ-Specific Proteome Deterioration in Old Rats	35
Summary	36
Results	37
Age Markers Were Consistently Identified	42
Identification of Common and Organ-Specific Alterations	43
Translation Output Contributes Significantly to Proteomic Alterations	48

Multiple Levels of Regulation Modulate Functional Networks between Young and Old Animals	52
Alternative Splicing.....	55
Discussion	58
Experimental Procedures	61
Author Contributions.....	62
Acknowledgements.....	63
Accession Numbers.....	63
 CHAPTER 4: TRANSLATIONAL CONTROL IN THE ACUTE GLUCOSE RESPONSE AND HIGH-FAT DIET - Results.....	 64
Pilot experiment results	64
Weights and blood glucose levels.....	67
High-fat diet response	69
Glucose response in normal and high-fat diets.....	70
Discussion	76
Methods.....	78
 CHAPTER 5: CONCLUSION	 81
 APPENDIX A: RESULTS FROM COLLABORATORS.....	 83
 APPENDIX B: SUPPLEMENTAL FIGURES	 94
 REFERENCES.....	 106
 CURRICULUM VITAE	 116

List of figures

Figure 2.1. Ribosome profiling of whole tissues	12
Figure 2.2. Pull-down of tagged Rpl10A with or without biotin supplementation.....	14
Figure 2.3. Enrichment of human transcripts in mixed profiling	16
Figure 2.4. SDS wash improves background binding.....	18
Figure 2.5. Ribosome Affinity Purification Separates 80S Footprints from Background RNA	25
Figure 3.1. Protein Translation Does Not Correlate with Protein Lifespan.....	32
Figure 3.2. Integrated Genomics and Proteomics Analysis of Aging Brain and Liver	42
Figure 3.3. Common and Organ-Specific Alterations of the Proteome in Old Rats	47
Figure 3.4. Changes in Translation Correspond to Changes in Protein Abundance	51
Figure 3.5. The Impact of Age on Functional Networks Occurs at Multiple Levels of Regulation	54
Figure 3.6. Alternative Expression of Splicing Isoforms	57
Figure 4.1. Results from pilot experiment.....	65
Figure 4.2. Weights and blood glucose levels.....	67
Figure 4.3. High-fat diet response	69
Figure 4.4. Glucose response in normal and high-fat diet.....	73
Figure 4.5. Gene ontology analysis of glucose response	74
Figure 4.6. Changes in gene ontology categories across time course	75
Figure A.1. Proteomic Changes Affect the Abundance and Composition of Protein Complexes	86
Figure A.2. Changes in Protein Localization and Phosphorylation.....	89
Figure S2.1. FLOSS analysis detects snoRNA-derived background that co-purifies with the ribosome.....	94

Figure S3.1. Reproducibility of proteomic measurements and variation of protein abundances between animals of different age.....	96
Figure S3.2. Replicate samples of RNA-Seq and Ribosome Profiling are consistent.....	97
Figure S3.3. Protein kinases and members of the ubiquitin-proteasome system and autophagy are affected between young and old animals.....	98
Figure S3.4. Increased abundance of ribosomal proteins in old brain...	99
Figure S3.5. Changes in PSI value for all transcripts.....	100
Figure S3.6. Conserved molecular alterations in aging brain between rat and human.....	101
Figure S4.1. Identification of outlier samples by blood glucose levels and Spearman's correlation	102
Figure S4.2. Glucose response at 10 and 30 minutes in normal and high-fat diet.....	103
Figure SA.1. Reproducibility of phosphoproteomic measurements and comparison of protein abundance and phosphorylation level changes	105

Chapter 1: Introduction

Translation is a crucial step in the expression of protein coding genes. While transcription, RNA processing, and RNA transport are important for providing mRNA to be translated, without translation those mRNAs have little impact on the cell. Translation also consumes a large fraction of a cell's resources. In most eukaryotes, including yeast, flies, mice, and human cells, a substantial portion of the proteome is devoted to translation (Nagaraj 2012, Brunner 2007, Geiger 2013, Geiger 2012). In mice, this is true across many tissue types, including liver and pancreas, both of which produce large amounts of protein (e.g. albumin and lipoproteins in liver, digestive enzymes and insulin in pancreas).

Because translation requires a large amount of cellular resources, it is a logical target for regulation. Large amounts of unnecessary translation would certainly impose a large fitness cost for cells, especially in non-optimal environments. It is also important to control translation so that proteins are synthesized when and where they are needed, as many proteins can have negative effects when expressed at the wrong time or place (Kong and Lasko 2012). Regulation of translation also offers a more rapid response than transcription or mRNA processing.

Transcriptional regulation requires time for the accumulation of the necessary transcripts, their processing and export, and translation. Translational regulation, by contrast, can respond without waiting for

transcripts to accumulate and be processed (Kong and Lasko 2012).

Translational regulation can also be used to ensure a protein is produced only in a particular region of the cell (Kong and Lasko 2012). This makes translational control particularly effective for pathways which respond to cellular stresses.

There are several pathways that are known to regulate protein production at the translational level, including mechanistic target of rapamycin (mTOR), a global translation regulator (Sengupta, 2010). The mTOR protein is a kinase that regulates translation and autophagy in response to many input signals, including cellular energy levels, amino acid availability, and growth factors. As a part of the mTORC1 complex, it promotes translation through phosphorylation of several targets. One target is eIF4E-binding protein 1 (4E-BP1), which blocks translation initiation factor eIF4E, which binds the 5' cap of the mRNA, from interacting with the scaffold protein eIF4G until phosphorylated by mTOR (Ma and Blenis 2009). Another target is S6K, a kinase that targets a number of different proteins involved in translation including the ribosomal protein Rps6 (Ma and Blenis 2009). Although much of the translational regulation downstream of mTOR is global, it also has a more specific regulatory effect on transcripts with 5' oligopyrimidine tracts (5' TOP), which include most ribosomal proteins and elongation factors (Laplanche and Sabatini, 2012). Although the mechanism of this control is unclear, recent studies have suggested that mTOR acts on

5'TOP mRNAs through La-related protein 1 (LARP1), which competes with eIF4G on 5'TOP mRNAs unless phosphorylated by mTOR (Fonseca et al., 2015; Mura et al., 2015).

Phosphorylation of eIF2 α , a subunit of eIF2, which recruits the initiator tRNA, is another well-characterized translational regulation mechanism. There are a number of kinases that target eIF2 α , including Gcn2, in response to amino acid starvation, and PERK, in response to ER stress (Ron and Walter 2007, Wek et al. 2006). Phosphorylation of eIF2 α prevents eIF2 from being recharged with GTP, which is required for its role in translation initiation (Wek et al., 2006). This phosphorylation event causes a global decrease in translation levels, but also a seemingly paradoxical increase in translation of a number of target genes. The best-known target of this induction is ATF4, a transcription factor, whose increase in translation depends on upstream open reading frames (uORFs) on the ATF4 transcript (Vattem and Wek 2004). Under normal conditions, these uORFs are translated, preventing translation because they overlap the start codon (Vattem and Wek 2004). However, when active eIF2 is low, the uORFs are more likely to be skipped in favor of the main ORF (Vattem and Wek 2004).

Both mTOR and eIF2 α phosphorylation are examples of translational regulatory pathways that respond to changes in nutrient levels. All organisms must balance their near constant need of nutrients with their

sporadic availability. In multicellular organisms, this balance is complicated by the varying needs of different cell types, and the sometimes contradictory requirements of the cell versus the organism. Glucose is one of the most closely regulated nutrients in many organisms, and is often one of the primary sources of energy for eukaryotic cells (Brown and Edelman 2010). Abnormal blood glucose levels can lead to many symptoms, ranging from temporary fatigue and confusion from hypoglycemia (low blood sugar) to significant kidney and neurological damage from chronic hyperglycemia (high blood sugar).

In humans (and other animals), misregulation of glucose levels results in diabetes, a metabolic disease that affects over 29 million people in the US alone (CDC, 2015). In healthy individuals, glucose levels in the blood are controlled by signals secreted by the pancreas. Insulin, secreted by β -cells, instructs liver hepatocytes (and other cells, such as skeletal muscle) to absorb glucose from the blood (Brown and Edelman 2010). Glucagon, secreted by α -cells, instructs liver hepatocytes to release stored glucose into the blood (Brown and Edelman 2010). Diabetes occurs when insulin is no longer produced properly, due to loss or dysfunction of β -cells, or hepatocytes and other target cells no longer respond to insulin properly.

There are a number of elements of the glucose control system that are translationally controlled. First, insulin has been shown to be

translationally regulated (Welsh et al. 1986, Kulkarni et al. 2011). Although the initial release of insulin is controlled post-translationally, these translational mechanisms increase insulin production, preparing for later changes in glucose levels and supporting sustained insulin secretion (Welsh et al. 1986, Kulkarni et al. 2011). Furthermore, a recent study found that insulin mRNA is present in glucagon-secreting α -cells, but no insulin protein is detected (Blodgett et al. 2015). Second, knockout of PERK, an eIF2 α kinase and component of the unfolded protein response (UPR), in mice causes the islets of Langerhans, the location of both α - and β -cells, to deteriorate (Zhang et al., 2002). PERK knockout mice are born normal, but gradually lose their islets, beginning with the β -cells. Lastly, mTOR responds to both cellular glucose levels and insulin levels (Laplante et al. 2012). This final observation combines both the cellular energy signals and organismal energy signals, lessening protein synthesis when either the cell or organism is lacking nutrients.

Diet-induced obesity, another major health concern, is often a contributing factor to the development of diabetes, among other metabolic diseases (Winzell and Ahrén, 2004). An estimated two-thirds of adults in the US are considered overweight or obese (Ogden et al., 2014). Diet-induced obesity, in part through the induction of oxidative stress, is thought to play a large role in the development of diabetes (Rani et al., 2016). However, there remains a fundamental gap in our understanding of this process. Insulin signaling to the liver regulates

both glucose and lipid metabolism. Knockdown of liver-specific insulin receptor (LIR) in mice blocks insulin communication to both glucose and lipid metabolic pathways, but high-fat diet primarily affects glucose metabolism, while lipid metabolism remains normal (Brown & Goldstein, 2008).

There is evidence that diet-induced obesity has specific effects on translation in the liver. Analysis of the ER-associated proteome in normal and obese mice suggests that, while lipid metabolic proteins are more prevalent in obese mice, those involved in protein production are down-regulated (Fu et al., 2011). These include translation initiation factors as well as other protein metabolism factors. Measurement of ER-associated translation by polysome profiling followed by microarray showed a large number of differentially translated transcripts (Fu et al., 2012).

Another basic biological process in which translational regulation plays a role is aging, a complex process, characterized by gradual deterioration of an organism. Many cells and tissues within an organism are post-mitotic, while at the molecular level they are subject to damage and turned over regularly. Some structures, however, are not subject to this turnover and their protein components are maintained over long periods of time (Savas et al., 2012). These represent a particularly interesting group, as one would expect their synthesis to decrease over the

organism's lifespan. Although several studies have independently characterized the global changes in mRNA and protein abundance between young and old organisms (Jiang et al., 2001; Lee et al., 2000; Lu et al., 2004; Wood et al., 2013; Walther and Mann, 2011), none have combined these approaches with measurements of translation levels. Combined measurement of mRNA levels, translation levels, and protein levels within the same set of organisms can provide a more complete picture of not only what changes are occurring, but also how they happen.

Ribosome profiling is used to investigate translation on a genome-wide scale with nucleotide resolution (Ingolia et al., 2009). Ribosome profiling simultaneously measures ribosome occupancy on all transcripts, presenting an unbiased and genome-wide view of protein production. At the same time, the exact location of ribosomes can be identified with nucleotide level resolution, revealing alternative translational events such as uORF translation and ribosome pausing. Ribosome profiling is performed by digesting lysates with an RNase, destroying all mRNAs not protected by a protein complex (Ingolia et al. 2012). Ribosomes can be isolated by centrifugation through a sucrose cushion, and the "footprints" of the ribosomes can be isolated. These short (about 28 nucleotide) fragments are used to create a DNA library which is then sequenced using "next-generation" sequencing platforms.

For many applications, including those discussed above, adaptation of ribosome profiling to use in whole tissues is essential. Although many interesting questions can be addressed in yeast or cell culture, there are a vast number of applications that are difficult or impossible to replicate outside of a full organism. Ribosome profiling was initially performed in yeast, and has since been adapted to mammalian cell culture (Ingolia et al., 2010; Ingolia et al., 2011). Profiling of whole tissues does, however present further challenges. Yeast for ribosome profiling are rapidly harvested by vacuum filtration and frozen, while cultured cells can be lysed directly on the dish they are grown in. Tissues to be profiled must be disrupted in a way that prevents degradation and changes in the translational landscape during preparation. This can be made even more challenging in certain tissues (e.g. pancreas) that produce a wide array of enzymes for digestion of protein and RNA. These challenges can be overcome by flash-freezing of tissues, cryogenic grinding, and addition of RNase and protease inhibitors to lysis buffer.

Cell type heterogeneity is another major concern introduced by profiling whole tissues. While some tissues (e.g. liver) are largely homogenous, others (e.g. pancreas) are highly heterogeneous. While beta-cells are of great interest in studying translational responses to glucose levels, they represent only 1-2% of the total pancreas, which is dominated by the “exocrine” pancreas, which produces vast amounts of enzymes for digestion. Unfortunately, microdissection and cell sorting techniques are

incompatible with protecting polysomes from degradation or changes in translation profiles. A promising avenue for ribosome profiling of specific cell lineages within heterogeneous tissues is lineage specific ribosome tagging. These systems apply a genetically coded affinity tag (e.g. HA, GFP) to ribosomes only in specific cell types (Sanz et al. 2009, Heiman et al. 2008, Heiman et al. 2014). Unfortunately existing systems were not effective for ribosome profiling in our hands due to non-specific background binding. I propose and have built, in collaboration with rotation students, a new system using a ubiquitous Avi tag, which can be biotinylated in a lineage specific manner by Cre-inducible expression of the BirA biotin ligase.

Another interesting application of ribosome profiling coupled with pulldown of tagged ribosomes is verification of ribosome association in non-canonical coding regions. These include long intergenic non-coding RNAs (lincRNAs), RNA polymerase II products with no clear coding potential (Bertone et al., 2004; Carninci et al., 2005; Guttman et al., 2009), and uORFs (Calvo et al., 2009; Wethmar et al., 2013). Previous ribosome profiling has suggested extensive translation in many of these regions, but questions remained as to whether these were bona-fide ribosome footprints (Ingolia et al., 2011; Chew et al., 2013; Guttman et al., 2013). Ribosome profiling of ribosome pull-down provides clear experimental evidence for these fragments being true ribosome-protected fragments.

Chapter 2: Ribosome profiling in whole tissues and ribosome affinity purification

Results

Ribosome profiling is a powerful technique that measures translation on a genome-wide scale with nucleotide resolution. Previously, the technique has been used in yeast and mammalian cell culture (Ingolia et al., 2009, Ingolia et al., 2012). While these systems can be very informative, some questions do not lend themselves to yeast or cell culture models. For these applications, ribosome profiling of whole tissues from an intact organism is essential.

I addressed several concerns relating to the use of ribosome profiling in tissues to obtain accurate and reproducible results. First, hypoxia induced by or occurring immediately after euthanasia could cause dramatic translational changes that would obscure meaningful biological changes. Hypoxia is known to activate mTOR, with strong translational effects (Sengupta et al., 2010). To address this concern, I used cervical dislocation as the primary method of euthanasia and harvested tissues as quickly as possible. The second concern I addressed is degradation or changes in the translational landscape during tissue homogenization and sample preparation. This was prevented by rapid freezing of dissected tissues in liquid nitrogen and cryogenic grinding of tissues in a Retch

MM400 mixer mill prior to resuspension in lysis buffer. With this procedure, tissues are maintained at extremely low temperatures while the macro-scale tissue structure is disrupted, and are only thawed as a powder in the presence of lysis buffer. Lastly, many tissues (e.g. pancreas) produce protein products that could degrade RNA or proteins, which could damage ribosomes and prevent footprint recovery. I address this concern by including murine RNase inhibitor, which will inhibit endogenous mouse RNases but not RNase I used for footprinting, and a protease inhibitor cocktail in the lysis buffer.

This protocol resulted in reproducible profiling from mouse liver (Figure 2.1A). While there is variation between replicates, the vast majority of transcripts vary by less than 2-fold. Enrichment of footprints within coding regions and 3 nucleotide periodicity, a hallmark of bona-fide translation, can also be seen in these data (Figure 2.1B). Comparing the data from liver to that of similar experiments using pancreas by gene ontology analysis, it is clear that the expression levels measured reflect the known roles of those tissues (Figures 2.1C-D). Specifically, transcripts associated with bile acid, small molecule metabolic processes, and lipid metabolism are enriched in liver profiling, while transcripts associated with digestion and peptidase activity are enriched in pancreas profiling.

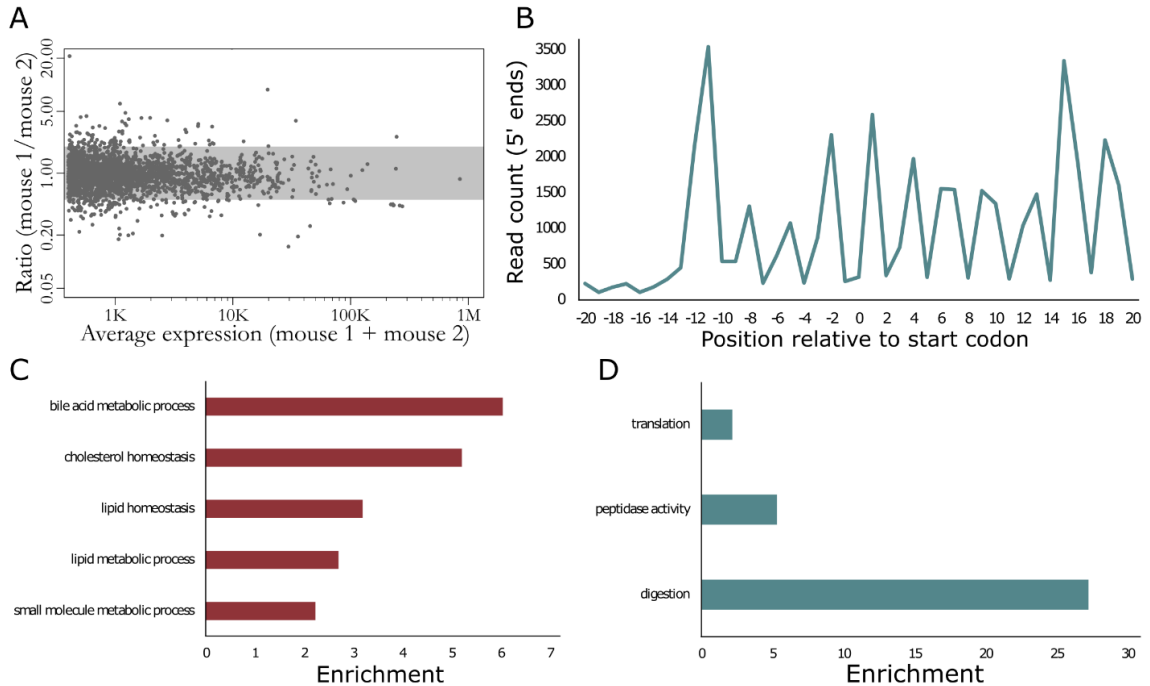


Figure 2.1. Ribosome profiling of whole tissues

(A) MA plot showing fold change between liver profiling from two untreated biological replicates. The shaded area indicates a range of 2-fold change.

(B) Metagene plot showing the counts of 5' ends of reads at positions relative to the start codon.

(C-D) Significantly enriched gene ontology categories in liver relative to pancreas (C) and pancreas relative to liver (D).

Analysis of translation in heterogeneous tissues (e.g. pancreas) requires a method for lineage specific ribosome profiling. As existing technologies were incompatible or insufficient for our needs, my advisor and I designed our own lineage-specific ribosome profiling system. Our system relies on the Avi tag, which is a short peptide able to be biotinylated by the BirA ligase. We plan to tag the endogenous Rpl10A (ribosomal protein 10A) locus with the Avi tag, resulting in the addition of the Avi tag to all ribosomes in every cell. The BirA ligase can then be expressed

in target cell types, for instance by Cre-mediated activation. In this way, only cells in the Cre-positive lineage used will have biotinylated ribosomes. These Avi-tagged Rpl10A constructs were prepared and initially tested in cell culture by rotation students in the Ingolia Lab. Their work demonstrated that the system could be used for ribosome profiling, and that mitochondrial transcripts were disenriched, suggesting real enrichment of tagged ribosomes.

I wanted to test the ribosome affinity purification system in an environment with many non-biotinylated ribosomes that could be tracked to report the quality of our purification. Lysate from Rpl1B-GFP yeast (Rpl1B is the yeast homolog of mouse/human Rpl10A) were mixed with Hek293 cell lysates with biotinylated ribosomes. This experiment showed that I could collect biotinylated ribosomes from a mixed population (Figure 2.2A). Unfortunately the Rpl1B-GFP was difficult to track by western blot, and was uninformative for measuring the extent of background binding. While I appeared to recover all biotinylated Rpl10A-Avi, this represented only a small fraction of the total Rpl10A-Avi present in the cells. This suggested that only a fraction of Rpl10A-Avi ribosomes were being biotinylated. To improve biotinylation, supplemental biotin was added to the cell culture medium about 24 hours before collection. Although I was still unable to pull down the majority of Rpl10A-Avi, I did see an improvement in how much Rpl10A-Avi was biotinylated (Figure 2.2B).

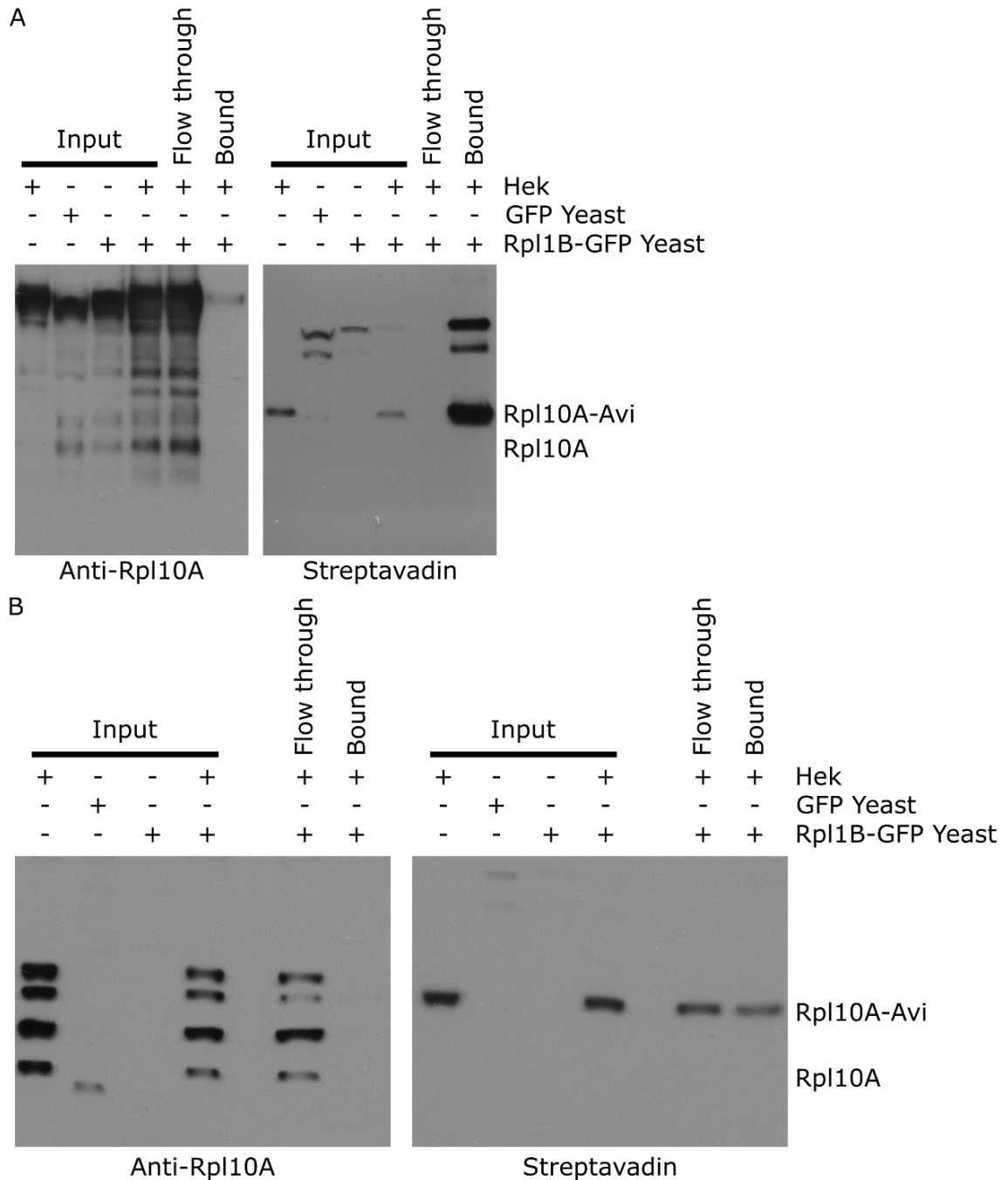


Figure 2.2. Pull-down of tagged Rpl10A with or without biotin supplementation

(A) Tagged Hek293 cell lysates were mixed with Rpl1B-GFP yeast lysates and bound to streptavidin beads, without biotin supplementation of media. All biotinylated Rpl10A-Avi appears to be bound.

(B) Tagged Hek293 cell lysates were mixed with Rpl1B-GFP yeast lysates and bound to streptavidin beads, following biotin supplementation of media.

I decided to try ribosome profiling of these mixed populations to determine how much enrichment I could get relative to untagged yeast ribosomes. Libraries were prepared from an input sample that was not enriched for biotinylated ribosomes and a sample that was bound to streptavidin beads. Reads were aligned to a combined human and yeast genome, with multiple alignments suppressed to prevent any cross-alignment. I saw a nearly 7-fold enrichment of human transcripts in the bound library relative to yeast (Figure 2.3A). Two well expressed yeast transcripts were enriched, one endogenously biotinylated protein, likely biotinylated while still attached to ribosomes, and one aminoacyl-tRNA synthetase. Several human mitochondrial transcripts were disenriched, consistent with previous results and the fact that they are translated by an independent pool of ribosomes.

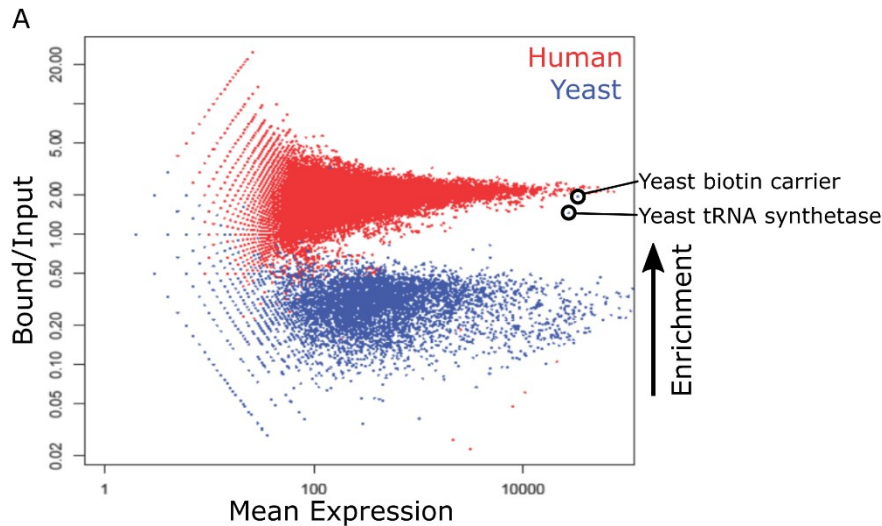


Figure 2.3. Enrichment of human transcripts in mixed profiling
 (A) A mixed lysate of Rpl10A-Avi tagged Hek293 lysate and Rpl1B-GFP tagged yeast lysate was bound to streptavidin beads and ribosome profiling was performed on input and bound lysates. Human transcripts are enriched approximately 6.7-fold in the bound library compared to yeast transcripts.

I further optimized ribosome affinity purification by measuring the amount of RNA recovered rather than by Western blots, which had proven uninformative, or by ribosome profiling, which is expensive and time consuming. I performed ribosome purification from untagged yeast and tagged human lysates independently, and the RNA concentration in the input and bound fractions was measured. RNA measurements showed a clear difference in the yield of ribosomes from yeast vs. human lysates, suggesting about 10-fold difference in their ability to be pulled down (Figure 2.4A). Several adjustments to the pull-down conditions were tested, but in the end SDS wash was the only condition that resulted in improved results. While the percent of RNA recovered from

human lysates decreased slightly with SDS wash, non-specific pull-down of yeast was reduced much more dramatically (Figure 2.4B).

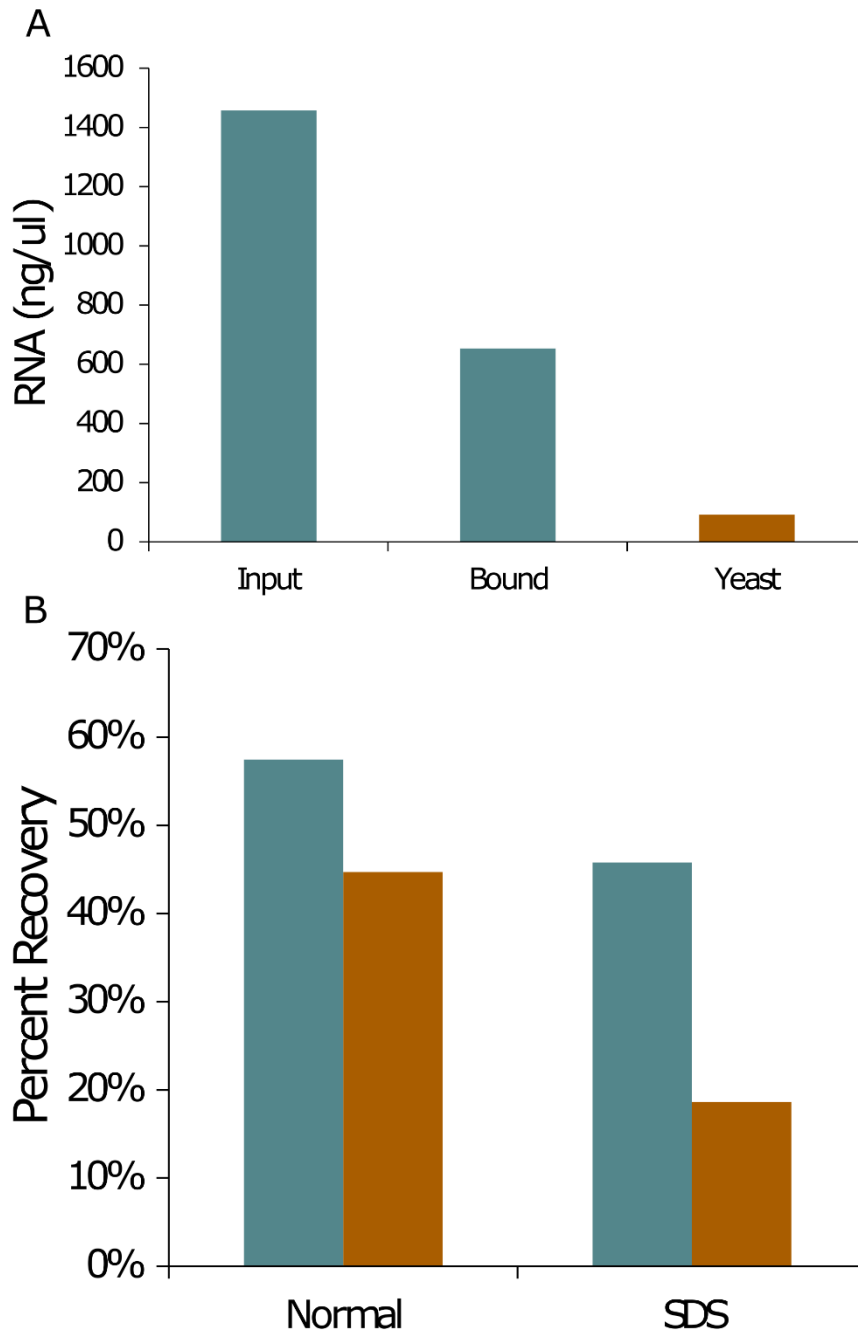


Figure 2.4. SDS wash reduces background binding

(A) RNA concentrations of input Rpl10A-Avi tagged Hek293 lysate and streptavidin bound Hek293 and Rpl1B-GFP yeast lysates are compared. (B) The percent recovery of RNA from tagged Hek293 lysate (teal) and untagged yeast lysate (orange) is shown using the previous pull-down conditions or SDS wash. SDS wash lowers non-specific recovery from yeast lysate, while having only a small effect on recovery from tagged Hek293 lysates.

The remainder of this results section was originally published in Cell Reports on Aug. 21, 2014. It is published under a creative commons license (CC BY 3.0), and as such may be reproduced here so long as appropriate credit is given. Only portions of this work that directly involve work performed by the thesis author (Michael Harris) are shown here. More specifically, I performed the ribosome affinity purification and profiling experiments and processed and analyzed the resulting data.

Ribosome Profiling Reveals Pervasive Translation Outside of Annotated Protein-Coding Genes

Nicholas T. Ingolia^{1,5}, Gloria A. Brar^{2,5}, Noam Stern-Ginossar^{2,6}, Michael S. Harris^{1,3,5}, Gaëlle J.S. Talhouarne^{1,3}, Sarah E. Jackson⁴, Mark R. Wills⁴, and Jonathan S. Weissman²

¹Department of Embryology, Carnegie Institution for Science, Baltimore, MD 21218, USA

²Department of Cellular and Molecular Pharmacology, Howard Hughes Medical Institute, Center for RNA Systems Biology, California Institute for Quantitative Biosciences, University of California, San Francisco, San Francisco, CA 94158, USA

³Department of Biology, The Johns Hopkins University, Baltimore, MD 21218, USA

⁴Department of Medicine, University of Cambridge, Cambridge CB2 0QQ, UK

⁵Present address: Department of Molecular and Cell Biology, University of California, Berkeley, Berkeley, CA 94720, USA

⁶Present address: Department of Molecular Genetics, Weizmann Institute of Science, Rehovot 76100, Israel

We next sought to verify that footprints seen outside of annotated coding regions copurified specifically with the ribosome. Ribosome affinity purification would provide strong evidence that footprints on lncRNAs and on 5' UTRs were bound to the ribosome (Figure 2.5A). We typically

recover ribosomes by sedimentation in an ultracentrifuge, but this purification provides little specificity for ribosomes over other large RNPs. The most prominent classical noncoding RNAs that contribute to background in ribosome-profiling experiments are components of nonribosomal RNPs, such as RNase P, telomerase, and the vault RNP. We infer that these RNP assemblies both protect RNA fragments from digestion and then sediment with ribosomes, and it seemed possible that some apparent ribosome footprints on lncRNAs actually reflected the incorporation of the lncRNA into a similar RNP complex.

Specific affinity purification of the ribosome would deplete background from these RNPs. The large (60S) subunit joins at the last step in translation initiation and does not associate with mRNA prior to this time, and so any footprint associated with the 60S subunit derives from a ribosome that has completed initiation and begun translation (Aitken and Lorsch, 2012). Ribosome-profiling data are unlikely to include footprints of small (40S) subunits scanning 5' UTRs prior to initiation, because these complexes are unstable in the absence of chemical crosslinking and are expected to protect a different mRNA footprint size from assembled 80S ribosomes (Valásek et al., 2007). Nonetheless, we wished to verify that footprints on 5' UTRs reflected postinitiation-assembled (80S) ribosomes.

In order to purify 80S (and 60S) ribosomes specifically, we developed an affinity-tagged version of large subunit ribosomal protein L1 (formerly RPL10A). Several ribosome epitope tags have been developed for lineage-specific polysome isolation, including the translating ribosome affinity purification tag, in which L1 is fused to enhanced GFP (Heiman et al., 2008). We believed that *in vivo* biotinylation of L1 would offer advantages over epitope tags, allowing us to exploit the high affinity and rapid association of biotin and streptavidin to purify tagged ribosomes. We placed a biotin acceptor peptide at the end of a long, flexible linker at the C terminus of L1 and coexpressed this tagged protein along with *birA*, the cognate *E. coli* biotin ligase, in human embryonic kidney 293 (HEK293) cells. Tagged L1 was biotinylated, dependent on the presence of *birA*, and L1-biotin was incorporated into ribosomes.

In order to test our enrichment of tagged ribosomes, we mixed lysate from human cells expressing L1-biotin (in addition to their endogenous L1) with a control yeast lysate lacking biotinylated ribosomes and compared the fate of the human ribosome footprints to footprints from yeast genes. We performed nuclease footprinting of this mixture, collected all ribosomes by filtration through Sephacryl S400 columns, and purified the tagged human ribosomes by streptavidin affinity. Footprints from human protein-coding genes were strongly enriched in the streptavidin-bound sample relative to footprints from yeast transcripts (Figure 2.5B). The only exception was the yeast gene *ACC1*,

which encodes the endogenous yeast biotin carrier protein. We assume that it is biotinylated cotranslationally in vivo and so footprints recovered by affinity purification through the nascent chain. Consistent with this model, only footprints from the 3' end of ACC1, corresponding to ribosomes that have synthesized the biotin acceptor site of Acc1p, are enriched. Importantly, the observed specificity for human mRNAs also excluded post lysis association of human ribosomes to yeast mRNAs, arguing strongly that footprints seen in ribosome-profiling experiments reflect translation that initiated in vivo prior to cell lysis. Fragment length distribution analysis provided further evidence against human ribosomes subject to affinity enrichment on yeast mRNAs, as protected fragments on human and yeast ribosomes are distinct in the mixed lysate and there was no evidence for a shift toward human fragment lengths on yeast messages following affinity purification. Human snoRNA reads also copurified with biotinylated L1, though somewhat less efficiently than ribosome footprints, as we expect due to their binding to preribosomal complexes in order to guide pre-rRNA modification (Figures S2.1A–C).

We then investigated the fate of other human-derived background reads following affinity purification of ribosomes. As noted above, profiling data after conventional ribosome sedimentation in HEK cells contained fragments mapping to several classical noncoding RNAs that also appeared in the mESC profiling, such as RNase P. Fragment length analysis using the FLOSS reliably discriminated this background from

footprints on coding sequences (Figure 2.5D). These same transcript fragments were also depleted in affinity-purified profiling samples, at least as strongly as were yeast-coding sequences (Figures 2.5E-F). Fragments from mitochondrial coding sequences were also strongly depleted, as the mitochondrial ribosome, which is entirely distinct from the cytosolic ribosome, lacked a biotin tag.

Having established affinity purification as a physical separation of background RNA fragments from true ribosome footprints, we next turned to investigate the status of apparent ribosome footprints in noncoding regions. We first verified that, as in mESCs, the protected fragments size distribution on HEK cell 5' UTRs closely resembled ribosome footprints from the coding sequences (Figure S2.1D). These 5' UTR protected fragments also copurified with the large ribosomal subunit in nearly all cases (Figure 2.5C). We thus conclude that these fragments are true 80S ribosome footprints and do not reflect scanning 40S subunits. Likewise, we find that protected fragments on most HEK lncRNAs are physically bound to the ribosome and likely reflect true translation of these noncoding RNAs (Figures 2.5G-I). Furthermore, the small number of lncRNAs yielding substantial non-ribosome-associated fragments were independently identified as sources of background by the FLOSS analysis.

Figure 2.5. Ribosome Affinity Purification Separates 80S Footprints from Background RNA (next page)

(A) Schematic showing that affinity purification of tagged 60S ribosome subunits recovers 80S footprints but depletes background from nonribosomal RNPs, potential scanning 40S footprints, and footprints of untagged yeast 80S ribosomes.

(B) Human ribosome footprints are retained during ribosome affinity purification whereas yeast ribosome footprints (excepting the yeast biotin carrier ACC1) are depleted.

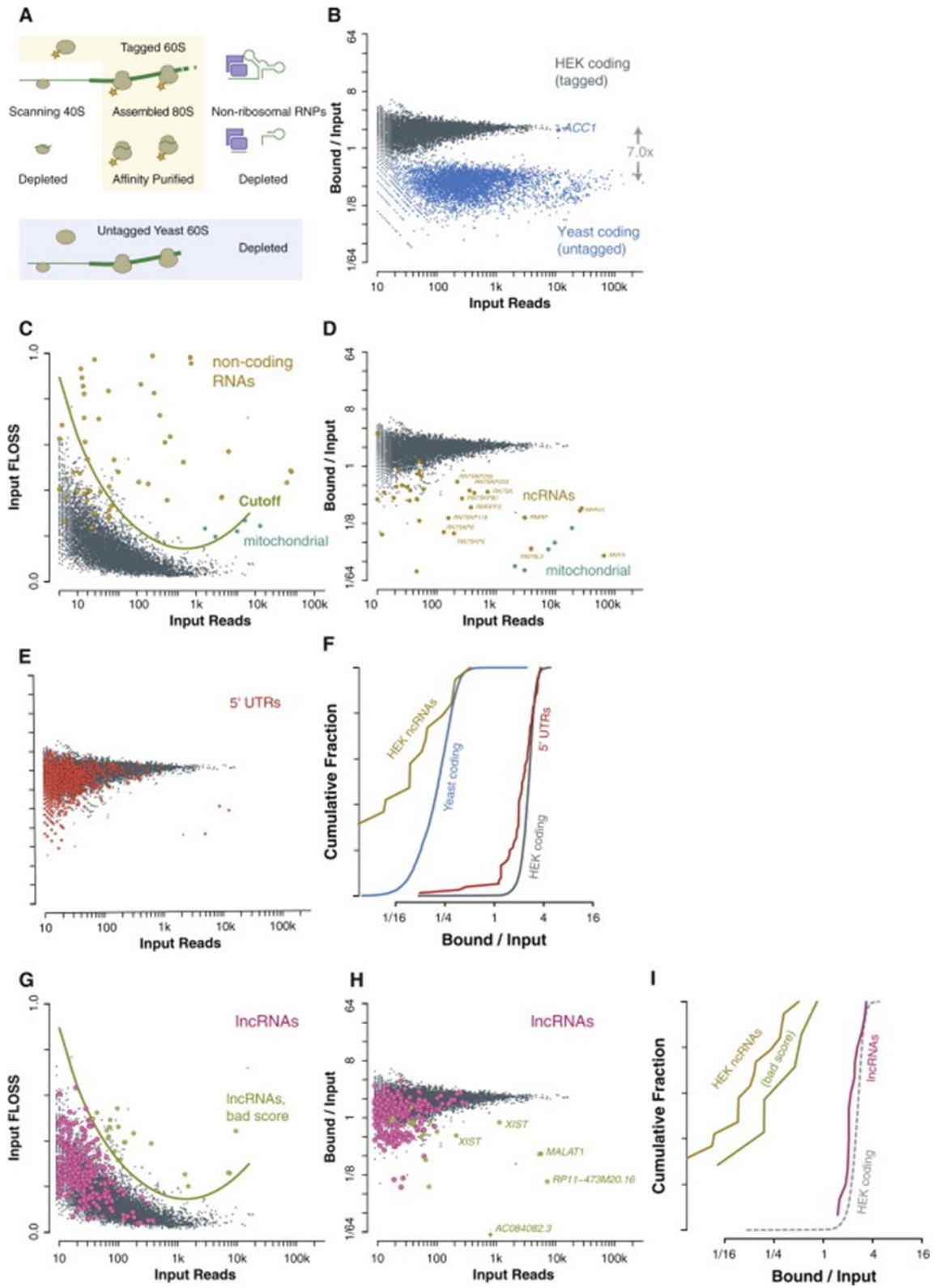
(C) Fragment length analysis of nuclear and mitochondrial coding sequences and of functional noncoding RNAs in HEK cells. A fragment length score cutoff based on extreme outliers relative to coding sequences excludes background fragments.

(D) Ribosome footprints are retained during ribosome affinity purification whereas mitochondrial footprints and noncoding RNAs are depleted.

(E and F) Ribosome footprints on 5' UTRs are retained during affinity purification of the 60S ribosomal subunit.

(G) Fragment length analysis of ENCODE lncRNAs, identifying a small number of transcripts with likely nonribosomal contamination.

(H and I) Ribosome footprints on lncRNAs are retained during ribosome affinity purification, whereas many sources of nonribosomal contamination, including the nuclear noncoding RNA XIST, are depleted.



Discussion

Adaptation of ribosome profiling to whole tissues is an important advancement in the use of the technique. Many biological questions, including those addressed in subsequent chapters of this thesis, are better suited to study in whole animals rather than cell culture. For example, while cell culture models of glucose response are available, they fail to fully capture the complex network of signals that give rise to *in vivo* responses. While some aspects of the liver's response to glucose may be a direct result of increased glucose levels, elevated insulin released from the pancreas is also a major contributor. Some responses may be mediated by other, less obvious, hormone factors. Studying this system with all the components intact provides a much better picture of this response.

The lineage-specific ribosome isolation strategy described here will further expand the range of systems that can be studied using ribosome profiling. For example, while the liver is relatively homogenous and can be meaningfully studied as a whole organ, translational regulation in β -cells can only be assayed with lineage-specific profiling, as they comprise a small percentage of the pancreas. Lineage-specific profiling will also be immensely helpful in studying translation in the brain, as the brain is highly complex and heterogeneous. The ability to select a small subset of cells using an existing Cre driver line would allow for studying of many

interesting phenomenon that may be specific to certain types of neurons. Although this system is incomplete, it has been shown to be effective at separating populations of ribosomes in mixed cell culture and yeast lysates. Transfer of the constructs used here to mice would likely provide the necessary lines for lineage specific profiling.

The discovery of ribosome footprints in non-coding regions suggested that these sequences are, in fact, translated to some degree. This has remained relatively controversial, due to concerns about these data representing bona-fide ribosomes footprints and not the footprints of some other ribonucleoprotein (RNP) complex. Among other evidence, the presence of these footprints in ribosome profiling libraries generated using this ribosome affinity purification system has clearly demonstrated that these fragments are in fact bona-fide ribosome footprints.

Chapter 3: Translational regulation in aging

While most proteins are turned over within hours to days to avoid accumulation of damaged proteins (Belle et al., 2006, Cambridge et al., 2011 and Price et al., 2010), this is not always the case. There are a number of proteins that have been shown to be extremely long-lived, ranging all the way up to several years (D'Angelo et al., 2009, Masters et al., 1977, Piha et al., 1966, Rodríguez de Lores et al., 1971, Savas et al., 2012 and Verzijl et al., 2000). A central question in the study of these long-lived proteins is whether they are continually translated in older animals. One might expect, because the old proteins remain, that far less new protein is produced in older animals.

I collaborated with Brandon Toyama and Martin Hetzer in their study of the long-lived proteins that they had identified in rat brain and liver (Savas et al., 2012). These proteins were primarily components of the nuclear pore complex and histones, some of which were maintained in the brain for up to 12 months. I performed ribosome profiling on young and old tissues to assess the levels of protein production for these long-lived proteins.

The following two paragraphs were originally published in Cell on Aug. 29, 2013. A license has been acquired from Elsevier (License # 3838920365480) for reproduction of these excerpts which contain the work contributed by the thesis author (Michael Harris). I performed the ribosome profiling experiment described here, and analyzed the resulting data.

Identification of Long-Lived Proteins Reveals Exceptional Stability of Essential Cellular Structures

Brandon H. Toyama^{1, 5}, Jeffrey N. Savas^{2, 5}, Sung Kyu Park², Michael S. Harris^{3, 4}, Nicholas T. Ingolia³, John R. Yates III², Martin W. Hetzer¹

¹Molecular and Cell Biology Laboratory, Salk Institute for Biological Studies, La Jolla, CA 92037, USA

²Department of Chemical Physiology, The Scripps Research Institute, La Jolla, CA 92037, USA

³Department of Embryology, Carnegie Institution for Science, Baltimore, MD 21218, USA

⁴Department of Biology, The Johns Hopkins University, Baltimore, MD 21218, USA

Results

In the case of eye lens crystallin, the lack of protein translation (and degradation) in lens fiber cells provides a rationale for their exceptional lifespan. To determine if lack of synthesis might explain the exceptional lifespans of the cellular proteins identified above, we determined the level of translation for all proteins expressed in liver and brain tissue through

deep sequencing of ribosome-protected mRNA footprints (Ingolia et al., 2009). Translation levels (i.e., density of ribosome footprints) were determined for over 11,000 proteins in 6-month-old liver and brain, and, unlike crystallin, we found evidence for translation of almost every long-lived protein. To test if there was a correlation between a protein's synthesis rate and its lifespan, we plotted translation levels versus ^{15}N fractional abundance at 6 months postchase (Figure 3.1A). Intriguingly, no strong correlation could be determined, with long-lived proteins possessing translation levels that span three orders of magnitude. Prevalent translation was also seen for all Nups regardless of their protein lifespan or tissue type (Figures 3.1A and 3.1B) and is particularly noteworthy for the NPC proteins Nup98 and Nup96. These nucleoporins are translated as a single precursor polypeptide that is autocatalytically cleaved into Nup98 and Nup96 (Fontoura et al., 1999). MS data on these two proteins 6 months postchase reveal that, despite their identical translation rates, Nup96 retains ^{15}N signal whereas Nup98 has been completely replaced with newly synthesized copies (Figures 3.1C and 3.1D). This difference is consistent with the structural and functional properties of these two Nups: although Nup98 is a peripheral and highly mobile nucleoporin with very low residence time at the NPC, Nup96 is a member of the Nup107/160 subcomplex and is therefore critical for the assembly and structural integrity of the nuclear pore (Hoelz et al., 2011 and Rabut et al., 2004). It thus appears that protein longevity is the

result of protein deposition into a stable complex rather than a lack of expression. Because the overall levels of Nup96 and NPC numbers do not increase with age (see below), these results also suggest that newly synthesized copies of Nup96, which are not incorporated into the NPC, are rapidly degraded.

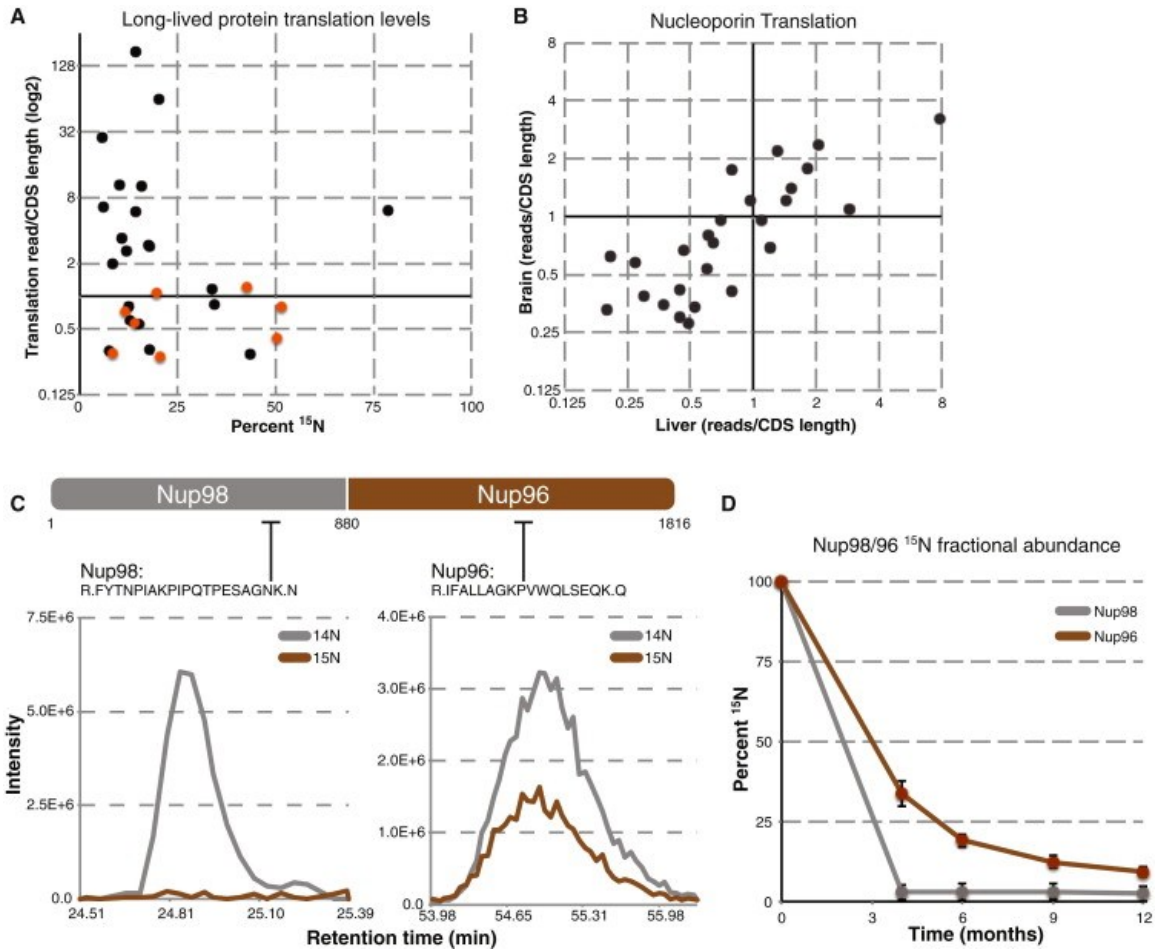


Figure 3.1. Protein Translation Does Not Correlate with Protein Lifespan

(A) Protein translation levels of long-lived proteins. Translation levels (reads/CDS length) of long-lived proteins are plotted (log₂) against their corresponding ¹⁵N fractional abundance at 6 months postchase. Translation levels of long-lived nucleoporins are plotted in orange.

(B) Translation levels of NPC proteins in liver and brain tissue. Translation levels of all NPC proteins were determined in liver (horizontal axis) and brain (vertical axis) tissue, and plotted against each other (log₂).

(C) Translation and stability of Nup98/96. Top: schematic of the Nup98/96 translated peptide, as well as the cleavage site (aa 880) that produces the separate Nup98 and Nup96 proteins. Lower: elution profile MS1 traces of the indicated peptides from the Nup98 and Nup96 region, plotted as describe for Figures 3.1D–3.1G.

(D) Stability of Nup98/96 over 12 months. Average ¹⁵N fractional abundance for Nup98 (gray) and Nup96 (orange) was determined from multiple peptides for each indicated time point and plotted over time.

Discussion

Another surprising result from our study is the continued translation of almost all long-lived proteins. This phenomenon is most clearly illustrated by the Nup98/Nup96 proteins, which are translated at identical rates from the same mRNA but exhibit divergent lifespans. Although Nup98 turns over rapidly, Nup96 is incorporated into the NPC scaffold, where it persists for months. This observation implies that the majority of newly synthesized Nup96 is immediately degraded in postmitotic cells. Why the coupling of translation of these two proteins is evolutionarily conserved when their cellular lifespans are divergent remains a mystery. Also unclear is the continuous production of long-lived proteins despite the fact that they are stably embedded in a cellular structure. One possibility is that long-lived proteins may exist in multiple functional populations within the cell, whereby one population is stable and long-lived, whereas another is dynamic and short-lived. Thus, translation would be needed to maintain constant turnover of the short-lived population. Alternatively, most of the newly synthesized copies may be unincorporated and subject to degradation. This possibility is consistent with protein turnover serving as a mechanism to buffer intracellular amino acid levels and with the reported immediate degradation of ~30% of all translated proteins (Schubert et al., 2000 and Vabulas and Hartl, 2005).

Related to the study of long-lived proteins and their production rates is the broader question of how the overall proteome changes with age. This includes identifying what proteins change in abundance between young and old animals, as well as understanding how these changes occur. Following the previous study of these long-lived proteins, I again collaborated with Brandon and Martin, along with Alessandro Ori and Martin Beck, in an integrative analysis of proteome change in aging.

The following was originally published in Cell Systems on Sept. 13, 2015.

It is published under a creative commons license (CC BY-NC-ND 4.0), and

as such may be reproduced here so long as appropriate credit is given.

Sections of the paper that are not directly related to work performed by the thesis author (Michael Harris) are included in the “Results from

collaborators” section. More specifically, I performed the ribosome profiling

and RNA-Seq experiments described here, processed and analyzed the

resulting data, cross referenced transcriptome and translatoome data with

proteomics data, and played a major role in the writing process.

Integrated Transcriptome and Proteome Analyses Reveal Organ-Specific Proteome Deterioration in Old Rats

Alessandro Ori^{1, 6, 7}, Brandon H. Toyama^{2, 6}, Michael S. Harris^{3, 4},

Thomas Bock¹, Murat Iskar¹, Peer Bork^{1, 5}, Nicholas T. Ingolia³ Martin W.

Hetzer² Martin Beck¹

¹European Molecular Biology Laboratory, Structural and Computational Biology Unit, Meyerhofstrasse 1, Heidelberg 69117, Germany

²Molecular and Cell Biology Laboratory, Salk Institute for Biological Studies, 10010 North Torrey Pines Road, La Jolla, CA 92037, USA

³Department of Molecular and Cell Biology, University of California, Berkeley, Berkeley, CA 94720, USA

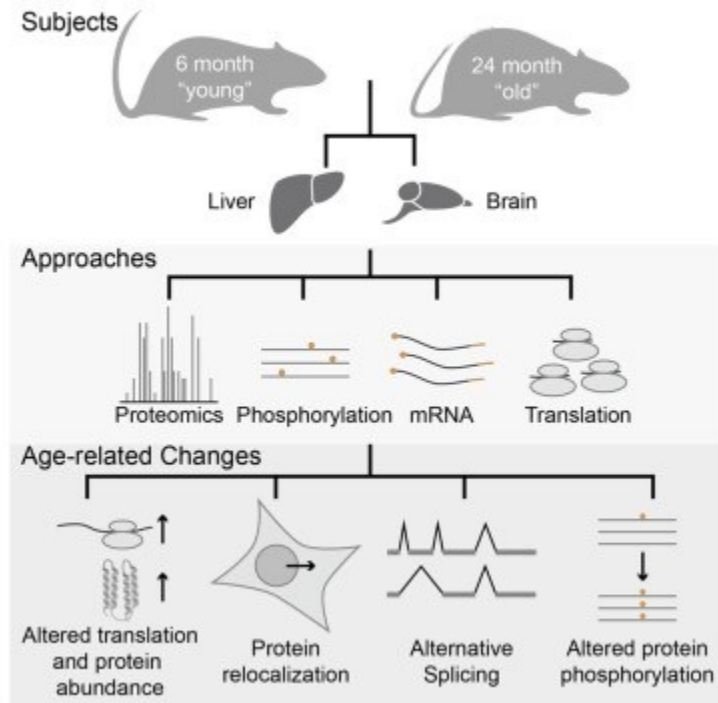
⁴Department of Biology, Johns Hopkins University, Baltimore, MD 21218, USA

⁵Max Delbrück Center for Molecular Medicine, Robert-Rössle-Strasse 10, Berlin 13125, Germany

Summary

Aging is associated with the decline of protein, cell, and organ function. Here, we use an integrated approach to characterize gene expression, bulk translation, and cell biology in the brains and livers of young and old rats. We identify 468 differences in protein abundance between young and old animals. The majority are a consequence of altered translation output, that is, the combined effect of changes in transcript abundance and translation efficiency. In addition, we identify 130 proteins whose overall abundance remains unchanged but whose sub-cellular localization, phosphorylation state, or splice-form varies. While some protein-level differences appear to be a generic property of the rats' chronological age, the majority are specific to one organ. These may be a consequence of the organ's physiology or the chronological age of the cells within the tissue. Taken together, our study provides an initial view of the proteome at the molecular, sub-cellular, and organ level in young and old rats.

Graphical Abstract



Results

To identify age-related molecular changes in the liver and brain, we sacrificed three “young” (6-month-old) and three “old” (24-month-old) rats from multiple litters, the latter of which represent old, but not dying, animals at the age of 50% expected survival. Brain and liver were harvested and identical samples were split for analysis at the transcription, translation and proteome levels by next-generation RNA sequencing, ribosome profiling and tandem shotgun mass spectrometry, respectively (Figure 3.2A). The mRNA abundance and translation output (total ribosome footprint reads) of 8,975 and 6,490 transcripts were

compared between young and old animals in brain and liver, respectively, and changes in translation efficiency were inferred by comparing these measured values. To increase proteomic coverage and obtain insights into subcellular localization, brain and liver samples were fractionated into nuclei, post-nuclear fraction 1 (pn1; enriched for mitochondria), post-nuclear fraction 2 (pn2; enriched for cytoplasmic membranes) and soluble cytosolic proteins (sol) according to a previously established procedure (Blobel and Potter, 1966 and Lovtrup-Rein and McEwen, 1966). All samples were analyzed by shotgun mass spectrometry, enabling us to perform 14,131 comparisons of protein abundances across two age groups and four subcellular fractions, covering 4,714 protein groups (i.e., collections of alternative protein isoforms containing shared peptides) mapping to 4,697 unique gene identifiers.

The proteomic measurements were highly reproducible, as indicated by the high correlation between technical replicates (on average Pearson's $r = 0.974$; Figure 3.2B). More importantly, correlation values across biological replicates of different age groups were significantly lower as compared to samples from the same age group (Wilcoxon rank sum test p value $2.5e-5$ and $8.1e-5$ for brain and liver, respectively; Figure 3.2C), demonstrating that the variation of protein abundance across age groups is more pronounced than the variation of protein levels across individuals of the same age. At the same time, the observed coefficients

of variation among both, young and old animals were very low (median coefficient of variation ~25%; Figure S3.1A). Similarly, both ribosome profiling and RNA sequencing (RNA-seq) were highly reproducible, as indicated by high correlation between replicates (Figures S3.2A-B, S3.2D-E). We thus conclude that the measured changes in protein and transcript abundance, and ribosome occupancy significantly discriminate samples obtained from the two age groups with the number of analyzed animals ($n = 3$ for each age group) using rigorous statistics (Figures S3.1B-C, S3.2C, and S3.2F).

In agreement with previous studies (Jiang et al., 2001, Lee et al., 2000, Lu et al., 2004, Toyama et al., 2013, Walther and Mann, 2011 and Wood et al., 2013), our data underline that age-specific variations of the transcriptome and proteome are much less pronounced than tissue-specific differences (Figure S3.1D). The majority of genes and proteins (>90%) are stably expressed and maintained in both the brains and livers of old animals (Figures 3.2D and 3.2E). Ribosome profiling provides an inclusive measure of “translation output” that reflects the net effect of changes in mRNA levels and ribosome occupancy. We identified 658 and 490 transcripts, in brain and liver respectively, with changes in translation output (adjusted p value < 0.01). Of these, 168 (brain) and 283 (liver) were caused exclusively by changes in mRNA abundance. The “translation efficiency” of an mRNA is the overall translation output from ribosome profiling normalized over the transcript abundance from RNA-

seq. Among differentially expressed transcripts, 96 (brain) and 9 (liver) displayed exclusively a change in translation efficiency but not in transcript abundance (Figure 3.2F). In order to directly relate changes in protein production to the observed alterations of protein abundance, we compared our translation output values from ribosome profiling to our proteomic measurements. At the proteomic level, significant abundance changes for 204 protein groups in young versus old organs (q value < 0.1) were detected. A total of 264 proteins were identified exclusively and consistently in all three replicates of one age group but in no replicates of the other age group; these were considered as potentially affected. We conclude that hundreds of genes and proteins were identified that differentiate young and old organs and constitute a comprehensive resource for the scientific community to query molecular alterations of cells in their physiological ground state during aging in mammals.

Figure 3.2. Integrated Genomics and Proteomics Analysis of Aging Brain and Liver (next page)

(A) Brain and liver samples obtained from three “young” (6-month-old) and three “old” (24-month-old) rats were compared by next-generation RNA sequencing, ribosomal profiling and shotgun mass spectrometry. Prior to mass spectrometry, organ homogenates were fractionated in four subcellular fractions: nuclei (nuc), post-nuclear fraction 1 (pn1; enriched for mitochondria), post-nuclear fraction 2 (pn2; enriched for cytosolic membranes) and soluble cytosolic proteins (sol). For proteomics measurements, each sample was analyzed in technical duplicate (repeated injection of the same sample).

(B) Reproducibility of protein abundance measurements. The histogram shows the distribution of pairwise correlations between all technical replicates for brain and liver.

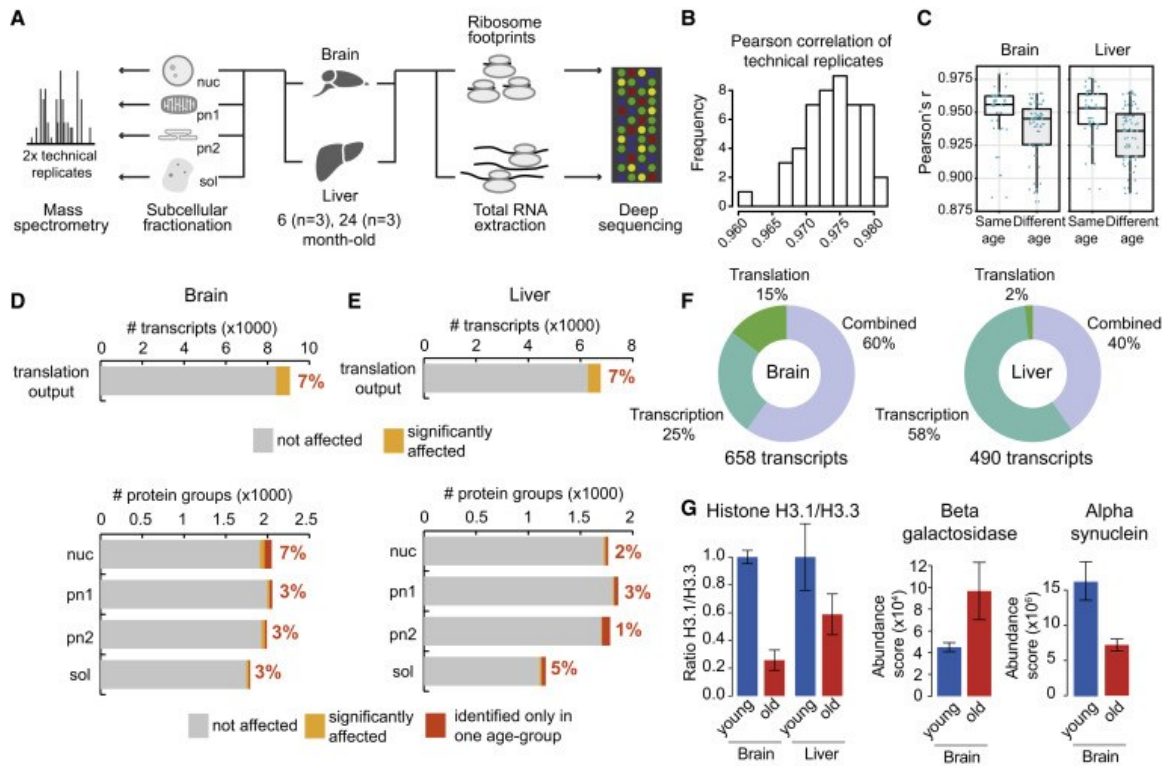
(C) The boxplots depict all the pairwise correlations between samples from all the subcellular fractions.

(D and E) Less than 10% of the quantified transcript and protein groups were affected in young versus old rats, both in brain (D) and liver (E). Differential protein expression was assessed by label-free quantification and significantly affected proteins were defined using a q value cut-off of 0.1. Additionally, proteins that were identified exclusively and consistently in one age group but not the other were considered as age-affected (dark orange). Translation output was measured by ribosome footprints. Significantly affected transcripts were defined using an adjusted p value cut-off of 0.01.

(F) Significantly affected transcripts were grouped according to whether they were affected by a change in transcript abundance (as quantified by RNA-seq), translation efficiency or by a combined effect.

(G) Established aging markers were recovered at the protein level. Histones H3.1 and H3.3 were quantified using proteotypic peptides measured by targeted proteomics (see Supplemental Experimental Procedures). The ratio between the two proteins is displayed relative to its value in young animals (set to 1) and it represents the average value \pm SEM (n = 3 animals per age group). For beta-galactosidase and alpha-synuclein, protein abundances are indicated as average abundance score (sum of peptide intensities normalized by protein molecular weight) \pm SEM (n = 3 animals per age group).

See also Figures S3.1 and S3.2.



Age Markers Were Consistently Identified

The sensitivity of our approach recovers alterations of previously established age markers. A global decrease in the abundance ratio between histone H3.1 and H3.3 was observed in both old organs (Figure 3.2G). Histone H3.1 is incorporated in nucleosomes only during mitosis (Wu et al., 1982) and is replaced by the H3.3 variant outside of mitosis, typically during transcription (Ahmad and Henikoff, 2002 and Schwartz and Ahmad, 2005). Thus, in a tissue that is largely post-mitotic such as the brain, the H3.1/H3.3 ratio is expected to decrease with age (Maze et al., 2015); this is what we observe. We also observed a 2-fold increase in the abundance of the enzyme beta-galactosidase in old brain (Figure 3.2G), a widely used marker of cellular senescence (Dimri et al., 1995).

Concurrently, we detected beta-galactosidase in old liver but not young. A decreased level of alpha-synuclein, a protein involved in synaptic plasticity and neurodegenerative disorders, was also detected in brain (Figure 3.2G), corroborating a previous study in mice (Mak et al., 2009). Additionally, we detected significant changes at the level of protein abundance or translation output for 97 age-related factors (Hühne et al., 2014). We conclude that our integrative analysis recapitulates trends of several known age markers but also identifies a large and comprehensive set of transcripts and proteins that are linked to age-specific alterations for the first time.

Identification of Common and Organ-Specific Alterations

Liver and brain have different regenerative capacities. Most neurons in the adult brain are non-dividing cells that must survive for an organism's lifespan (Spalding et al., 2005). In contrast, liver cells, such as hepatocytes, are replaced every few months throughout adult life in rodents (Arber et al., 1988 and Toyama et al., 2013). One would thus predict that age-related effects onto the proteome are organ-specific. A comparison of proteomic changes across the different biochemical fractions supports this hypothesis: we identified the highest number of differentially expressed proteins in the nuclear fraction of the brain (7% of nuclear proteins affected: Figure 3.2D), whereas in the liver the most changes were found in the cytosolic fraction (5% of cytosolic proteins

affected: Figure 3.2E). Overall, a larger fraction of the proteome was affected in brain, the tissue with lower regenerative capacity: 8% of all quantified proteins versus 5% in liver (Figures 3.2D and 3.2E).

The identities of the transcripts and proteins affected were also indicative of organ-specific differences between young and old animals. Out of 1,099 transcripts abundances that were altered, only 48, considerably less than expected (Fisher's exact test: p value < 0.0001 , odds ratio 0.04), were common to brain and liver and 37 of them (77%) changed concordantly (Figure 3.3A). Most of these transcripts are involved in the regulation of the immune system and stress response. The protein abundance data showed a similar trend: only eight out of the 447 affected protein groups are common to brain and liver (Fisher's exact test: p value < 0.001 , odds ratio 0.02; Figure 3.3B).

Gene ontology analysis confirmed that different functional modules are affected in brain and liver, but also underlined the existence of common aspects of altered protein function in old tissues. Commonalities include the enrichment of altered genes encoding for factors involved in cell communication, hormone response, immune response/inflammation, and the depletion of respiratory chain components (Figures 3.3C-F). The latter, previously described at the mRNA level across multiple organs and species (Zahn et al., 2006), likely arises from mitochondrial dysfunction and might be accompanied by an increase of reactive oxygen species and

generation of pro-inflammatory signals (Green et al., 2011). Another common feature is the regulation of proteins involved in post-translational modifications, although different pathways are affected in the two organs. Whereas several protein kinases (Figure S3.3A) and methyltransferases are altered in brain (Figure 3.3D), it is largely acetyltransferases that are affected in liver (Figure 3.3F). We speculate that some of these alterations might be responsible for the changes in the epigenetic landscape described in aged cells (Rhie et al., 2013 and Sun et al., 2014).

Organ-specific alterations appear to be linked to their physiology. In brain, alterations of neuronal communication and synaptic transmission occur at multiple levels: we observed depletion of intracellular mediators of signaling such as protein kinases, multiple ion channels and G protein-coupled receptors, in the brains of old rats (Figure 3.3C). In liver, several metabolic networks are altered (Figures 3.3E-F). In particular, we observed an increased abundance of enzymes involved in pyruvate metabolism and the tricarboxylic acid cycle, lipid catabolism (in particular fatty acid oxidation), and maintenance of redox homeostasis (Figure 3.3F). These alterations are consistent and might underlie the metabolic changes that have been observed in old liver in mice (Houtkooper et al., 2011).

In summary, by providing a detailed picture of the molecular alterations that distinguish young and old organs, our data suggest a molecular basis for several hallmarks of aging including mitochondrial dysfunction, increased inflammation, and changes in regulators of the epigenetic landscape (López-Otín et al., 2013).

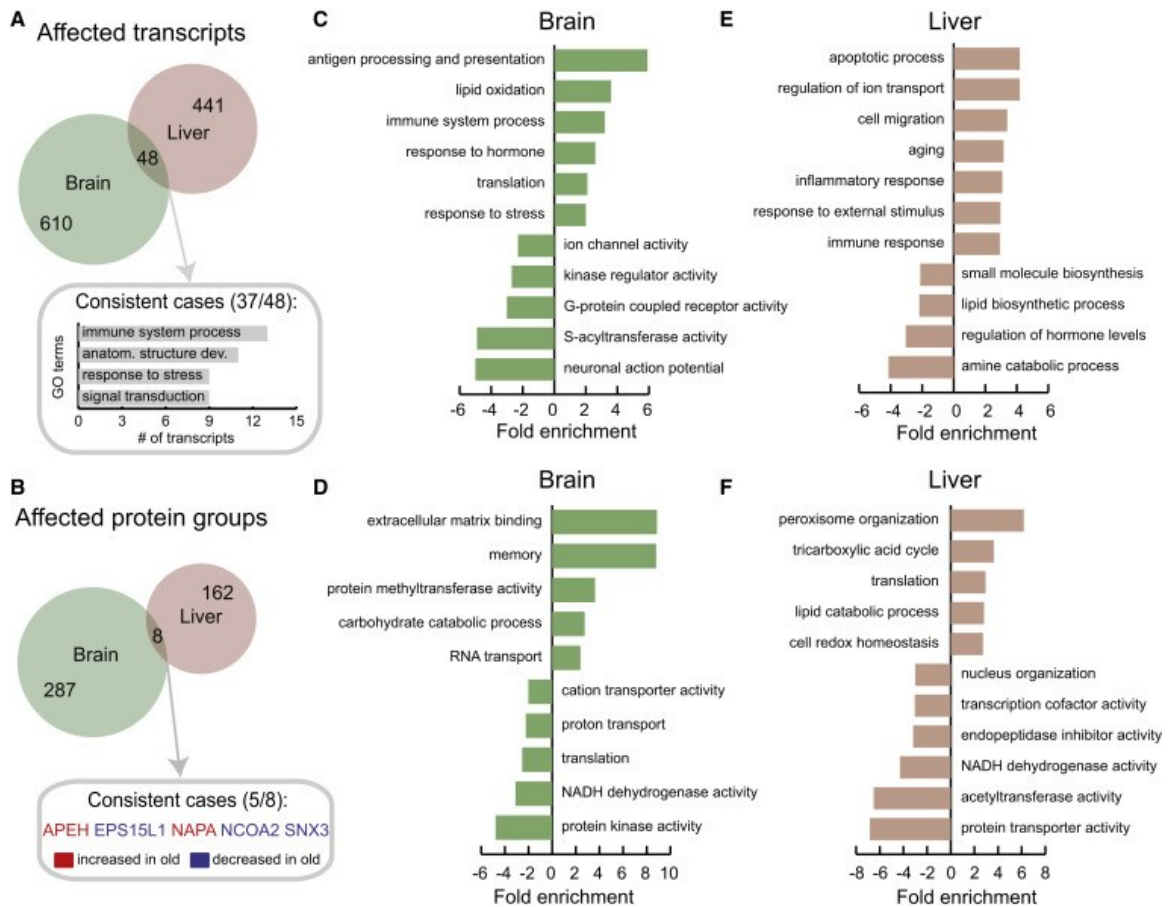


Figure 3.3. Common and Organ-Specific Alterations of the Proteome in Old Rats

(A and B) We identified only 48 transcripts affected at the level of translation output (A) and eight proteins affected at the level of protein abundance (B) that were altered in both brain and liver. The most represented gene ontology (GO) terms among consistently affected transcripts are shown in (A) while the five consistently affected proteins are indicated in (B).

(C–F) Functional enrichment was performed on the list of quantified transcripts and proteins that were ranked according to the level of differential expression (fold change) using GOrilla (Eden et al., 2009). Displayed GO terms are representative cases selected from among those significantly enriched (cut-off for transcripts: q value < 0.05, minimum number of transcript >4, fold enrichment ≥ 2 ; for proteins the same criteria were applied with the exception of q value < 0.2). The fold enrichments are plotted using positive values for terms enriched in transcripts/proteins that are increased in old animals, or using negative values for terms enriched in transcripts/proteins that are decreased in old animals.

See also Figure S3.3.

[One section from the published work has been removed here (“Protein Complexes Are Affected at Multiple Levels”), and can be found in “Results from collaborators.”]

Translation Output Contributes Significantly to Proteomic Alterations

The combination of ribosome profiling and shotgun proteomics data allowed us to determine the contribution of translation output, and thus protein synthesis, to alteration of protein abundances (Battle et al., 2015 and Guo et al., 2010). Globally, we found that the changes in translation output between young and old animals are reflected by consistent changes in protein level. We categorized all transcripts into three groups: significantly increased, significantly decreased, and not affected at the level of translation output. The corresponding proteomic fold changes of altered transcripts were shifted substantially and significantly relative to transcripts without evidence for significant translational change (Figures 3.4A-B).

Notably, for ~75% of these transcripts, the changes in translation output and protein abundance are concordant in directionality (Figures 3.4A-B, dashed lines). Also, the observed fold-changes in translation output and protein abundances in both brain and liver were positively correlated, meaning that we see a correlation between the changes in the abundance of a protein, as assessed by proteomics, and the abundance and/or translation of the mRNA that encodes it in our ribosome profiling experiments (Spearman's rank correlation coefficient between translation and protein abundance fold changes: 0.13 and 0.25 for brain and liver, respectively: Figures 3.4C and 3.4D). Conversely, if proteins are

categorized into groups that are significantly increased, significantly decreased, and not affected in their abundance, their respective fold changes in translation output are similarly shifted, although with smaller effect size (compare Figures 3.4E-F to 3.4A-B).

Taken together, this analysis suggests that differences in protein synthesis (translation output) give rise to an appreciable fraction of the observed changes in protein abundance that discriminate young and old organs (Figures 3.4E-F). This overall correspondence emerges despite limited overlap between datasets (Figures 3.4C-D), suggesting that many genes might be showing subtle changes in synthesis and abundance that do not rise to statistical significance when studied with only one of the techniques. We show that on a global scale, changes in translation output—although small—impact on protein abundance between young and old animals, as exemplified by the increase of chaperonin alpha-crystallin B in old brains (Figure 3.4G).

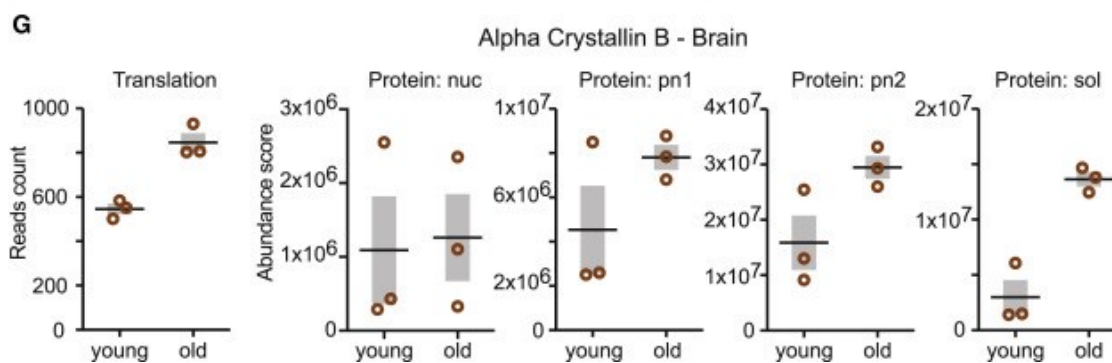
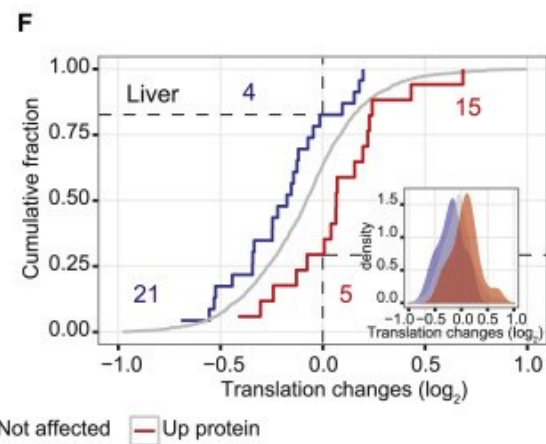
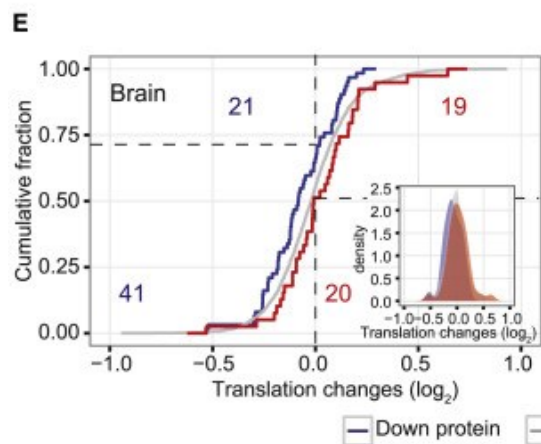
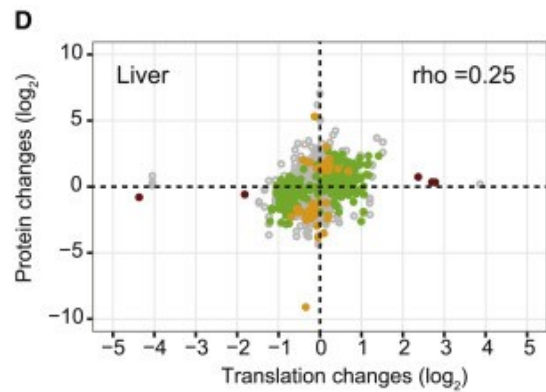
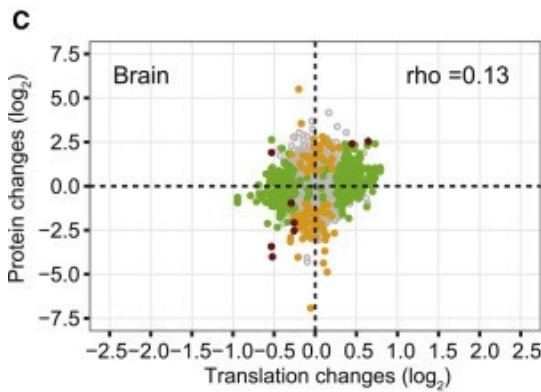
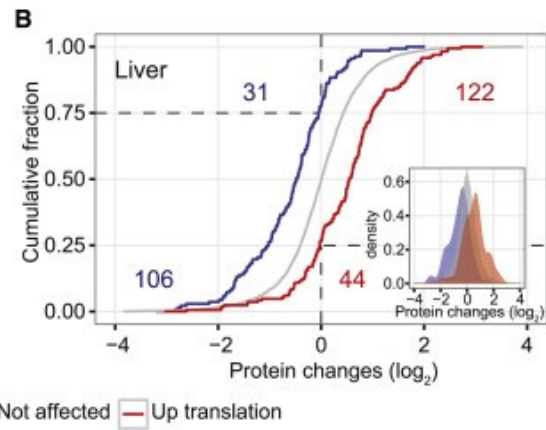
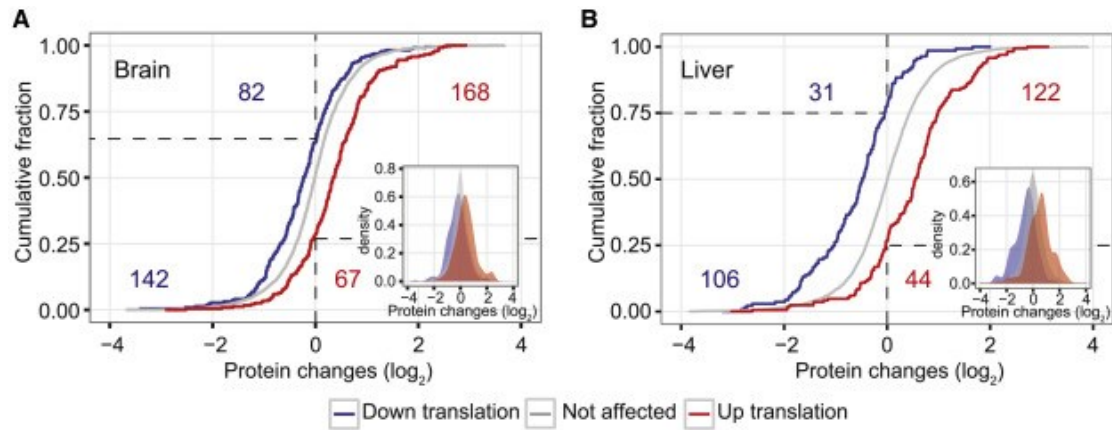
Figure 3.4. Changes in Translation Correspond to Changes in Protein Abundance (next page)

(A and B) The distribution of the corresponding protein changes for transcripts showing increased (red) or decreased (blue) translation output in old animals is significantly and consistently shifted relative to that of unaffected transcripts (gray).

(C and D) Changes in translation output and protein abundance are positively correlated despite the limited overlap in cases that rise to significance using both methods. We assessed the correlation between translation and protein abundance by calculating the Spearman's rank correlation coefficient between the respective fold changes: 0.13 and 0.25 for brain and liver, respectively. The correlation coefficients increased to 0.37 for brain and 0.42 for liver when only significant cases (either at the translation or protein level) were taken into account.

(E and F) The distribution of the corresponding changes in translation for proteins increased (red) or decreased (blue) in old animals is significantly and consistently shifted relative to the distribution of unaffected proteins (gray).

(G) The chaperonin alpha-crystallin B is shown as an example of a protein that is affected at the level of translation output, and it is consistently changed at the protein level in multiple subcellular fractions.



[Two sections from the published work has been removed here (“Altered Protein Localization”, “Changes in Protein Phosphorylation”), and can be found in “Results from collaborators.”]

Multiple Levels of Regulation Modulate Functional Networks between Young and Old Animals

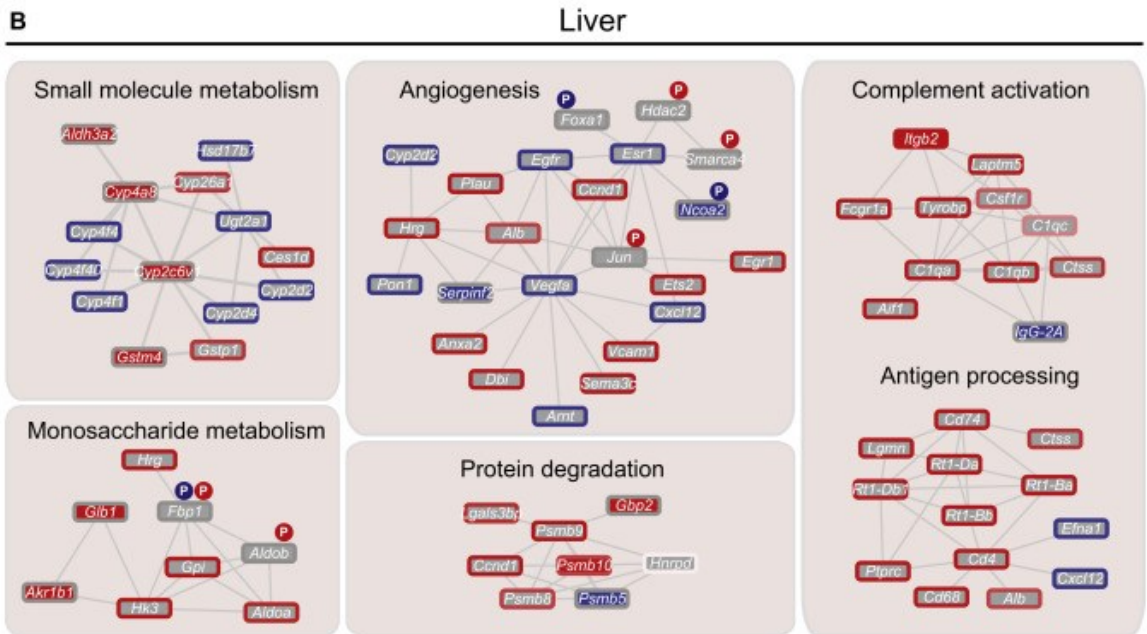
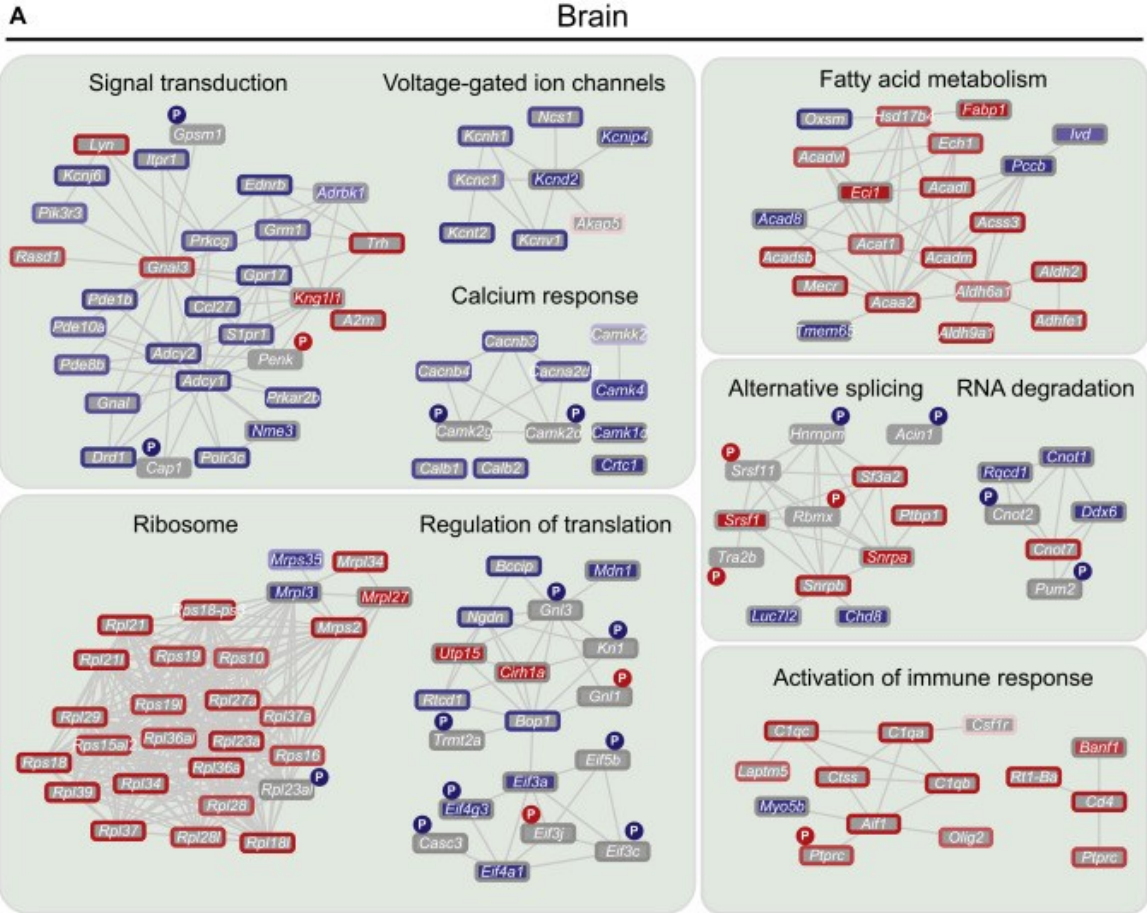
The integration of multiple measurements on the same sample provides a powerful approach to capture functional modules that discriminate between different cellular states. To take advantage of this, we combined genes affected at the level of translation, protein abundance and protein phosphorylation and used them to reconstruct functional networks (see Supplemental Experimental Procedures) that are altered between young and old animals (Figure 3.5). Specifically in brain, we identified three related networks that are involved in signal transduction. The majority of the nodes in these networks displayed reduced translation output or protein abundance in old animals. Among these, several mediators of the calcium signaling pathway, such as the kinases CAMK1D and CAMK4, were reduced in their protein abundance, while the kinases CAMK2D and CAMK2G were affected in their phosphorylation state (Figure 3.5A). We found up-stream mediators of calcium signaling to be affected, including several voltage-gated channels and calcium transporters, as well as down-stream effectors such as the CREB-regulated transcription

coactivator 1 (CRTC1; Figure 3.5A). Taken together, our data suggests that the response to stimuli might be modified at multiple levels in the brain of old animals, mainly through the depletion of several factors involved in mediating calcium signaling.

We also found two related functional networks that are common to both brain and liver. These clusters comprise multiple mediators of the immune response such as proteins involved in antigen processing and presentation, including all the three components of the C1q complex that are involved in the first step of the classical complement activation pathway by direct recognition of pathogens or antibody:antigen complexes (Figures 3.5A-B). As many of these proteins are generally not expressed in hepatocytes and neuronal cells, such as CD4, we speculate that the observed abundance increase derives from an increased number of immune cells that are recruited into the old organ by pro-inflammatory stimuli.

Figure 3.5. The Impact of Age on Functional Networks Occurs at Multiple Levels of Regulation (next page)

(A and B) Selected functional networks that are altered between young and old rats are displayed. The node fill color indicates significant fold change in protein abundance and the node border color indicates significant fold change in translation output. Changes in phosphorylation status are represented by the circled letter "P." Increased abundance in old animals is indicated in red and decreased abundance is indicated in blue. See also Figures S3.4 and S3.6.



Translation old/young (log₂) Protein old/young (log₂) Phosphosite, in old animals:

-0.5 0.5 -2 2 P decreased P increased

Alternative Splicing

Another potential source of age-related alterations of the cellular proteome is the process of alternative splicing, which results in a single gene coding for multiple proteins (Wood et al., 2013). Inspired by the fact that multiple factors involved in the regulation of alternative splicing and RNA processing were affected in old animals (Figure 3.5A), we analyzed potential differences in mRNA splicing between young and old animals (see Supplemental Experimental Procedures). We found significant differences in the expression of 41 and 61 transcript isoforms from 24 and 39 genes in brain and liver, respectively (Figure S3.5). Among these were two isoforms in the brain of *Sgk1*, a serine/threonine protein kinase that plays an important role in cellular stress response and two isoforms in the liver of *Whsc1*, a histone H3K36 N-methyltransferase (Figure 3.6A). A longer isoform (ENSRNOT00000016121) of *Sgk1* predominates in old brain, whereas a shorter isoform (ENSRNOT00000040736) is equally prevalent in young animals (Figure 3.6B). Comparison of the number of isoform-specific reads suggests that this change is primarily due to a large increase in the levels of the long isoform with age (Figure 3.6C). In liver, the short isoform (ENSRNOT00000050238) of *Whsc1* is more prevalent in young animals compared to the long isoform (ENSRNOT00000021952), whereas in old animals the two isoforms are expressed at similar levels (Figure 3.6B). For *Whsc1*, this is due primarily to an increase in expression of the longer isoform with age, bringing it to

a similar expression level as the short isoform (Figure 3.6C). Our analysis of alternative splicing demonstrates that there are age-related changes in the abundance of specific transcript isoforms with distinct coding potential, which might result in functional proteome diversification in old organs.

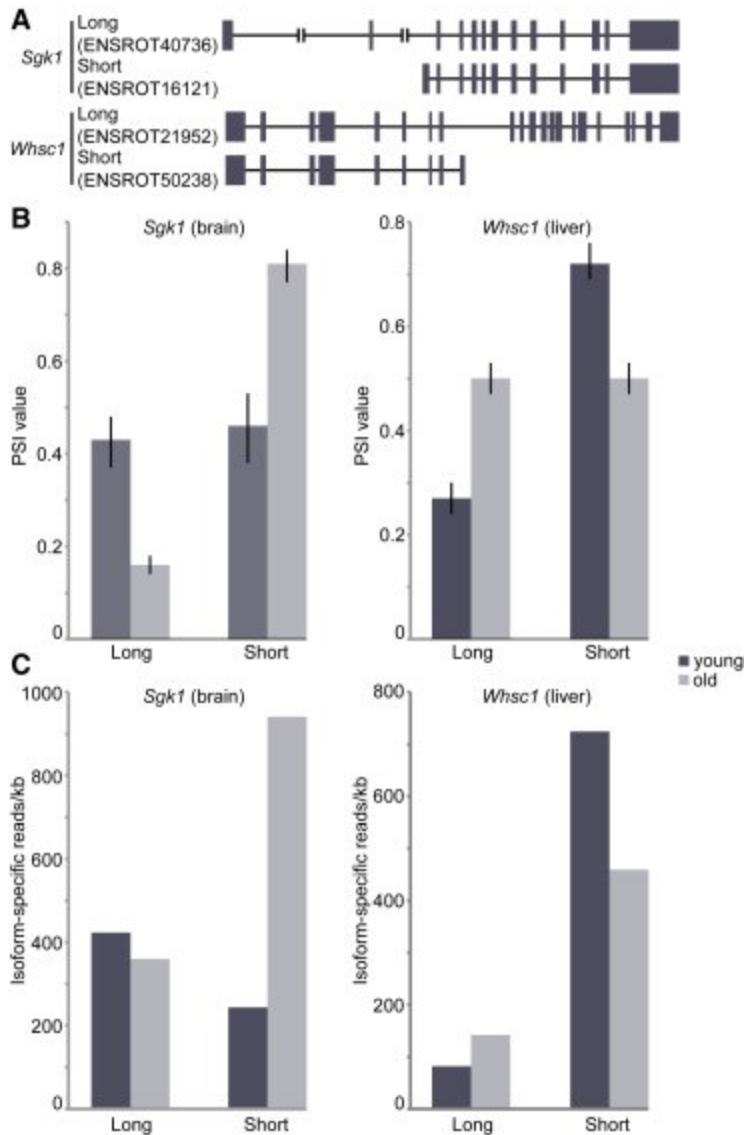


Figure 3.6. Alternative Expression of Splicing Isoforms

(A) *Sgk1* and *Whsc1* each have two isoforms with substantial expression in brain and liver, respectively. The lengths of *Whsc1* introns have been scaled down by a factor of 2 for display purposes.

(B) A comparison of percent spliced-in (PSI) values generated by MISO (Katz et al., 2010) shows a significant difference in isoform expression levels between young and old animals (for each isoform, Bayes factor ≥ 1012). Error bars represent 95% confidence intervals.

(C) Isoform-specific expression (reads per kb, normalized for overall sequencing depth) shows the underlying changes in isoform abundances responsible for differences in PSI values.

See also Figure S3.5.

Discussion

Here, we present an integrated comparison of gene expression, translation, protein abundance, and phosphorylation in organs from young and old rats. Our work expands the list of proteins that are affected by chronological age in mammals. Although some of the functional modules discussed above were previously identified as hallmarks of aging (López-Otín et al., 2013), we identified hundreds of molecular events underlying these processes that were previously unknown to be affected by age. We thus provide a rich resource that should stimulate the generation of new, experimentally testable hypotheses, leading to a better understanding of aging on the organism level.

The comparison of two organs with different physiology and regenerative capacity enabled us to distinguish organ-specific effects from more systemic effects of aging. Intuitively, our results suggest that organ-specific effects of age are tightly linked to the organ function. For example, in brain, multiple alterations of key signaling mediators are observed. We speculate that these alterations might be part of a progressive functional deterioration that affect the maintenance of neuronal plasticity in old brains (Bading, 2013) and other phenotypes observed the aging brain (Burke and Barnes, 2006). Notably, 45 of the changes that we identified in old rat brains are consistent with a

previous transcriptomics study of aging human brains (Lu et al., 2004) (Figure S3.6), suggesting that age-related changes in the proteome and transcriptome are to some extent conserved from rat to humans.

The systemic impact of chronological age on proteome homeostasis manifests on many levels. In the liver, the majority of age-dependent changes are driven by alteration of transcript abundance (58% of the affected transcripts versus only 25% in brain; Figure 3.1F), suggesting the occurrence of age-related changes in transcriptional regulation. In contrast, the brain appeared to be affected by age largely at the translational level. For example, specifically in aged brain, we observed that the translational output of multiple ribosomal subunits increased (Figure 3.5A); these subunits were also more abundant on the protein level (Figure S3.4). A similar effect of orchestrated ribosomal gene expression was described throughout the lifespan of the short-lived fish *Nothobranchius furzeri* (Baumgart et al., 2014), suggesting that this phenomenon might represent a conserved feature of the aging brain. Conversely, a decreased protein level of multiple factors involved in translation initiation accompanied the increased abundance of ribosomal subunits (Figure 3.5A). Taken together, our data suggest that an age-associated remodeling of the translation machinery in the brain may ultimately lead to alterations of the translation efficiency of a subset of transcripts in old animals. Specifically, we identified 15% of the brain

transcripts to be affected by a change in translation (versus only 2% in liver).

Despite the correlation between translation output and protein abundances, not all the observed changes of protein abundance could be explained by changes in translation output, particularly in brain (Figure 3.4E). This phenomenon strongly indicates a higher degree of post-translational control in the brain as compared to the liver. Indeed, our proteomic analysis revealed that key regulators of protein homeostasis were altered in aged brain, including several components of the ubiquitin-proteasome and autophagy systems (Figure S3.3B). These findings imply that altered protein homeostasis, which has been shown to affect organism longevity under stress-response conditions (Kevei and Hoppe, 2014), also leads to detectable proteomic alterations that occur between young and old animals. The exact consequences and targets of such alterations are likely complex and remain to be explored in detail. In addition, more fine-grained genomic and proteomic investigations at multiple time points across organism life-span are required to shed light on the dynamics and interplay between systemic and organ-specific effects of aging and thus reveal which alterations are causative of, or a result of, aging.

From our measurements performed on the bulk organ lysate, it is impossible to estimate whether the observed changes affect most of the

cells within an organ or whether they originate from a subpopulation of cells that is more prone to the effects of aging or from a change in the proportion between cell types in an organ. Most of the proteomics changes that we describe at the level of both protein abundance and phosphorylation level are quite large (typically >2-fold). It is therefore reasonable to assume that they might affect a major proportion of cells. However, we cannot exclude that events occurring in a minor fraction of cells will be missed by our approach. Higher resolution studies focusing on specific anatomical regions or cell subpopulations will be required to detect more subtle alterations.

Experimental Procedures

Determination of Transcription and Translation Changes

RNA-seq and ribosome profiling libraries were prepared using an Illumina TruSeq kit and standard ribosome profiling protocols (Ingolia et al., 2009 and Ingolia et al., 2012), and sequenced using the Illumina HiSeq platform. The data discussed in this publication have been deposited in NCBI's Gene Expression Omnibus (Edgar et al., 2002) and are accessible through GEO: GSE66715 (<http://www.ncbi.nlm.nih.gov/geo/query/acc.cgi?acc=GSE66715>).

[Two sections from the published work has been removed here (“Tissue Fractionation”, “Determination of Protein and Phosphosite Abundance Changes”), and can be found in “Results from collaborators.”]

Supplemental Experimental Procedures

Determination of transcription and translation changes

Ribosome profiling libraries were prepared as described previously (Toyama et al., 2013). Total RNA libraries were prepared from homogenized tissue using TruSeq stranded kits with RiboZero gold (Illumina). Libraries for both ribosome profiling and total RNA were sequenced using the Illumina HiSeq platform. Mapping of RNA-Seq and ribosome profiling data was performed using TopHat (Trapnell et al., 2009), a splice-aware aligner. For differential expression analysis of ribosome profiling and total RNA sequencing, a generalized linear model (GLM) was constructed using DESeq (Anders and Huber, 2010). This analysis differentiates between specifically transcriptional and translational changes. Individual, highly variable outlier transcripts (colored red in Figure S2) were identified and removed from downstream analysis by testing for excess residual deviation between replicates (209 transcripts for brain and 281 transcripts for liver). Outlier samples were assessed by hierarchical clustering and excluded from dispersion estimates. Significantly affected transcripts were defined using an adjusted p value cut-off of 0.01.

Author Contributions

A.O., B.H.T., M.S.H., N.T.I., M.W.H., and M.B. designed experiments and wrote the manuscript. A.O., B.H.T., M.S.H., and T.B. performed

experiments and analyzed data. M.I. and P.B. designed algorithms for protein complex analysis. M.W.H. and M.B. oversaw the project.

Acknowledgments

We gratefully acknowledge support from EMBL's Proteomics Core Facility, Centre for Statistical Data Analysis, in particular Dr. Bernd Klaus, and the Centre for Biomolecular Network Analysis, in particular Dr. Matt Rogon. We thank Drs. Oliver Rinner and Lukas Reiter for access to the software SpectroDive (Biognosys AG). A.O. was supported by postdoctoral fellowships from the Alexander von Humboldt foundation and Marie Curie Actions. T.B. was supported by EMBL Interdisciplinary Postdoc Programme (EIPOD) under Marie Curie Actions COFUND. N.T.I. is supported from the Searle Scholars Program (11-SSP-229) and the Paul F. Glenn Center for Aging Research. M.B. acknowledges funding by EMBL.

Accession Numbers

The accession number for the data reported in this paper is GEO: GSE66715 and ProteomeXchange: PXD002467.

Chapter 4: Translational control in the acute glucose response and high-fat diet

Results

Pilot experiment results

To investigate the role of translational control in the acute glucose response and understand how this effect is modified by a chronic high-fat diet, I performed ribosome profiling on liver samples from mice given a high-fat or normal-chow diet for one week, and a controlled dose of either glucose or water. This 2-factor design allows for analysis of changes associated with both glucose and high-fat diet alone, as well as the effect of high-fat diet on the glucose response. A time period of one week was chosen for high-fat diet to concentrate on the early changes associated with the diet (Andrikopoulos et al., 2008). Tissues were collected 20 minutes following glucose administration, a time point near the peak of blood glucose and insulin levels (Andrikopoulos et al., 2008).

The change caused by high-fat diet was associated with many significant changes in gene expression (Figure 4.1A). Because no matched RNA-Seq is available, these data reflect changes in transcription, mRNA processing, degradation, and translation. A gene ontology analysis identified several categories of transcripts that were up- or down-regulated (Figure 4.1D). These include repression of lipid and small-molecule metabolic processes, as well as induction of sulfotransferase activity and membrane and extracellular components.

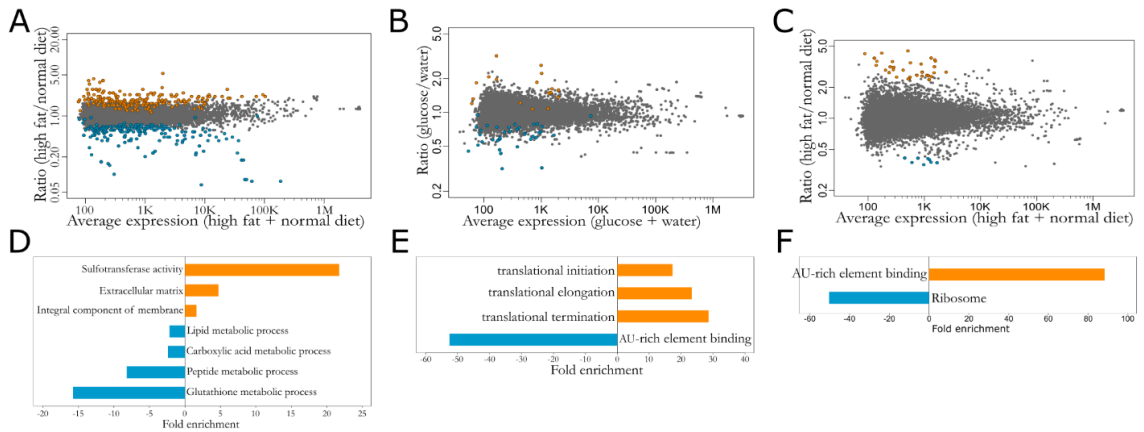


Figure 4.1. Results from pilot experiment

(A-C) MA-plots showing fold change of individual transcripts in high-fat vs. normal diet (A), glucose vs. no glucose (B), or glucose in high-fat vs. glucose in normal diet (C). Significant changes ($p < 0.01$) are marked in blue (down) or orange (up). (D-F) Significantly up- or down-regulated GO categories in high-fat vs. normal diet (D), glucose vs. no glucose (E), or glucose in high-fat vs. glucose in normal diet (F). For all GO categories shown, $p < 0.01$.

Analysis of changes associated with glucose response also revealed several significant changes in individual transcript levels (Figure 4.1B). Due to the short time frame used in this experiment (20 minutes) it is unlikely that these changes are a result of changes in transcription or

RNA processing. While some down-regulation could be the result of rapid mRNA degradation, up-regulation is almost certainly the result of translational changes. Gene ontology analysis suggests that translational components are strongly up-regulated, while AU-rich element binding proteins are down-regulated. The up-regulation of translation factors, which includes many ribosomal proteins, is likely a result of mTOR activation (Laplante et al. 2012).

The final and most informative analysis of these data is assessing how the glucose response changes with the addition of high-fat diet. There are many differences between the glucose response of high-fat fed animals and normal animals at the transcript level (Figure 4.1C). Gene ontology suggests that many of these changes are simply the loss of the normal glucose response (Figure 4.1F). While this pilot study yielded informative and encouraging results, this experiment had a few flaws including limited replicates (2 animals for each condition, but only 1 for high-fat, no glucose), limited time points for glucose response, and lack of additional data (e.g. weights of animals, blood glucose levels).

Based on these promising results, I decided to follow this experiment with a similar, yet larger-scale experiment to more fully understand these responses. The follow-up experiment was designed to address the shortcomings of the original study by including 4 replicates for each condition, three time points for glucose response (10, 20, and 30

minutes), and physiological measurements such as animal weight while on the diet and glucose levels at the time of tissue collection.

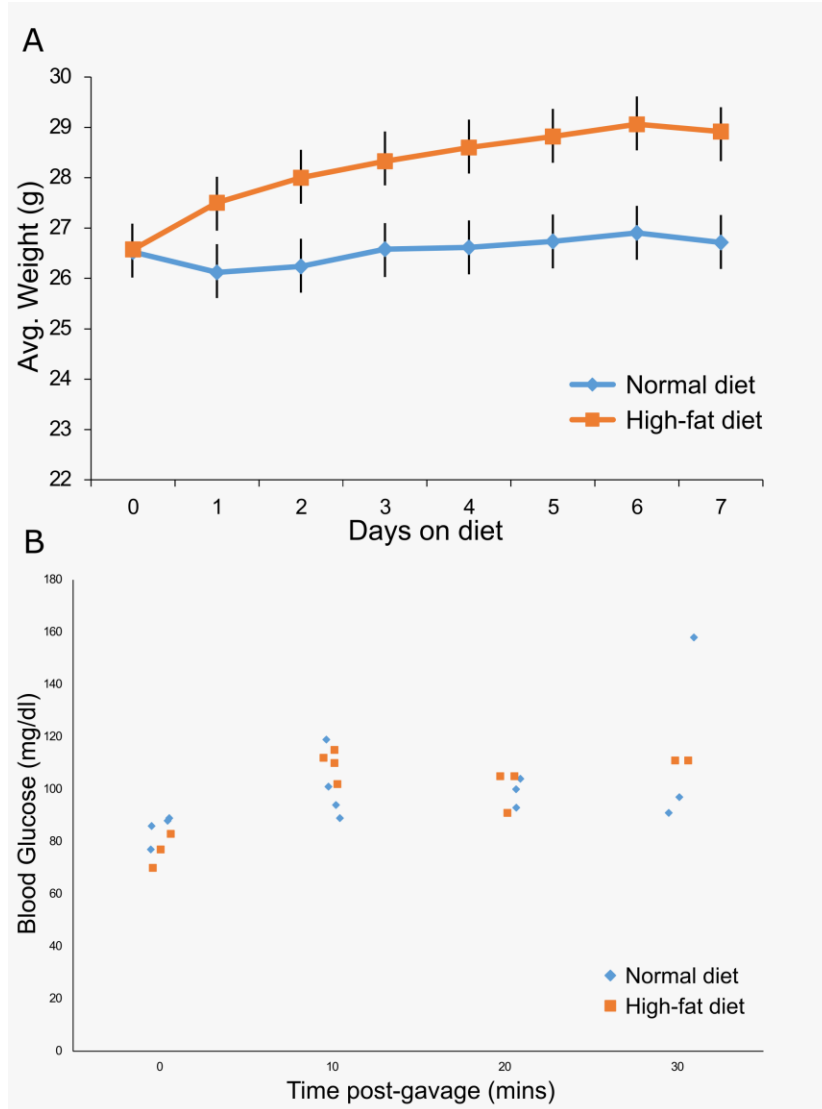


Figure 4.2. Weights and blood glucose levels

(A) Average weights for high-fat and normal diet animals over the week. Error bars represent 95% confidence intervals.

(B) Blood glucose levels for all animals used in ribosome profiling analysis.

Weights and blood glucose levels

The high-fat diet induced significant and substantial weight gain relative to the normal diet (almost 10% over the course of one week). All mice

used in the experiment were weighed each day while on the experimental diet. At day 0, all animals weighed approximately 26.5g, and there was no significant difference between animals receiving high-fat or low-fat diets (Figure 4.2A; $p \gg 0.05$). After 6-7 days however, animals on the high-fat diet had gained significantly more weight than those on the low-fat diet (Figure 4.2A; $p < 0.01$). High-fat fed animals were now about 2.5g heavier than low-fat fed animals, on average. A small decrease in weight can be seen in both populations on day 7, when animals had already been fasted for several hours in preparation for glucose administration and tissue collection.

As expected, blood glucose levels were higher in animals given glucose (Figure 4.2B). Very little difference could be seen between early or late time points, or between normal and high-fat glucose levels. This is perhaps unsurprising as one week is a relatively short exposure to the high-fat diet. A few samples were removed from further analysis based on their blood glucose measurements. One control and two high-fat glucose animals were identified as outliers based on measuring the median \pm interquartile range (IQR) for plus or minus glucose populations (Figure S4.1A). Two additional low-fat glucose animals were removed due to having glucose levels in the range of control animals, suggesting a problem with their glucose administration (Figure S4.1A). These animals also stood out in a correlation matrix of all samples, likely a result of low

sequencing coverage due to under-representation in multiplexing pools (Figure S4.1B).

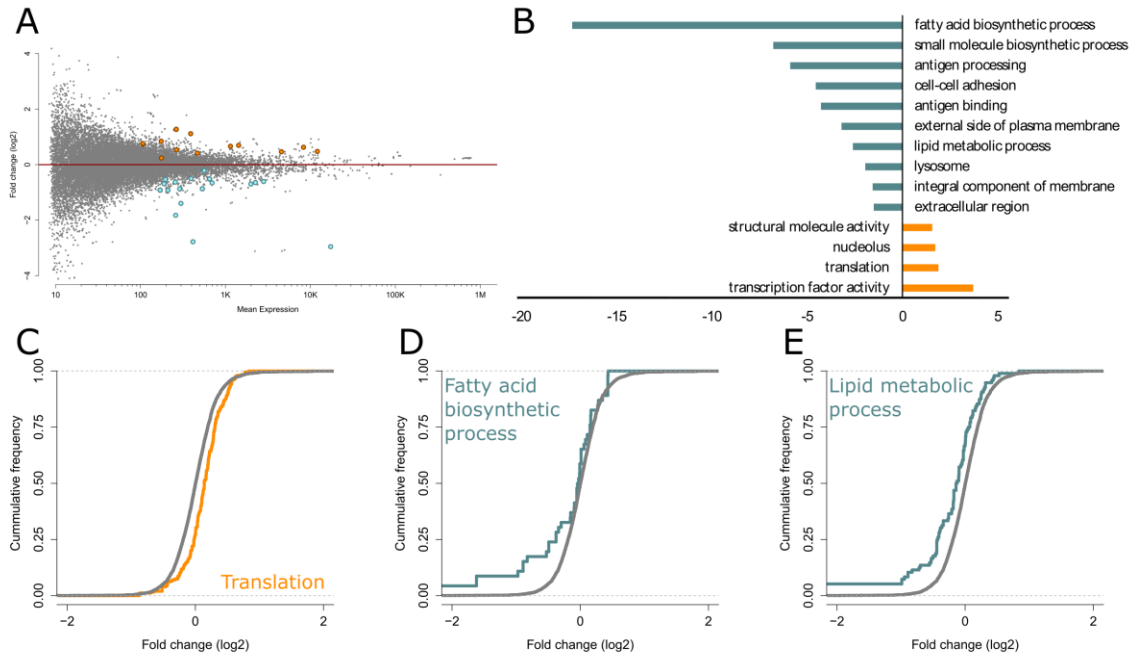


Figure 4.3. High-fat diet response

(A) MA-plot showing fold change of individual transcripts in high-fat vs. normal diet. Significant changes ($p < 0.05$) are highlighted in blue (down) or orange (up).

(B) Significantly up- or down-regulated GO categories in high-fat vs. normal diet ($p < 0.01$).

(C-E) Cumulative distribution functions (CDFs) of fold change for all transcripts (gray) and transcripts associated with the indicated GO term (colored) in high-fat vs. normal diet.

High-fat diet response

Several changes in individual transcript levels could be identified in response to high-fat diet (Figure 4.3A). As before, these changes are the combined effects of all the steps in protein expression, from mRNA transcription through translation. Most striking is the strong down-

regulation of a number of the Scd genes, which are involved in processing lipids in the ER (Hulver et al. 2005). Interestingly, SCD1 has been found to be up-regulated in muscle of obese humans (Hulver et al., 2005). A gene ontology analysis of changes resulting from high-fat diet suggests a number of broader changes (Figure 4.3B). Translation is moderately up-regulated, a change which was not seen in the earlier experiment. This change appears to be driven by small shifts in the expression of a large portion of the associated transcripts (Figure 4.3C). In contrast, down-regulation of both fatty acid biosynthetic processes and lipid metabolic processes appear to be driven largely by large changes in a select number of associated transcripts (Figures 4.3D-E). These include the Scd genes, along with other less dramatic changes.

Glucose response in normal and high-fat diets

Broader gene expression programs can be detected by gene ontology, in spite of the limited changes seen in individual transcripts. Analysis of the glucose response in normal diet identified only a single significant change at 20 minutes, down-regulation of SH2B1 (Figure 4.4A). SH2B1 is also significantly down-regulated at 30 minutes, but not at 10 minutes (Figures S4.2A-B). Capable of binding to insulin receptors, SH2B1 plays a role in activation of the insulin response (Rui, 2014). Down-regulation of SH2B1 in response to glucose may be a feedback mechanism intended to return the cell to a normal state. No individual transcripts were

significantly different between the high-fat and normal glucose responses (Figure 4.4B). Looking at all transcripts with a log₂ fold change of at least 0.5 regardless of significance, a number of patterns can be seen between time points (Figure 4.4C). First, there is a subset of transcripts not strongly up-regulated until 20 minutes. An additional group is up-regulated at 10 and 20 minutes, but less changed at 30 minutes. Lastly, a small group of transcripts is down-regulated strongly at 10 minutes, but less so at 20 and 30 minutes. The change in glucose response due to high-fat diet is relatively consistent across time points, although there is variation (Figure 4.4D).

Gene ontology on a ranked list of transcripts can extract biological insight despite the lack of significant changes on the individual transcript level. This analysis suggests a number of changes in response to glucose, and several modifications to the glucose response as a result of high-fat diet (Figures 4.5A-B). As seen in the smaller experiment, translation is significantly up-regulated in response to glucose, and this up-regulation is lost or lessened in high-fat fed animals. As in the high-fat response, this change appears to be driven by a relatively modest change in most associated transcripts (Figures 4.5C, D). The up-regulation of translation in response to glucose appears to be much stronger than in response to high-fat (Figures 4.3C, 4.5C). Another change in response to glucose is a down-regulation of lipid metabolic processes. This change is also reversed in high-fat fed animals. As with

the high-fat response, change in expression of lipid metabolic associated transcripts seems to be primarily driven by change in a smaller number of transcripts (Figures 4.5E-F). In contrast to the up-regulation of translation, down-regulation of lipid metabolic processes seems to be weaker in glucose response than high-fat response (Figures 4.3E, 4.4E). A small number of transcripts associated with adherens junctions also seems to be up-regulated in response to glucose, but not in high-fat animals.

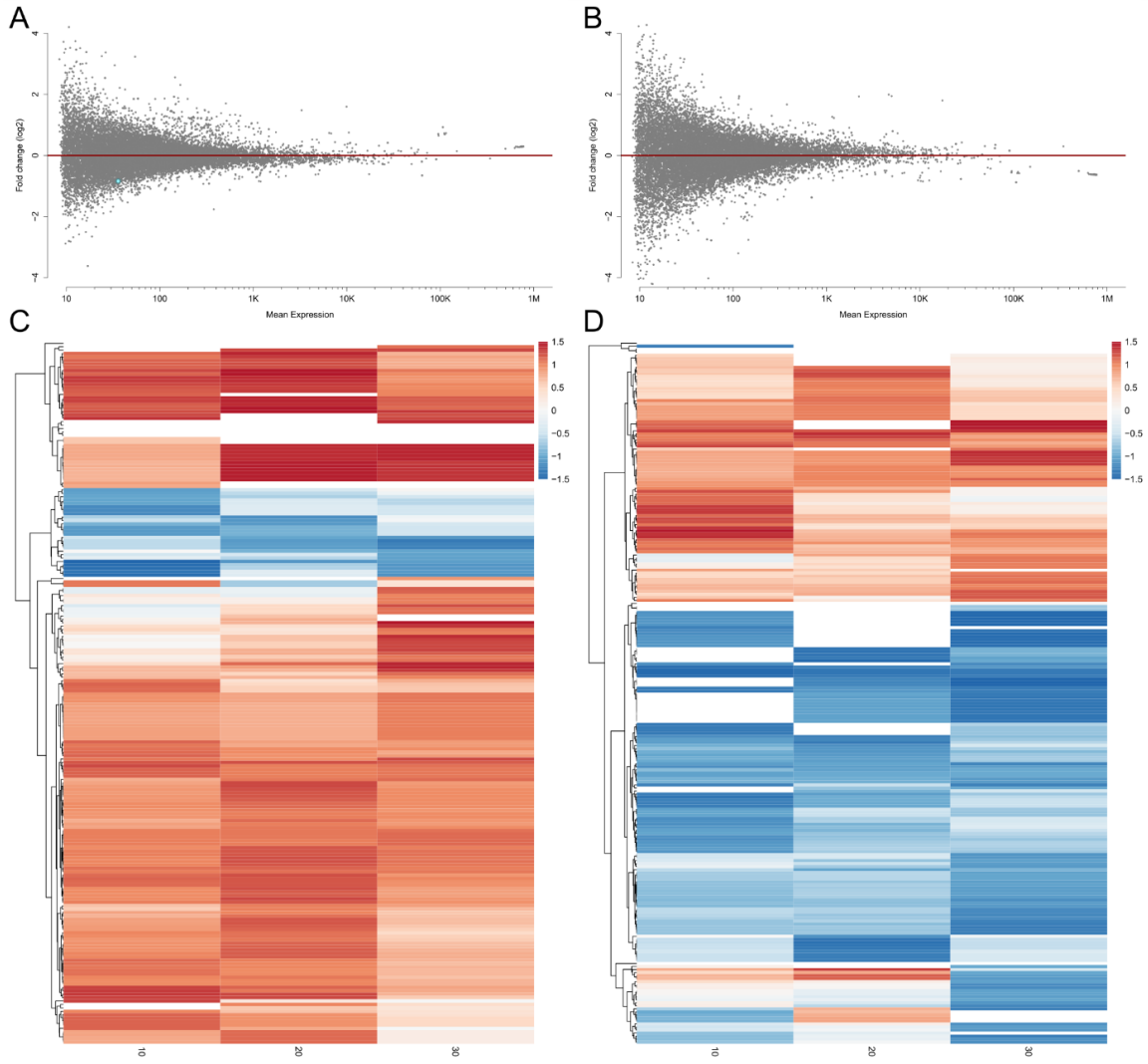


Figure 4.4. Glucose response in normal and high-fat diet

(A-B) MA-plots showing fold change of individual transcripts in glucose vs. no glucose (A), or glucose in high-fat vs. glucose in normal diet (B) at 20 minutes. Significant changes ($p < 0.05$) are marked in blue (down) or orange (up).

(C-D) Heatmap showing fold change of individual transcripts across time points in glucose vs. no glucose (C), or glucose in high-fat vs. glucose in normal diet (D). Only transcripts with at least 0.5 fold change at one time point and mean expression of at least 100 are shown.

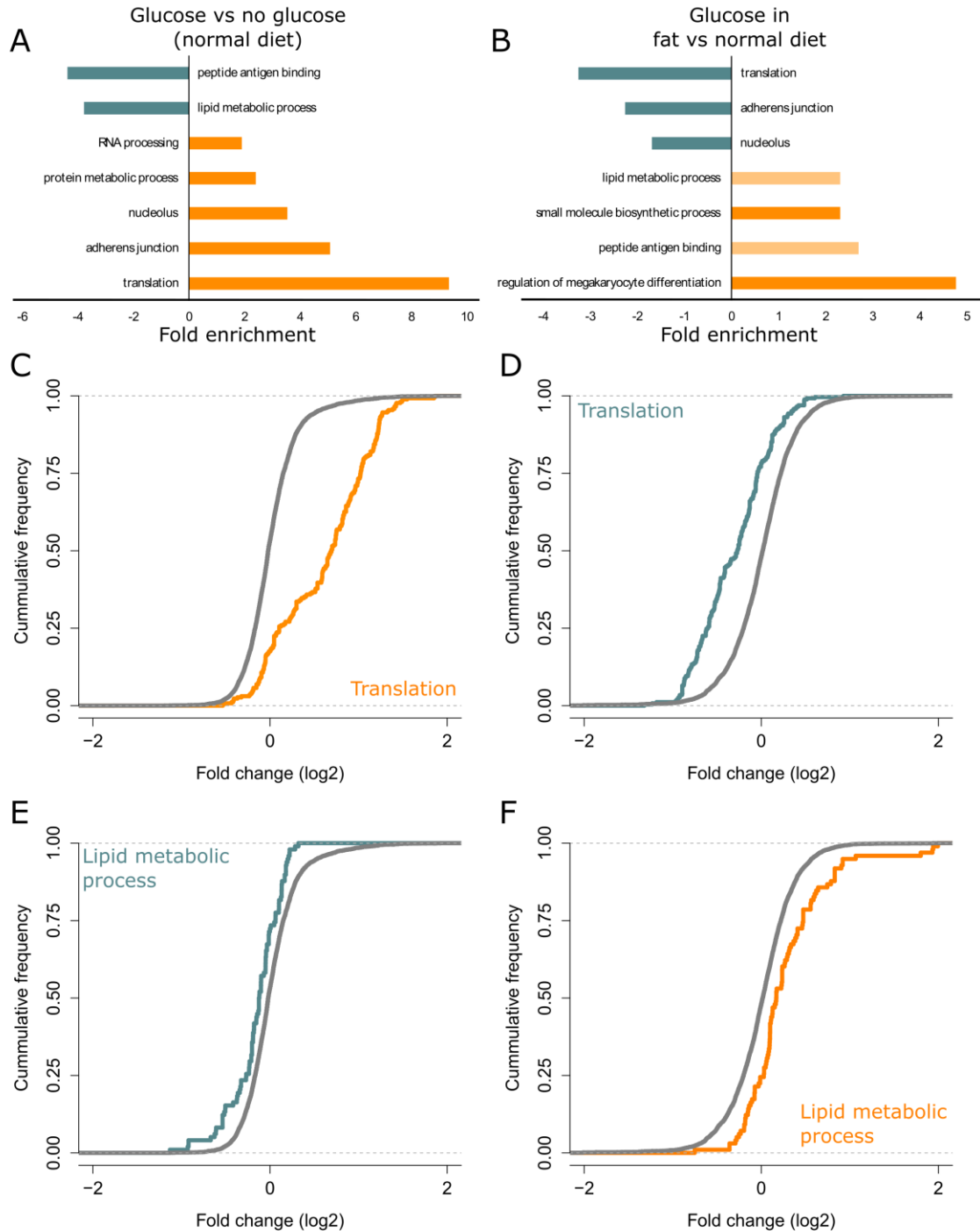


Figure 4.5. Gene ontology analysis of glucose response

(A-B) Significantly up- or down-regulated GO categories in glucose vs. no glucose (A), or glucose in high-fat vs. glucose in normal diet (B) at 20 minutes. $p < 0.01$ for non-faded bars, $0.01 < p < 0.05$ for faded bars.

(C-F) Cumulative distribution functions (CDFs) of fold change for all transcripts (gray) and transcripts associated with the indicated GO term (colored) in glucose vs. no glucose (C,E), or glucose in high-fat vs. glucose in normal diet (D,F).

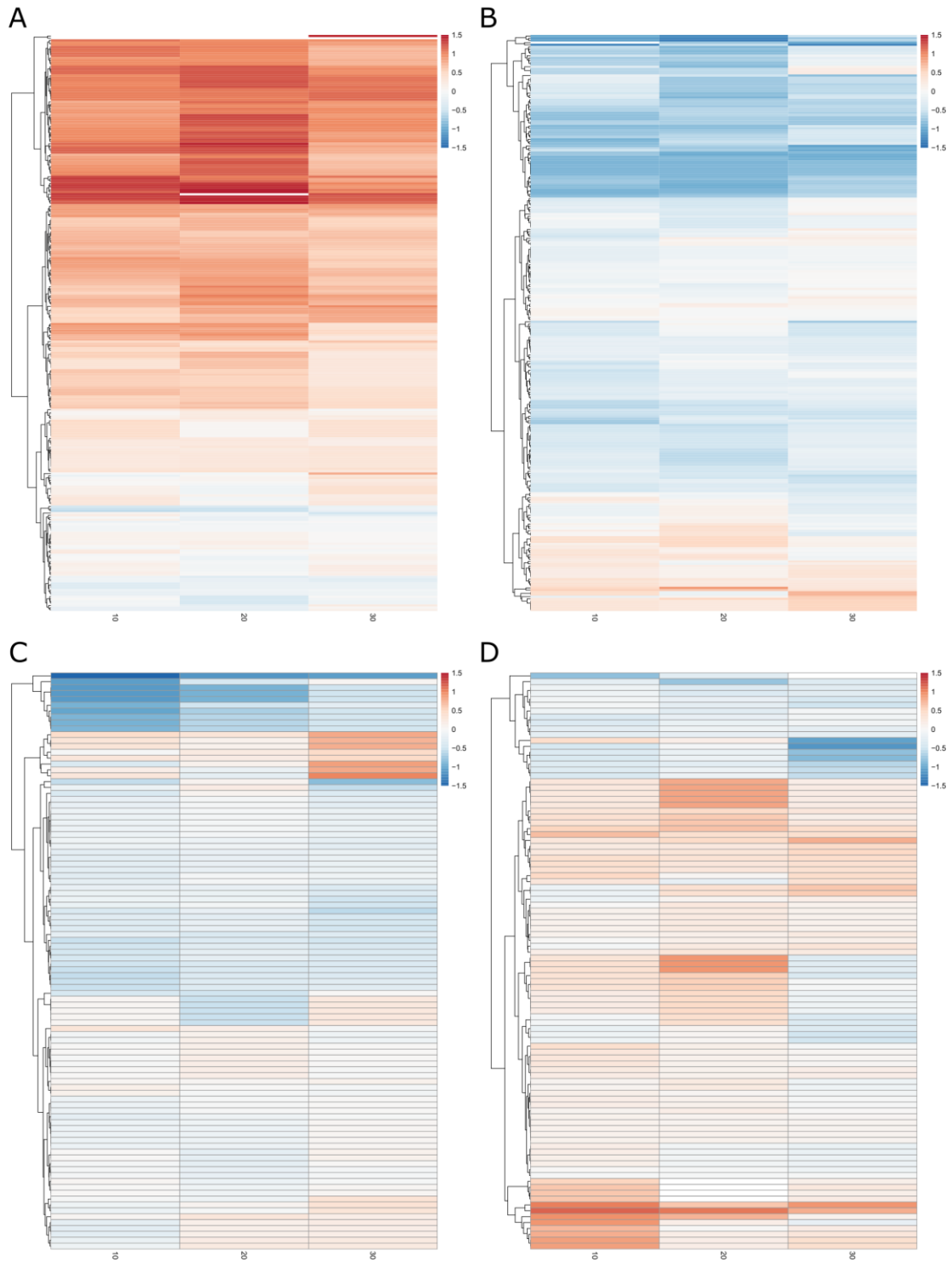


Figure 4.6. Changes in gene ontology categories across time course
 (A-D) Heatmap showing fold change of individual transcripts associated with translation (A-B) or lipid metabolic process (C-D) across time points in glucose vs. no glucose (A,C), or glucose in high-fat vs. glucose in normal diet (B,D).

The time course following glucose administration provides an opportunity to see when these responses occur, and how quickly they dissipate. Changes in transcripts associated with translation peak at 20 minutes, and appear noticeably diminished by 30 minutes (Figure 4.6A). The decrease of this response in high-fat fed animals follows a similar pattern, suggesting a general dampening of the response rather than a delay (Figure 4.6B). The down-regulation of transcripts associated with lipid metabolic processes is strongest at 10 minutes, and tapers off at 20 and 30 minutes (Figure 4.6C). Interestingly, there is a small subset of transcripts that seem to be up-regulated at 30 minutes. The changes in this response between normal and high-fat animals follow a similar pattern, again suggesting a dampened, rather than delayed, response (Figure 4.6D).

Discussion

These data provide a comprehensive view of changes in protein expression in response to high-fat diet and glucose. I have identified changes in both individual transcript levels, as well as coordinated changes in groups of transcripts associated with various biological processes or functions. In addition to characterizing the responses to high-fat diet and glucose, I have also characterized how the glucose response changes in high-fat fed animals.

Many of the changes I have seen here in response to high-fat diet differ from those previously seen in obese mice (Fu et al. 2011). There are a number of factors that may be responsible for these differences. First, the Fu et al. study used leptin-deficient mice rather than high-fat diet. This means that these mice are eating a normal diet, but in vast quantities. This is in contrast to the mice in this study, which were eating an extremely high-fat diet, but presumably in relatively normal quantities (food was provided ad libitum, but there was no noticeable difference in the quantity of food eaten by high-fat fed animals). Second, the Fu et al. study focused on ER associated proteins, so they could not distinguish changes in protein synthesis from relocalization or degradation, whereas my study focuses on expression specifically.

Several changes I have identified in the high-fat and glucose responses are similar in nature, yet differ by degree. For example, up-regulation of translation and down-regulation of lipid metabolism are present in both responses. However, the up-regulation of translation is stronger in response to glucose, while the down-regulation of lipid metabolism is stronger in response to high-fat. This suggests that many of these changes may be primarily driven by general availability of resources. For translational responses especially this would be consistent with current theories in the field, as translation consumes vast amounts of resources and is closely tied to growth.

These data provide clear evidence for the disruption of the translational response to glucose by high-fat diet. Since many of these changes are also present in high-fat diet animals already, it is possible that the loss of regulation is simply a result of an altered basal state limiting the regulation that can occur. If translation factors are already up-regulated, there may be less room for up-regulation in response to glucose. The other logical explanation for the changes in glucose response in high-fat diet is that the abundance of fat directly interferes with the response to glucose. The loss of these translational responses, as well as chronic activation from high-fat diet, is likely to impair the ability of the liver to function properly.

Methods

Animals

All animals used for this study were C57BL/6J obtained from Jackson Laboratory. Mice were maintained on a standard 24hr light cycle. High-fat animals were fed Research Diets diet #D12492, a 60% fat diet. Control animals were switched to Research Diets diet #D12450J, a matched low-fat control diet, simultaneously. Mice were weighed each day before and during the high-fat diet period, at approximately the same time each day. On day 7, food was removed from the cage about 2 hours into the light period, and animals were collected for glucose gavage and tissue collection 6 hours later.

Tissue collection

After euthanizing by cervical dislocation at the indicated time point post-gavage, animals were immediately necropsied. Tissues were rinsed in sterile PBS and immediately flash-frozen in liquid nitrogen. The left lobe of the liver was specifically set aside for profiling, while the remainder was collected for further experiments. The right quadriceps was collected for muscle profiling, and blood was collected from the abdominal cavity after removal of the liver and flash-frozen for blood glucose and insulin measurements.

Ribosome profiling

Ribosome profiling was performed as previously described (Ingolia et al., 2009, Ingolia et al., 2012), using the adaptations described in the “Ribosome profiling of animal tissues” section of this thesis.

Data analysis

Sequencing reads were processed as described previously (Ingolia et al., 2012). Differential expression analysis was performed using DESeq2 likelihood ratio testing (Love et al. 2014). A significance cutoff of $p < 0.05$ was used. Gene ontology analysis was performed using Gorilla using a list of transcripts ranked by fold-change (Eden et al., 2009, Eden et al., 2007). REVIGO was used to identify redundant GO categories, followed

by manual curation to avoid overlapping or misleading categories (Supek et al., 2011).

Blood glucose measurements

Frozen blood was thawed at 37°C, and 5µl was taken for blood glucose measurement using a Clarity Advanced glucose meter (Diagnostic Test Group). The remaining blood was allowed to coagulate for 30 minutes and centrifuged to isolate plasma for insulin tests.

Chapter 5: Conclusion

Translation is a crucial step in the production of active protein, and an energy and resource intensive process. As with other important cellular activities, it is subject to significant regulation. Not only does this prevent resources from being wasted on unnecessary protein production, but it also prevents production of proteins when they are not needed and could be disruptive, and provides a rapid means of responding to external stimuli. Understanding mechanisms of translational regulation is important to inform our general understanding of cellular processes, as well as specific processes such as nutrient response.

Ribosome profiling is a powerful technique for understanding translation and translational regulation. Its adaptation to whole tissues here is important for understanding translational regulation in systems that do not lend themselves to cell culture or yeast models. While the examples studied in this thesis include nutrient response and aging, there are many other systems that could benefit from ribosome profiling of whole tissues. Although not yet incorporated into animals, the ribosome affinity purification method demonstrated here will further expand the systems to which ribosome profiling can be applied to small cell populations in heterogeneous tissues. In cell culture, our ribosome affinity purification has provided key physical evidence for translation outside canonical coding regions.

The application of ribosome profiling, combined with RNA-Seq and protein mass spectrometry, has furthered our understanding of protein expression changes in aging. Many organ-specific changes in protein expression were identified, and a strong correlation was seen between change in translation output and protein levels. Changes in splicing patterns were also seen for several genes using RNA-Seq data. Along with the changes discussed here, this data set is a resource that enhances the understanding of protein production changes in aging for the field as a whole.

Ribosome profiling experiments described here in mouse liver have provided a detailed picture of changes in translation output from short term high-fat diet and the translational response to glucose. While the translational changes in response to high-fat diet and glucose are similar, they appear to have more substantial changes in different areas. While up-regulation of translation factors is stronger in response to glucose, down-regulation of lipid metabolic processes is more pronounced in response to high-fat diet. These data also suggest that much of the normal translational response to glucose is substantially disrupted by high-fat diet, including both up-regulation of translation factors and down-regulation of lipid metabolic processes. The changes identified here can be further studied in cell-culture models to establish the mechanism by which they occur.

Appendix A: Results from collaborators

The following was originally published in Cell Systems on Sept. 13, 2015.

It is published under a creative commons license (CC BY-NC-ND 4.0), and

as such may be reproduced here so long as appropriate credit is given.

These sections of the paper that are not directly related to work performed by the thesis author (Michael Harris), however due to the integrated nature of the work, they are important for establishing the overall impact and results.

Integrated Transcriptome and Proteome Analyses Reveal Organ-Specific Proteome Deterioration in Old Rats

Alessandro Ori^{1, 6, 7}, Brandon H. Toyama^{2, 6}, Michael S. Harris^{3, 4}, Thomas Bock¹, Murat Iskar¹, Peer Bork^{1, 5}, Nicholas T. Ingolia³, Martin W. Hetzer², Martin Beck¹

¹European Molecular Biology Laboratory, Structural and Computational Biology Unit, Meyerhofstrasse 1, Heidelberg 69117, Germany

²Molecular and Cell Biology Laboratory, Salk Institute for Biological Studies, 10010 North Torrey Pines Road, La Jolla, CA 92037, USA

³Department of Molecular and Cell Biology, University of California, Berkeley, Berkeley, CA 94720, USA

⁴Department of Biology, Johns Hopkins University, Baltimore, MD 21218, USA

⁵Max Delbrück Center for Molecular Medicine, Robert-Rössle-Strasse 10, Berlin 13125, Germany

Results

Protein Complexes Are Affected at Multiple Levels

We have previously shown that the composition of the nuclear pore complex (NPC) is altered during aging through the loss of long-lived scaffold components (D'Angelo et al., 2009 and Toyama et al., 2013), affecting its permeability barrier. We wanted to investigate the maintenance of protein complexes more generally and found that the alterations of the proteome that occur between young and old animals affect protein complexes in two different ways.

First, the overall abundance of some protein complexes is different in young and old rat. Consistent with a previous study in mice and worms (Houtkooper et al., 2013), we observed that the abundance of components of the mitochondrial ribosome was lower in old versus young brain (Figure A.1A). This phenomenon was not observed in the liver. However, other protein complexes in liver were similarly affected by age: the abundance of cytosolic proteasomes was higher in old liver versus young (Figure A.1B) and the abundance of NPCs was lower (Figure A.1C). Such changes might result in a reduced functional output and longevity, as in the case of the mitochondrial ribosome (Houtkooper et al., 2013).

Second, a subset of protein complexes undergoes compositional changes in young versus old animals. Using algorithms that we have previously developed (Ori et al., 2013), we identified changes in protein abundance

for specific members of complexes involved in chromatin regulation (e.g., polycomb repressive complex I), RNA processing and transport (e.g., TREX and exon junction complex), and complexes involved in vesicular transport (e.g., COPI, COPII, retromer complex: Figure A.1D). Our data suggests that changes of composition that occur in old animals might cause loss of protein complex function due to complex mis-assembly, as described for the nuclear pore (D'Angelo et al., 2012 and Lessard et al., 2007), or might mediate adaptation of its functionality, for example, under increased stress conditions.

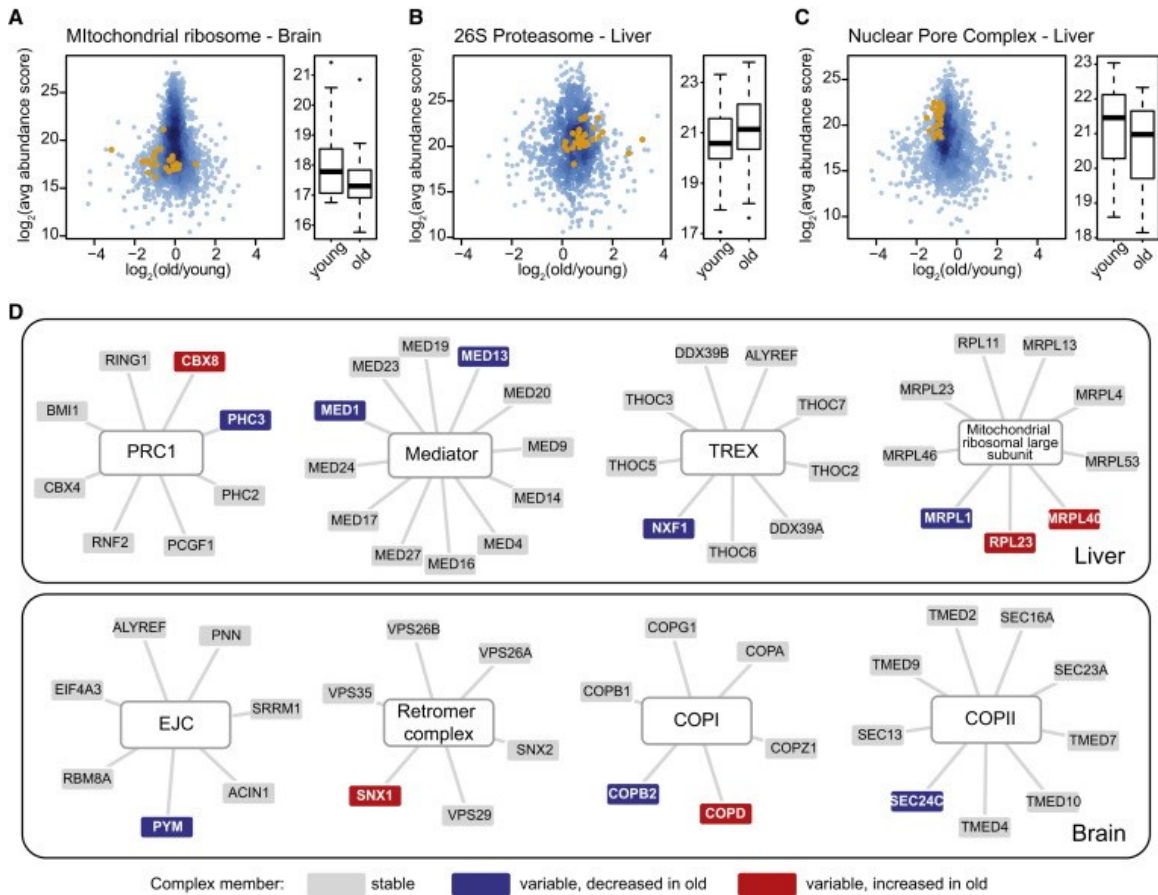


Figure A.1. Proteomic Changes Affect the Abundance and Composition of Protein Complexes

(A–C) We analyzed changes in protein complex abundance using a gene-set enrichment approach (see Supplemental Experimental Procedures). Definitions covering 270 large protein complexes curated from different resources and the literature (A.O., M.I., et al., unpublished data) were used. Only protein complexes that had at least five members quantified were considered. A q value cut-off of 0.1 was used to determine significantly affected protein complexes. All proteins identified in the respective sample are plotted according to their average abundance score and average fold change between young and old animals (both \log_2 -transformed). Positive values indicate higher expression in old animals and negative values indicate higher expression in young animals. Orange dots indicate the identified members of the affected complex. Boxplots show the distribution of abundances of complex members in young and old animals.

(D) Changes in protein abundance affect the composition of several protein complexes in old rats. For each selected example, the quantified complex members are displayed and the significantly affected cases are highlighted in red (indicating increased abundance in old animals) or blue (indicating decreased abundance in old animals). Compositional changes were inferred from protein abundance scores obtained by tandem mass spectrometry as previously described (Ori et al., 2013). A q value cut-off of 0.2 was used to determine significantly affected protein complex members.

Altered Protein Localization

The data integration also revealed exceptions from the overall trend, in which significant changes in protein abundance could not be explained by changes in translation output, particularly in brain (Figure A.2A). These discrepancies point to alternative mechanisms that differentially control protein abundance across age groups, such as protein degradation, or changes in protein localization. In the latter case, the increased abundance of a protein in one compartment might be counterbalanced by a decrease in another, leading to a signal we can observe in our subcellular fractions that would not be detectable by proteomics on total lysates or measurements of translation output. Indeed, we observed opposite abundance changes in different subcellular fractions for nine proteins—seven in brain and two in liver. We interpreted these data as indicative of change in subcellular localization. The potentially relocated proteins include RNA and protein-modifying enzymes, proteins involved in translation, and nuclear transport factors (Figure A.2B). For example, exportin 5, which interacts with NPCs during the export of miRNAs (Lund et al., 2004) and tRNAs (Calado et al., 2002), shows an increased abundance in the cytoplasm of cells from old brains, implying a potential alteration of nuclear transport activity. Two protein kinases—TRAF2- and NCK-interacting kinase (TNIK) and brain-specific kinase (BRSK1, also referred to as SAD-B)—also show proteomic alterations suggestive of subcellular redistribution with no changes in

translation output. Whereas TNIK showed an increased abundance at cytosolic membranes, BRSK1 was less abundant there and more in soluble cytosol of old brains (Figure A.2A). These potential relocalization events highlight an additional level of proteome alteration between young and old animals. Our data, along with the previously described age-related deterioration of the NPC (D'Angelo et al., 2009), suggest a remodeling of the protein and RNA transport machineries that is associated with animal age.

Figure A.2. Changes in Protein Localization and Phosphorylation
(next page)

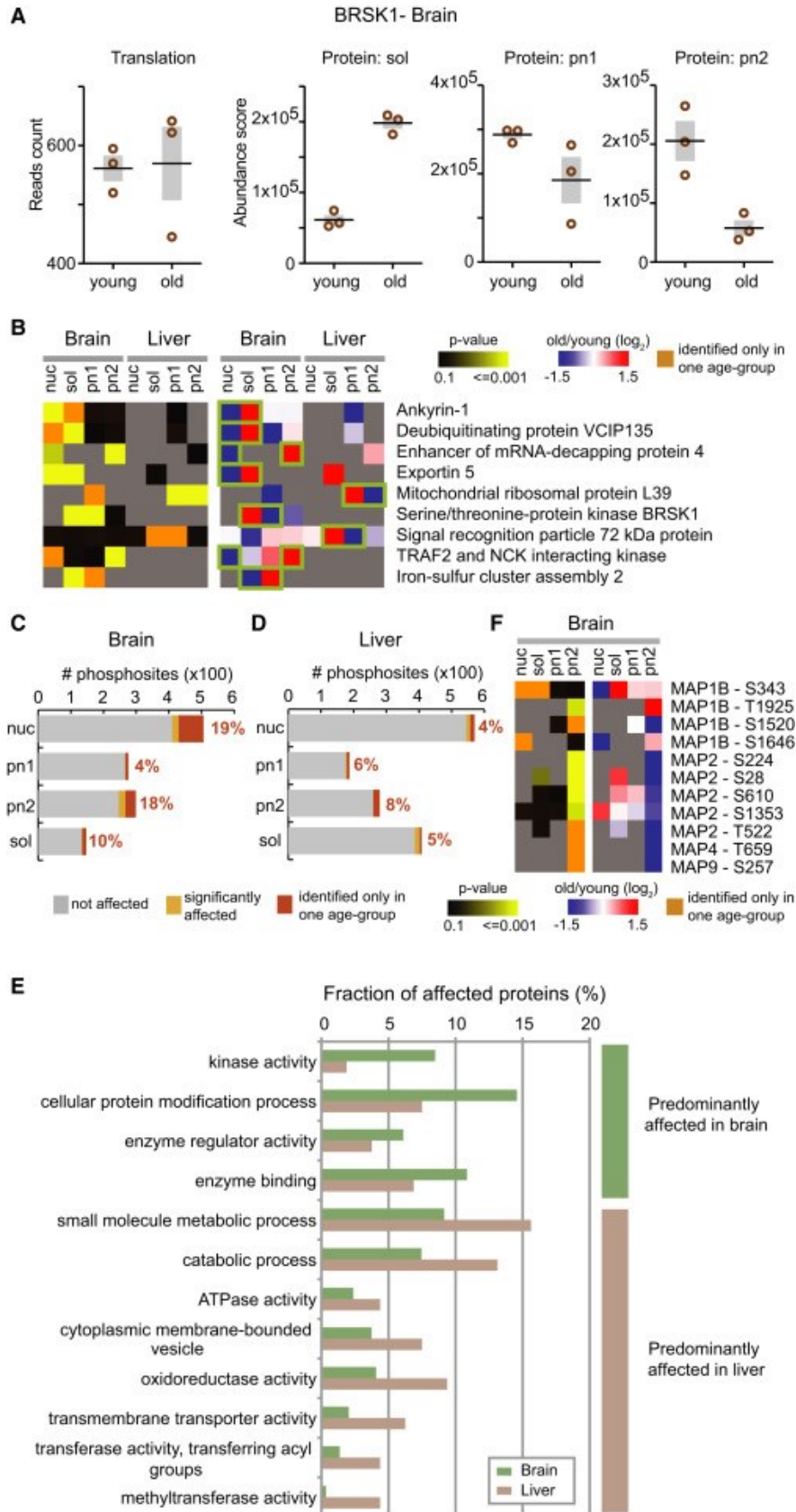
(A) The intracellular distribution of the kinase BRSK1 changes between young and old brain. BRSK1 shows significant changes in protein abundance with opposite signs in two distinct subcellular fractions, whereas it is not affected at the level of translation output.

(B) Another eight proteins display behavior similar to BRSK1, suggesting that their intracellular distribution might change in young versus old animals.

(C and D) Changes in phosphopeptide abundance were assessed by label-free quantification using the same procedure used for protein quantification (q value < 0.1). In addition, phosphopeptides identified exclusively and consistently in one age group but not the other were considered as age-affected (dark orange).

(E) Comparison of functional annotations between affected phosphosites in brain and liver. Affected phosphosites were annotated using the GO slim annotation associated to the corresponding protein group using QuickGO (Binns et al., 2009). Annotations were compared by selecting terms that were at least 1.5 times more frequent among affected phosphosites in one of the two organs. Only the 15 most represented categories per organ were considered.

(F) We identified a decreased level of phosphorylation of several microtubule-associated proteins (MAPS) in membrane fractions that mimics the relocalization of BRSK1 (A). See also Figure SA.1.



Changes in Protein Phosphorylation

Changes in post-translational modifications, such as phosphorylation, have been shown to drive cancer (Krueger and Srivastava, 2006) and a series of developmental processes (Huang and Reichardt, 2001 and Sancho et al., 2004). However, in the context of aging, evidence for alterations of post-translational modifications remain largely anecdotal. We identified several kinases that are differentially expressed between young and old animals, particularly in the brain (Figure S3.3A). In total, we found perturbations in the levels of 12 protein kinases belonging to different families. These include the major kinases that control cell growth, neuronal morphogenesis and plasticity such as the beta-adrenergic receptor kinase 1, the calcium/calmodulin-dependent protein kinases (CAMK) types I and IV, the cyclin-dependent kinases 5 and 19, and the serine/threonine-protein kinase mTOR (Figure S3.3A).

We next tested whether these changes in kinase levels impact downstream target phosphorylation levels by performing a phosphoproteomic analysis of all subcellular fractions, tissues, and age groups described above. Similarly to the protein abundance measurements, we observed high reproducibility between technical replicates (on average Pearson's $r = 0.957$; Figure S A.1A), lower correlation values across age groups as compared to samples from the same age group (Figure S A.1B), and median coefficient of variation $\sim 25\%$ (Figure S A.1C). Across all four

subcellular fractions and two organs, we made 2,497 comparisons of phosphosite abundance, covering 1,437 unique phosphosites, of which 75 (occurring on 68 proteins) were found to change significantly (q value < 0.1 ; Figures A.2C-D). In addition, we found 168 phosphosites (on 160 proteins) that were uniquely and consistently identified in all the replicates of one age group but not the other. For 136 affected phosphosites, we covered both changes in protein abundance and phosphorylation state on the same set of samples and thus could infer changes in the fraction of protein molecules phosphorylated (Figure S A.1D). In 19 out of the 136 phosphosites both the protein and phosphosite level changed in the same organ and subcellular fraction. In 17 of these 19 cases the fold changes were consistent (Figure SA.1E), implying that the phosphorylation state of the protein is not changed. In contrast, 2 of the 19 phosphosites had opposing fold changes, and the remaining 117 phosphosites had not-affected protein abundances while phosphosite level changed. The latter two scenarios are indicative of an alteration of the fraction of protein molecules phosphorylated (Figure SA.1D).

In liver, we found effects on the phosphorylation of proteins involved in metabolic processes and energy production, similarly to the biological processes impacted at the protein abundance level (Figure A.2E).

However, we also identified several altered phosphosites in transcriptional regulators, including c-JUN and FOXA1, as well as

proteins involved in stress responses and homeostatic processes. Similarly to the observed protein abundances, a larger fraction of phosphosites changed in brain as compared to the liver, which is consistent with the large number of protein kinases affected in brain. In addition to those kinases affected at the protein level, we also found changes in phosphorylation of a different subset of kinases, possibly because their activity is regulated through their phosphorylation status. Interestingly, the affected phosphosites were not equally distributed between cell compartments of brain, but primarily identified in membrane (pn2) and nuclear fractions (Figures A.2C and A.2D). A very prominent fraction of altered phosphosites was detected in cytoskeletal proteins (mostly in pn2), in particular in multiple microtubule-associated proteins (MAPS) (Figure A.2F). We speculate that this observation is related to the above-discussed redistribution of BRSK1 kinase away from membranes in old brain (Figure A.2A). BRSK1 is known to associate with synaptic vesicles (Inoue et al., 2006) and it is required to control the polarization of neurons (Kishi et al., 2005) through a mechanism that ultimately leads to the phosphorylation of MAPS (Barnes et al., 2007). While this specific hypothesis remains to be tested, the overall dataset suggests that altered protein phosphorylation and localization might have important physiological outcomes in old animals.

Experimental Procedures

Tissue Fractionation

Liver and brain were harvested from three Fischer 344 rats for each age group. Nuclei were purified according to previously described protocols (Blobel and Potter, 1966 and Lovtrup-Rein and McEwen, 1966). Further fractionation was based on previous descriptions (Toyama et al., 2013).

Determination of Protein and Phosphosite Abundance Changes

Proteins from subcellular fractions were solubilized and digested into peptides as described in Ori et al. (2014). For phosphoproteome analysis, phosphopeptides were isolated from peptide mixtures by TiO₂-based affinity enrichment using the Titansphere Phos-TiO Kit (MZ Analysentechnik) as described in Bui et al. (2013). All samples were measured by shotgun mass spectrometry (see Supplemental Experimental Procedures). The mass spectrometry proteomics data have been deposited to the ProteomeXchange Consortium (<http://proteomecentral.proteomexchange.org>) (Vizcaíno et al., 2014) via the PRIDE partner repository (Vizcaíno et al., 2013) with the dataset identifier PXD002467.

Appendix B: Supplemental figures

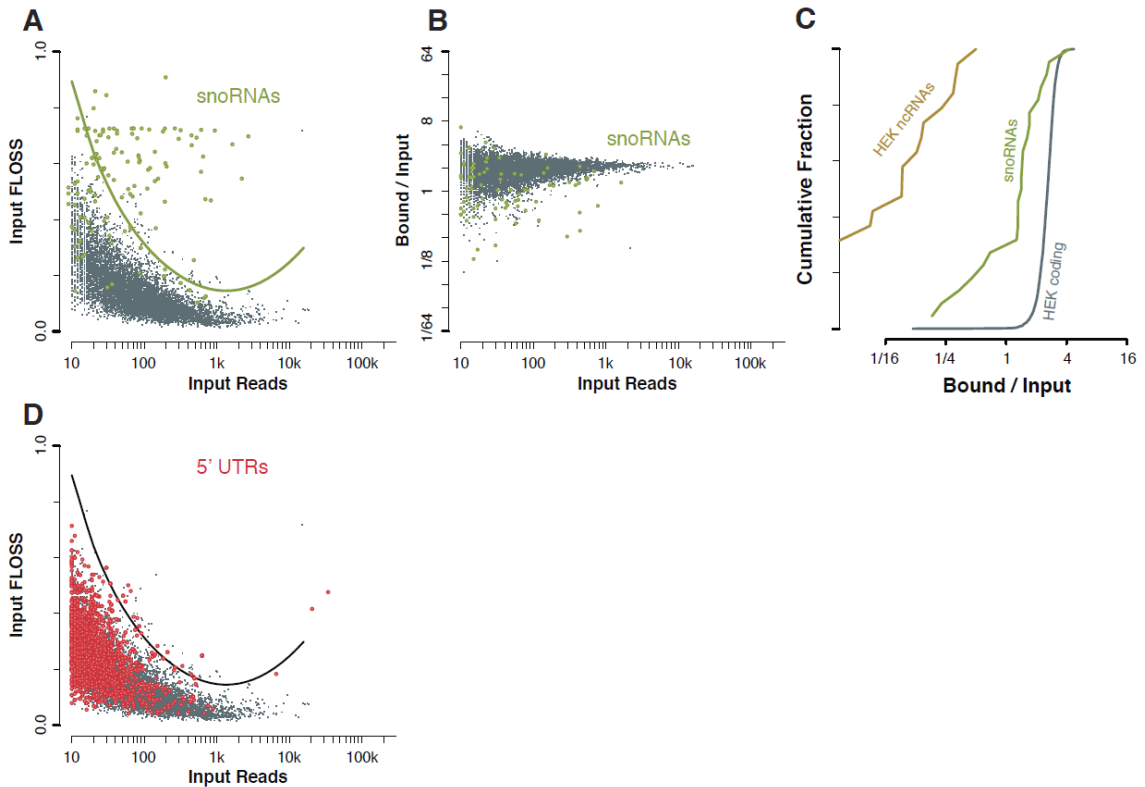


Figure S2.1. FLOSS analysis detects snoRNA-derived background that co-purifies with the ribosome.

(A) FLOSS analysis distinguishes snoRNA-derived background from true ribosome footprints.

(B, C) SnoRNAs are substantially retained during ribosome affinity purification.

(D) FLOSS analysis confirms that nearly all 5' UTRs resemble coding sequences in total HEK cell ribosome profiling.

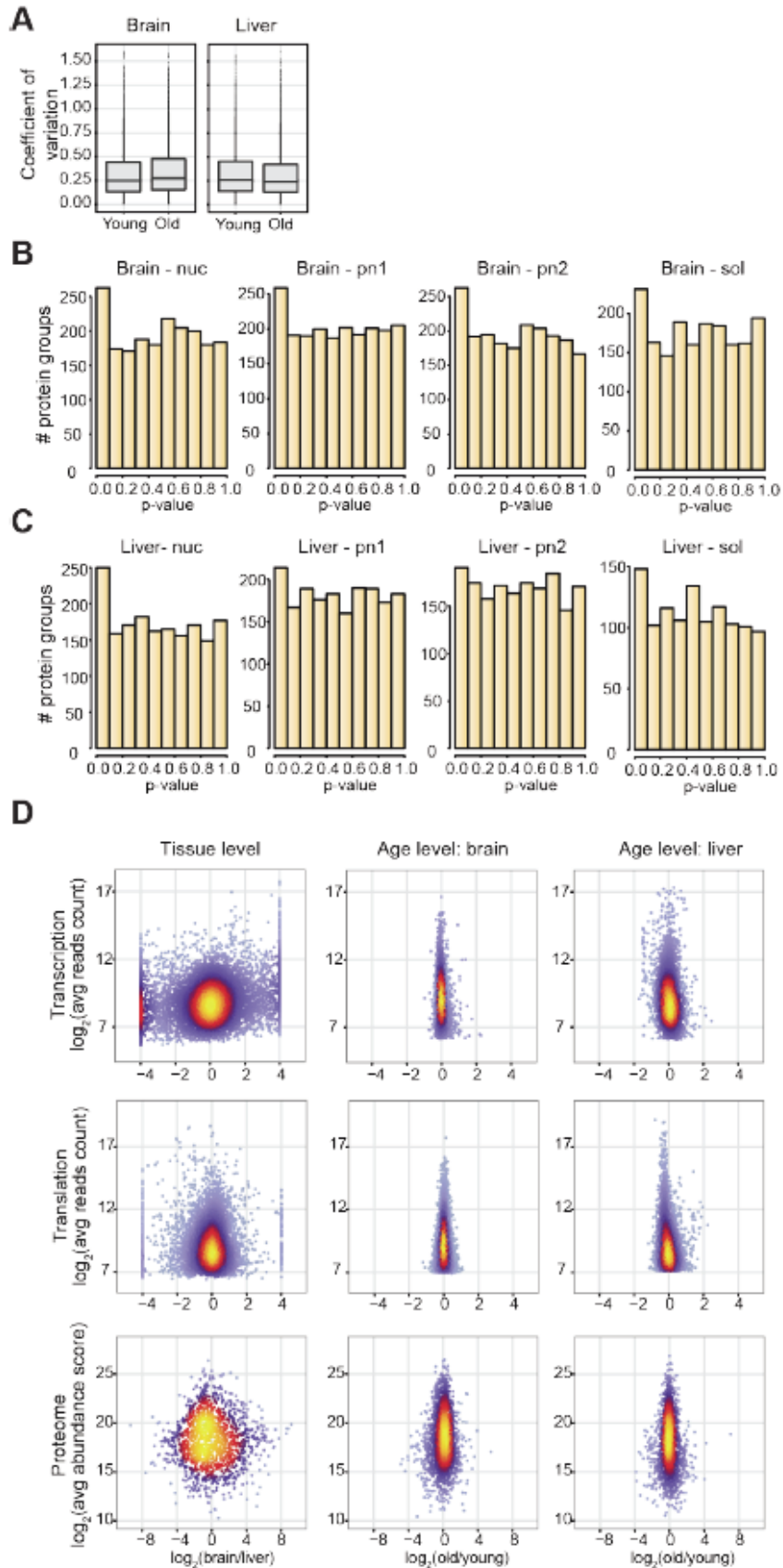
Figure S3.1. Reproducibility of proteomic measurements and variation of protein abundances between animals of different age.

(next page)

(A) Coefficients of variation (standard deviation / mean calculated on raw protein abundance scores) between animals of the same age were computed for all the protein groups quantified across subcellular fractions. The low coefficients of variation indicate minimal within-age-group variation in protein abundance both in brain and liver.

(B and C) Distribution of p values for all the subcellular fractions analyzed. The enrichment of protein groups having low p values (< 0.1) indicates deviation from the null-hypothesis (i.e. presence of proteins that vary in abundance between young and old animals). As discussed in the manuscript, brain samples are generally more affected than liver one. P values were calculated using fdrtool (Strimmer, 2008) from the t-statistics computed by limma (Smyth et al 2005).

(D) Molecular alterations during physiological aging are mild. The effect of aging at the level of transcription, translation output and protein abundance is compared to differences between the two organs. Age-related changes are characterized by small effect sizes and they affect a limited number of transcripts and proteins. For proteomic data, the comparison of the nuclear fractions is shown as a representative example.



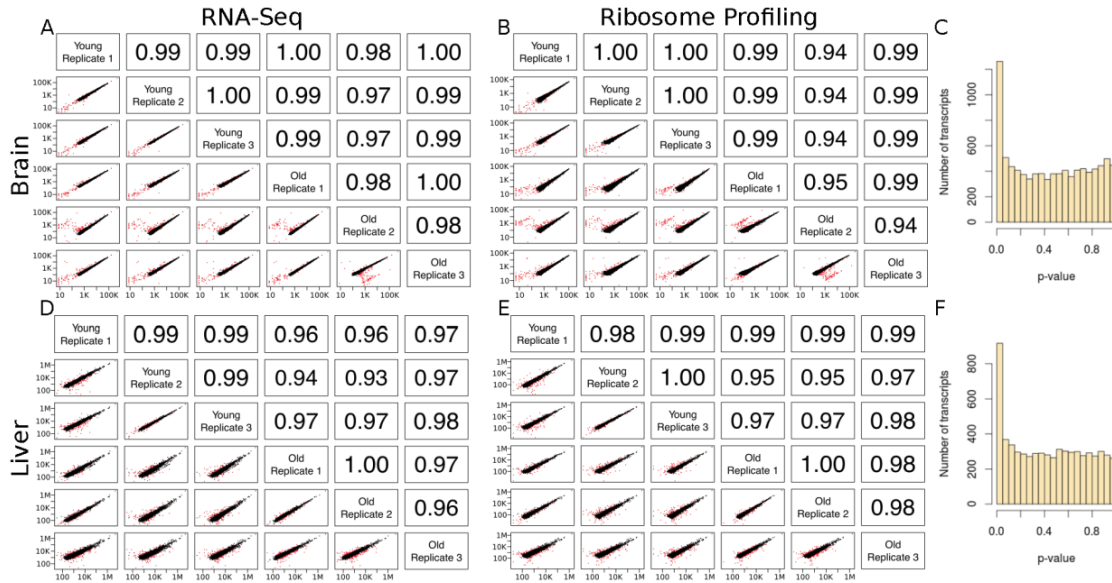


Figure S3.2. Replicate samples of RNA-Seq and Ribosome Profiling are consistent.

(A-B, D-E) Pairwise scatterplots and Pearson correlations are given for RNA-Seq (A, D) and Ribosome Profiling (B, E) counts. Samples from different animals show high correlation in both measurements for both tissues. Points in red were filtered from final analysis due to high dispersion.

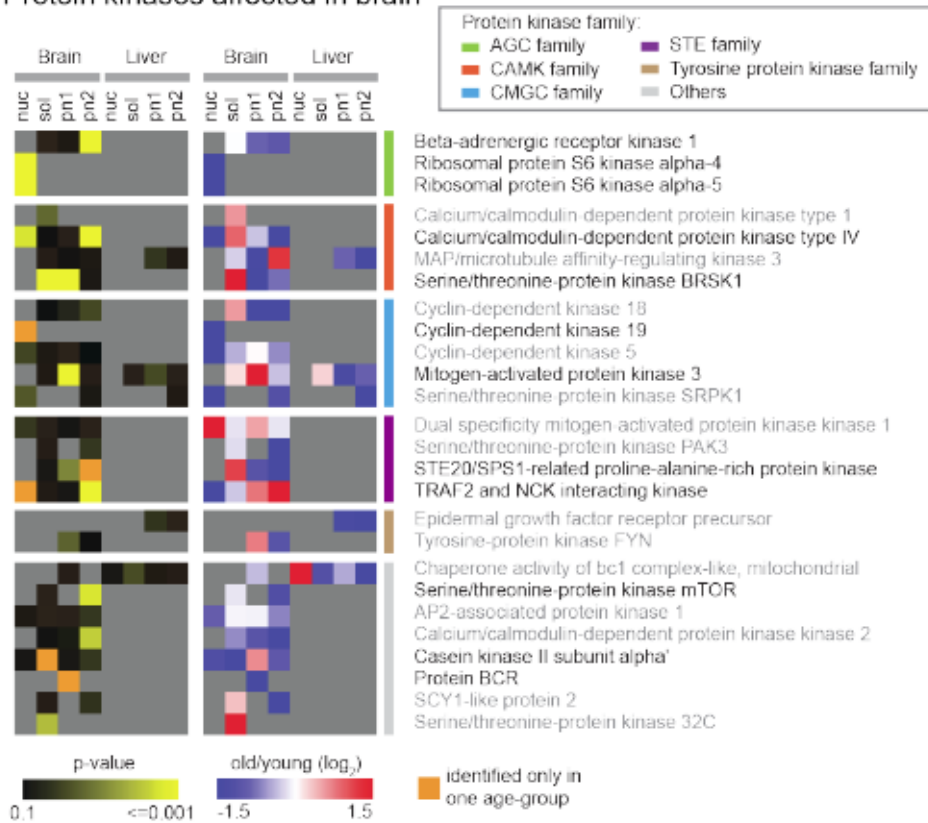
(C, F) Distribution of p values for translation output in brain (C) and liver (F). Enrichment of low p values indicates statistically significant changes.

Figure S3.3. Protein kinases and members of the ubiquitin-proteasome system and autophagy are affected between young and old animals. (next page)

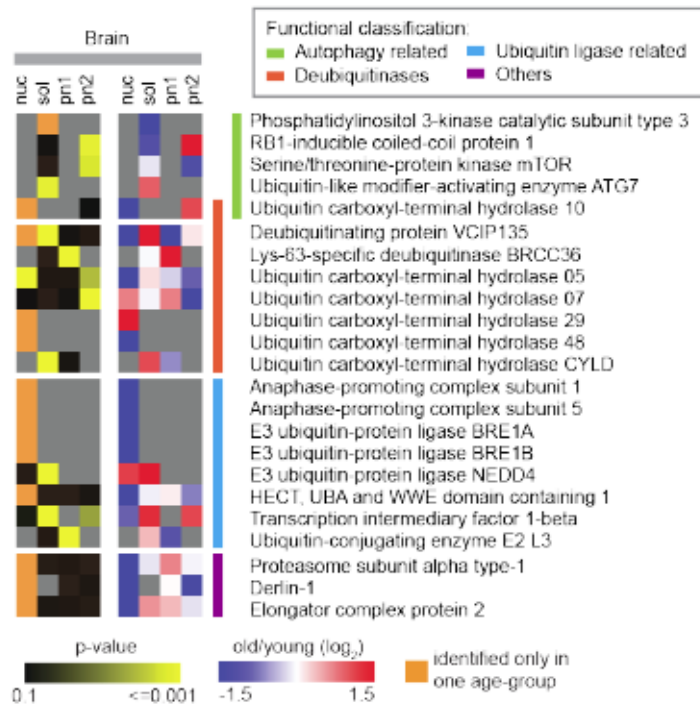
(A) Kinases are grouped in families as classified in UniProt (UniProt Consortium, 2009). The names of twelve significantly affected cases (q value < 0.1) are indicated in black font, while the names of additional 14 kinases that showed a strong trend (p value < 0.05) but did not raise to significant level (q value > 0.1) are indicated in gray font.

(B) Several proteins functionally related to the ubiquitin proteasome system and autophagy change abundance in brain from old animals. Proteins are grouped according to their functional classification.

A Protein kinases affected in brain



B Proteins of the ubiquitin-proteasome system and autophagy affected in brain



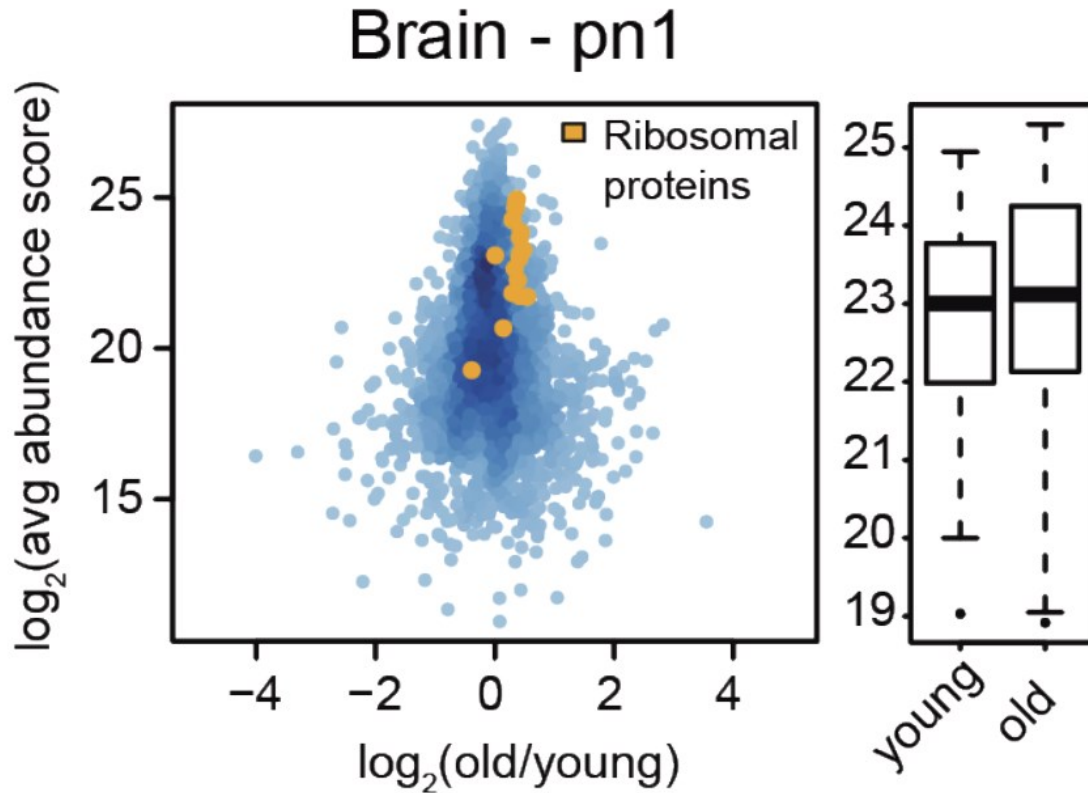


Figure S3.4. Increased abundance of ribosomal proteins in old brain. All proteins identified in the pn2 fraction of brain are plotted according to their average abundance score and average fold change between young and old animals (both \log_2 -transformed). Positive values indicate higher expression in old animals and negative values indicate higher expression in young animals. Orange dots indicate the identified members of the cytosolic ribosome. Boxplots show the distribution of abundances of ribosomal proteins in young and old animals.

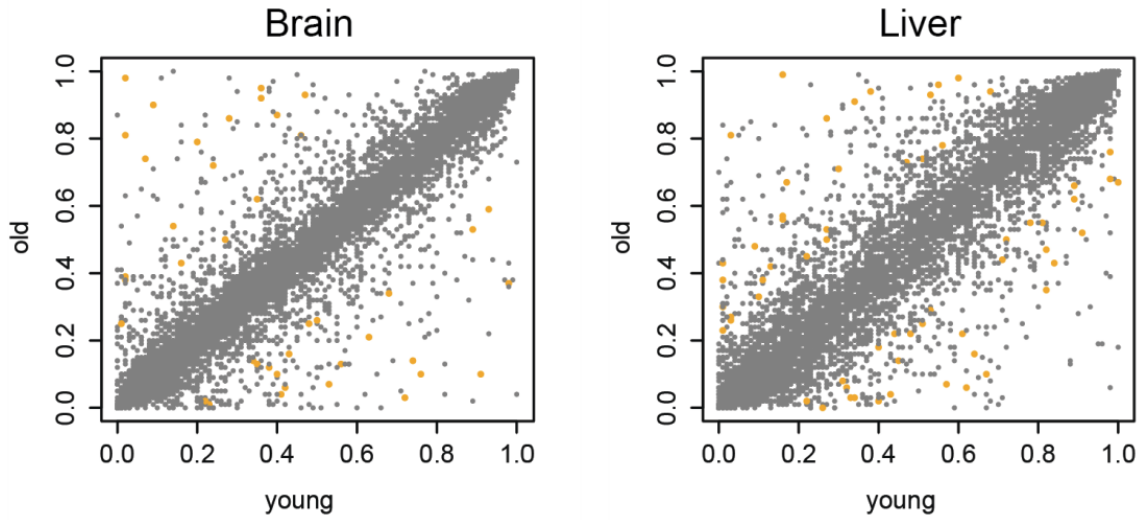


Figure S3.5. Changes in PSI value for all transcripts.

Percent Spliced In (PSI) values are mostly consistent across age, but with a moderate number of differentially expressed transcripts. Significantly changed transcripts, marked in orange, had Bayes factor ≥ 10 and difference ≥ 0.2 in merged and at least 5/9 individual analyses.

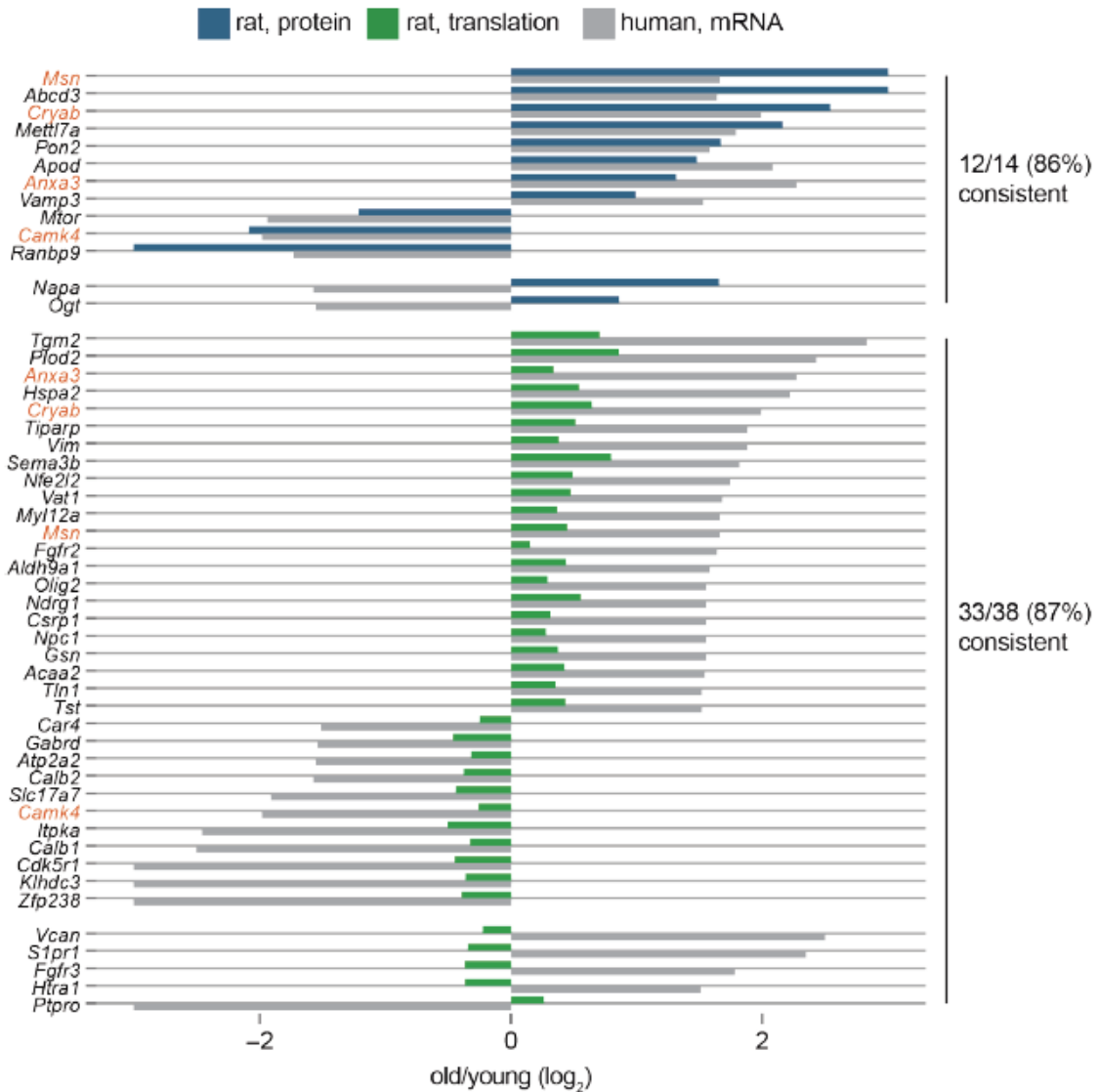


Figure S3.6. Conserved molecular alterations in aging brain between rat and human.

We compared significant changes in protein abundance or translation output that we identified in aging rat brain to changes in transcript level associated to age in human brain (Lu et al., 2004). 12 out of 14 (86%) changes in the protein abundance level and 33 out of 38 (87%) alterations in translation output that were identified as significant in both our and the human dataset are consistent having fold changes with the same sign. This suggests that conservation of age-associated molecular events between rodents and humans. Cases that were identified as significantly affected both at the level of translation output and protein abundance are highlighted in orange.

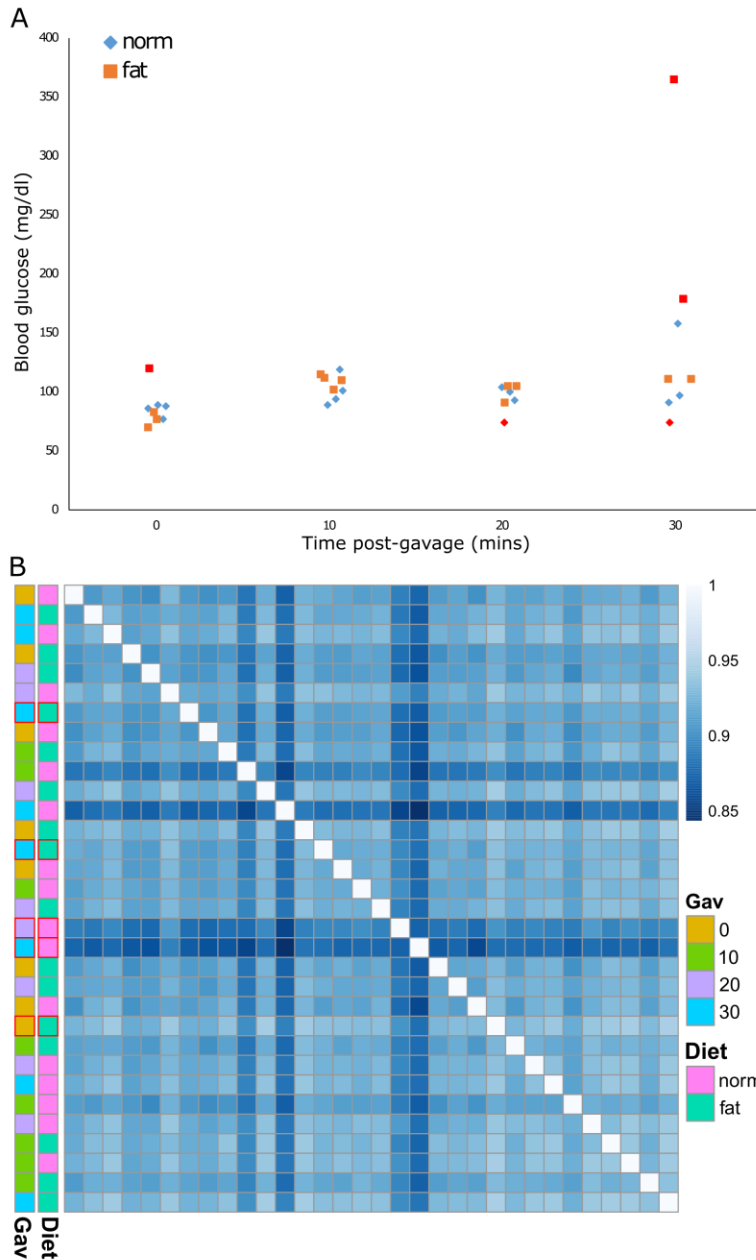


Figure S4.1. Identification of outlier samples by blood glucose levels and Spearman's correlation

(A) Blood glucose levels for all animals. Points in red were considered outliers and removed from further analysis.

(B) Spearman's correlation matrix for all samples. Samples outlined in red on the left were removed from further analysis.

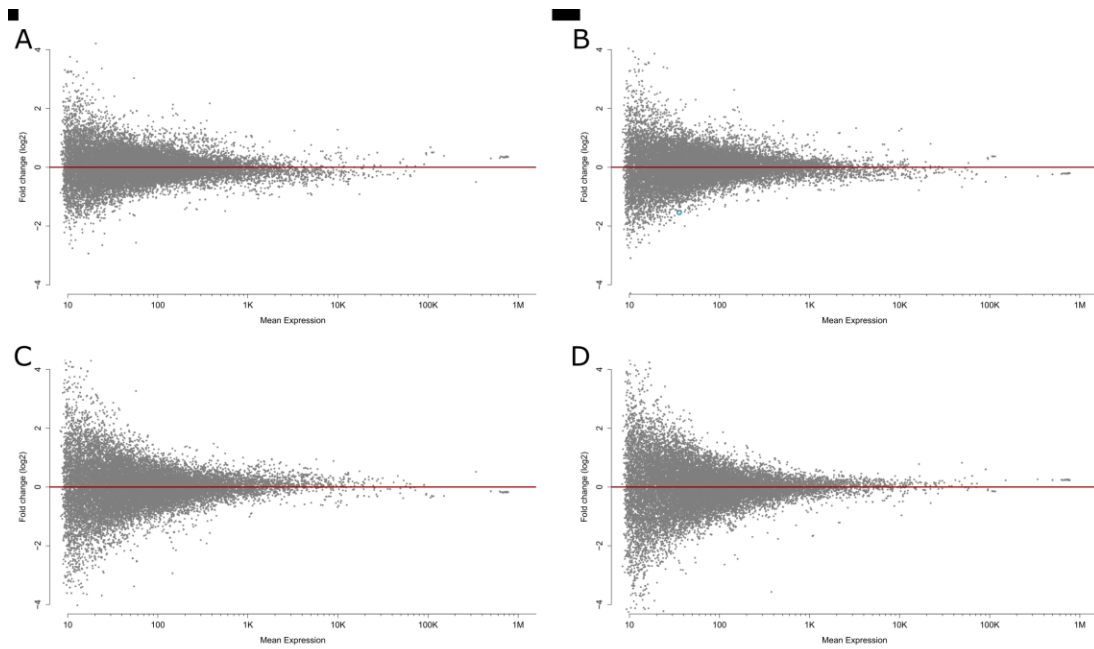


Figure S4.2. Glucose response at 10 and 30 minutes in normal and high-fat diet

(A-D) MA-plots showing fold change of individual transcripts in glucose vs. no glucose (A-B), or glucose in high-fat vs. glucose in normal diet (C-D) at 10 (A,C) or 30 (B,D) minutes. Significant changes ($p < 0.05$) are marked in blue (down) or orange (up).

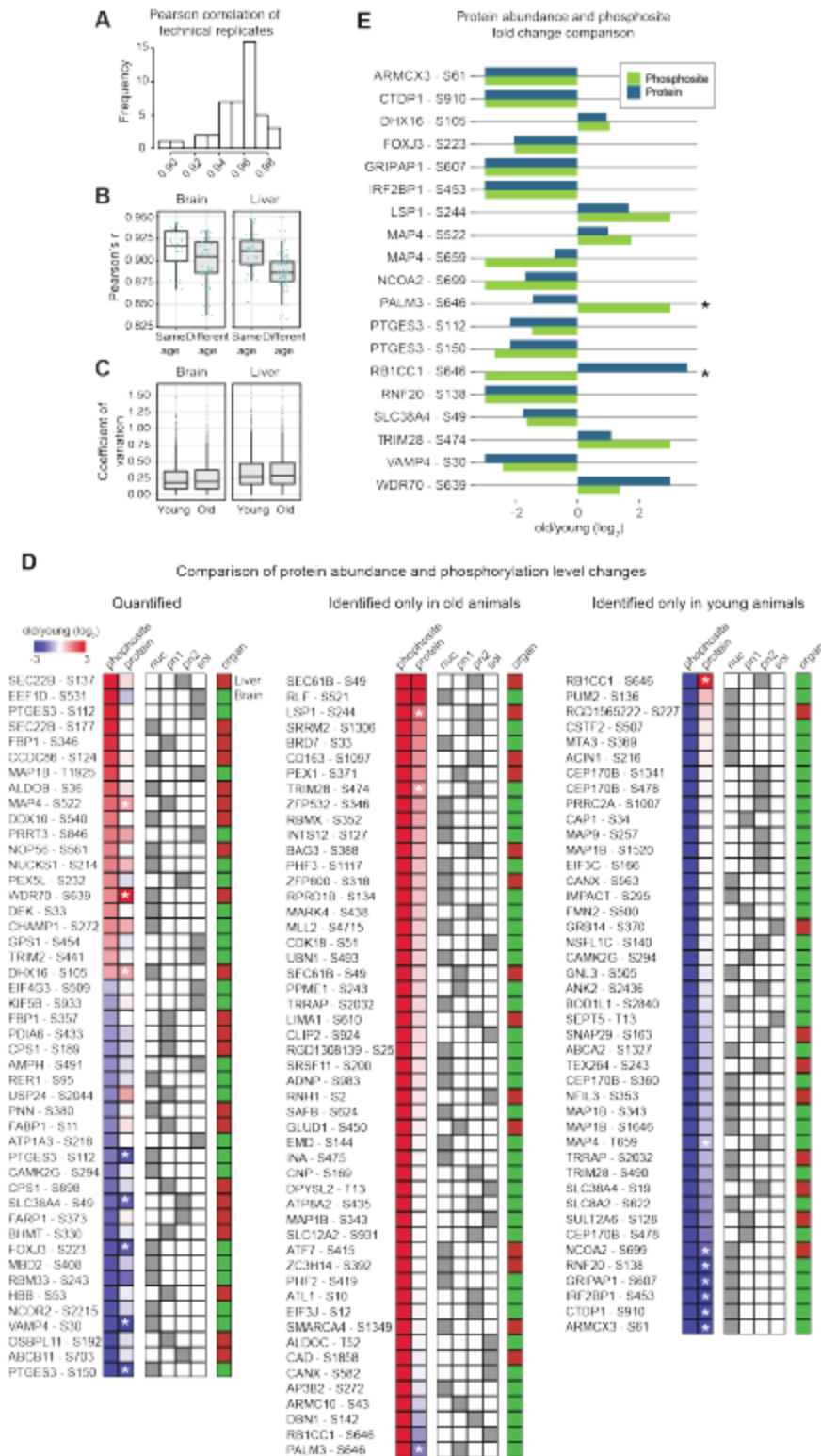
Figure SA.1. Reproducibility of phosphoproteomic measurements and comparison of protein abundance and phosphorylation level changes (next page)

(A) Reproducibility of phosphopeptide abundance measurements. The reproducibility of phosphopeptide abundance measurements was assessed by correlating protein abundance scores between technical replicates. The histogram shows the distribution of pairwise correlations between all technical replicates for brain and liver. The average pairwise correlation was Pearson's $r = 0.957$, indicating high reproducibility.

(B) As for protein abundance measurements (Figure 3.2C), samples from the same age group displayed consistently higher correlation than samples from different age groups. The boxplots depict all the pairwise correlations between samples from all the subcellular fractions. For both brain and liver, the correlation coefficients of samples from the same age group are significantly higher than samples from different age groups (Wilcoxon rank sum test p value $2.0e-2$ and $3.2e-4$, respectively).

(C) Coefficients of variation (standard deviation / mean calculated on raw phosphopeptide intensities) between animals of the same age were computed for all the phosphopeptides quantified across subcellular fractions. The low coefficients of variation indicate minimal within-age-group variation in phosphopeptide levels both in brain and liver.

(D) Comparison of protein abundance and phosphorylation level changes. For 136 affected phosphosites, we had measurements of both protein abundance and phosphorylation level in the same subcellular fraction. The heatmap show side-by-side comparison of protein abundance and phosphorylation level fold changes. For 19 of these phosphosites (indicated by a white star), we detected changes at both protein (p value < 0.05) and phosphopeptide level. These cases are highlighted in (E): the barplot compares fold changes measured at the protein (dark blue) and phosphopeptide level (green) in the two independent experiments. In 17 out of 19 cases (90%) the fold changes measured at the protein and phosphopeptide level are in agreement (fold change with same sign). A star indicates not consistent cases that are suggestive of an alteration of the fraction of protein molecules phosphorylated. Proteins and phosphosites identified only in one age group were assigned an arbitrary log₂ fold change of +3 (identified only in old animals) or -3 (identified only in young animals).



References

- Ahmad, K., and Henikoff, S. (2002). The histone variant H3.3 marks active chromatin by replication-independent nucleosome assembly. *Mol Cell* 9, 1191-1200.
- Aitken C & Lorsch J (2012). A mechanistic overview of translation initiation in eukaryotes. *Nat Struct Mol Biol* 19, 568–76.
- Anders, S., and Huber, W. (2010). Differential expression analysis for sequence count data. *Genome Biol* 11, R106.
- Andrikopoulos S, Blair A, Deluca N, Fam B & Proietto J (2008). Evaluating the glucose tolerance test in mice. *Am J Physiology - Endocrinol Metabolism* 295, E1323–E1332.
- Arber, N., Zajicek, G., and Ariel, I. (1988). The streaming liver. II. Hepatocyte life history. *Liver* 8, 80-87.
- Arnaiz G, Canal M & Robertis E (1971). Turnover of proteins in subcellular fractions of rat cerebral cortex. *Brain Res* 31, 179–184.
- Bader, G.D., and Hogue, C.W. (2003). An automated method for finding molecular complexes in large protein interaction networks. *BMC Bioinformatics* 4, 2.
- Bading, H. (2013). Nuclear calcium signaling in the regulation of brain function. *Nat Rev Neurosci* 14, 593-608.
- Barnes, A.P., Lilley, B.N., Pan, Y.A., Plummer, L.J., Powell, A.W., Raines, A.N., Sanes, J.R., and Polleux, F. (2007). LKB1 and SAD kinases define a pathway required for the polarization of cortical neurons. *Cell* 129, 549-563.
- Battle, A., Khan, Z., Wang, S.H., Mitrano, A., Ford, M.J., Pritchard, J.K., and Gilad, Y. (2015). Genomic variation. Impact of regulatory variation from RNA to protein. *Science* 347, 664-667.
- Baumgart, M., Groth, M., Priebe, S., Savino, A., Testa, G., Dix, A., Ripa, R., Spallotta, F., Gaetano, C., Ori, M., et al. (2014). RNA-seq of the aging brain in the short-lived fish *N. furzeri* - conserved pathways and novel genes associated with neurogenesis. *Aging Cell* 13, 965-974.
- Belle A, Tanay A, Bitincka L, Shamir R & O’Shea E (2006). Quantification of protein half-lives in the budding yeast proteome. *Proc Natl Acad Sci* 103, 13004–13009.
- Bertone P, Stolc V, Royce T, Rozowsky J, Urban A, Zhu X, Rinn J, Tongprasit W, Samanta M, Weissman S, Gerstein M & Snyder M (2004).

Global Identification of Human Transcribed Sequences with Genome Tiling Arrays. *Science* 306, 2242–2246.

Bindea, G., Mlecnik, B., Hackl, H., Charoentong, P., Tosolini, M., Kirilovsky, A., Fridman, W.H., Pages, F., Trajanoski, Z., and Galon, J. (2009). ClueGO: a Cytoscape plug-in to decipher functionally grouped gene ontology and pathway annotation networks. *Bioinformatics* 25, 1091-1093.

Binns, D., Dimmer, E., Huntley, R., Barrell, D., O'Donovan, C., and Apweiler, R. (2009). QuickGO: a web-based tool for Gene Ontology searching. *Bioinformatics* 25, 3045-3046.

Blobel, G., and Potter, V.R. (1966). Nuclei from rat liver: isolation method that combines purity with high yield. *Science* 154, 1662-1665.

Blodgett D, Nowosielska A, Afik S, Pechhold S, Cura A, Kennedy N, Kim S, Kucukural A, Davis R, Kent S, Greiner D, Garber M, Harlan D & diIorio P (2015). Novel Observations From Next-Generation RNA Sequencing of Highly Purified Human Adult and Fetal Islet Cell Subsets. *Nestle Nutr Works* Se 64, 3172–3181.

Brown & Edelman (2010). Optimal Control of Blood Glucose: The Diabetic Patient or the Machine? *Sci Transl Medicine* 2, 27ps18–27ps18.

Brown M & Goldstein J (2008). Selective versus Total Insulin Resistance: A Pathogenic Paradox. *Cell Metab* 7, 95–96.

Brunner E, Ahrens C, Mohanty S, Baetschmann H, Loevenich S, Potthast F, Deutsch E, Panse C, Lichtenberg U, Rinner O, Lee H, Pedrioli P, Malmstrom J, Koehler K, Schrimpf S, Krijgsveld J, Kregenow F, Heck A, Hafen E, Schlapbach R & Aebersold R (2007). A high-quality catalog of the *Drosophila melanogaster* proteome. *Nat Biotechnol* 25, 576–583.

Bui, K.H., von Appen, A., DiGuilio, A.L., Ori, A., Sparks, L., Mackmull, M.T., Bock, T., Hagen, W., Andres-Pons, A., Glavy, J.S., et al. (2013). Integrated structural analysis of the human nuclear pore complex scaffold. *Cell* 155, 1233-1243.

Burke, S.N., and Barnes, C.A. (2006). Neural plasticity in the ageing brain. *Nat Rev Neurosci* 7, 30-40.

Calado, A., Treichel, N., Muller, E.C., Otto, A., and Kutay, U. (2002). Exportin-5-mediated nuclear export of eukaryotic elongation factor 1A and tRNA. *EMBO J* 21, 6216-6224.

Calvo, S., Pagliarini, D., and Mootha, V. (2009). Upstream open reading frames cause widespread reduction of protein expression and are polymorphic among humans. *Proc Natl Acad Sci* 106, 7507–7512.

Cambridge S, Gnad F, Nguyen C, Bermejo J, Krüger M & Mann M (2011). Systems-wide proteomic analysis in mammalian cells reveals conserved, functional protein turnover. *J Proteome Res* 10, 5275–84.

Carninci, P., Kasukawa, T., Katayama, S., Gough, J., Frith, M., Maeda, N., Oyama, R., Ravasi, T., Lenhard, B., Wells, C., et al. (2005). The Transcriptional Landscape of the Mammalian Genome. *Science* 309, 1559–1563.

CDC (2015). Diabetes Report Card 2014. Atlanta, GA: Centers for Disease Control and Prevention, US Dept of Health and Human Services.

Chew, G.-L., Pauli, A., Rinn, J., Regev, A., Schier, A., and Valen, E. (2013). Ribosome profiling reveals resemblance between long non-coding RNAs and 5' leaders of coding RNAs. *Development* 140, 2828–2834.

D'Angelo, M.A., Gomez-Cavazos, J.S., Mei, A., Lackner, D.H., and Hetzer, M.W. (2012). A change in nuclear pore complex composition regulates cell differentiation. *Dev Cell* 22, 446-458.

D'Angelo, M.A., Raices, M., Panowski, S.H., and Hetzer, M.W. (2009). Age-dependent deterioration of nuclear pore complexes causes a loss of nuclear integrity in postmitotic cells. *Cell* 136, 284-295.

David, D.C., Ollikainen, N., Trinidad, J.C., Cary, M.P., Burlingame, A.L., and Kenyon, C. (2010). Widespread protein aggregation as an inherent part of aging in *C. elegans*. *PLoS Biol* 8, e1000450.

de Magalhaes, J.P., Curado, J., and Church, G.M. (2009). Meta-analysis of age-related gene expression profiles identifies common signatures of aging. *Bioinformatics* 25, 875-881.

Dimri, G.P., Lee, X., Basile, G., Acosta, M., Scott, G., Roskelley, C., Medrano, E.E., Linskens, M., Rubelj, I., Pereira-Smith, O., et al. (1995). A biomarker that identifies senescent human cells in culture and in aging skin in vivo. *Proc Natl Acad Sci U S A* 92, 9363-9367.

Durieux, J., Wolff, S., and Dillin, A. (2011). The cell-non-autonomous nature of electron transport chain-mediated longevity. *Cell* 144, 79-91.

Eden E, Lipson D, Yogev S & Yakhini Z (2007). Discovering Motifs in Ranked Lists of DNA Sequences. *PLoS Computational Biology* 3, e39.

Eden, E., Navon, R., Steinfeld, I., Lipson, D., and Yakhini, Z. (2009). GOrilla: a tool for discovery and visualization of enriched GO terms in ranked gene lists. *BMC Bioinformatics* 10, 48.

Ermolaeva, M.A., Segref, A., Dakhovnik, A., Ou, H.L., Schneider, J.I., Utermohlen, O., Hoppe, T., and Schumacher, B. (2013). DNA damage in

germ cells induces an innate immune response that triggers systemic stress resistance. *Nature* 501, 416-420.

Fonseca B, Zakaria C, Jia J-J, Graber T, Svitkin Y, Tahmasebi S, Healy D, Hoang H-D, Jensen J, Diao I, Lussier A, Dajadian C, Padmanabhan N, Wang W, Matta-Camacho E, Hearnden J, Smith E, Tsukumo Y, Yanagiya A, Morita M, Petroulakis E, González J, Hernández G, Alain T & Damgaard C (2015). La-related Protein 1 (LARP1) Represses Terminal Oligopyrimidine (TOP) mRNA Translation Downstream of mTOR Complex 1 (mTORC1). *J Biol Chem* 290, 15996–16020.

Fontoura B, Blobel G & Matunis M (1999). A Conserved Biogenesis Pathway for Nucleoporins: Proteolytic Processing of a 186-Kilodalton Precursor Generates Nup98 and the Novel Nucleoporin, Nup96. *J Cell Biology* 144, 1097–1112.

Geiger T, Velic A, Macek B, Lundberg E, Kampf C, Nagaraj N, Uhlen M, Cox J & Mann M (2013). Initial Quantitative Proteomic Map of 28 Mouse Tissues Using the SILAC Mouse. *Mol Cell Proteomics* 12, 1709–1722.

Geiger T, Wehner A, Schaab C, Cox J & Mann M (2012). Comparative Proteomic Analysis of Eleven Common Cell Lines Reveals Ubiquitous but Varying Expression of Most Proteins. *Mol Cell Proteomics* 11, M111.014050.

Green, D.R., Galluzzi, L., and Kroemer, G. (2011). Mitochondria and the autophagy-inflammation-cell death axis in organismal aging. *Science* 333, 1109-1112.

Guo, H., Ingolia, N.T., Weissman, J.S., and Bartel, D.P. (2010). Mammalian microRNAs predominantly act to decrease target mRNA levels. *Nature* 466, 835-840.

Guttman M, Amit I, Garber M, French C, Lin M, Feldser D, Huarte M, Zuk O, Carey B, Cassady J, Cabili M, Jaenisch R, Mikkelsen T, Jacks T, Hacohen N, Bernstein B, Kellis M, Regev A, Rinn J & Lander E (2009). Chromatin signature reveals over a thousand highly conserved large non-coding RNAs in mammals. *Nature* 458, 223–7.

Guttman, M., Russell, P., Ingolia, N.T., Weissman, J.S., and Lander, E.S. (2013). Ribosome Profiling Provides Evidence that Large Noncoding RNAs Do Not Encode Proteins. *Cell* 154, 240–251.

Heiman M, Schaefer A, Gong S, Peterson J, Day M, Ramsey K, Suárez-Fariñas M, Schwarz C, Stephan D, Surmeier J, Greengard P & Heintz N (2008). A Translational Profiling Approach for the Molecular Characterization of CNS Cell Types. *Cell* 135, 738–748.

- Heiman M, Kulicke R, Fenster R, Greengard P & Heintz N (2014). Cell type-specific mRNA purification by translating ribosome affinity purification (TRAP). *Nat Protoc* 9, 1282–91.
- Hekimi, S., Lapointe, J., and Wen, Y. (2011). Taking a "good" look at free radicals in the aging process. *Trends Cell Biol* 21, 569-576.
- Hoelz A, Debler E & Blobel G (2011). The Structure of the Nuclear Pore Complex. *Annual Review of Biochemistry* 80, 613–643.
- Houtkooper, R.H., Argmann, C., Houten, S.M., Canto, C., Jenninga, E.H., Andreux, P.A., Thomas, C., Doenlen, R., Schoonjans, K., and Auwerx, J. (2011). The metabolic footprint of aging in mice. *Sci Rep* 1, 134.
- Houtkooper, R.H., Mouchiroud, L., Ryu, D., Moullan, N., Katsyuba, E., Knott, G., Williams, R.W., and Auwerx, J. (2013). Mitonuclear protein imbalance as a conserved longevity mechanism. *Nature* 497, 451-457.
- Huhne, R., Thalheim, T., and Suhnel, J. (2014). AgeFactDB--the JenAge ageing factor database--towards data integration in ageing research. *Nucleic Acids Res* 42, D892-896.
- Hulver M, Berggren J, Carper M, Miyazaki M, Ntambi J, Hoffman E, Thyfault J, Stevens R, Dohm G, Houmard J & Muoio D (2005). Elevated stearoyl-CoA desaturase-1 expression in skeletal muscle contributes to abnormal fatty acid partitioning in obese humans. *Cell Metab* 2, 251–61.
- Ingolia, N.T., Brar, G.A., Rouskin, S., McGeachy, A.M., and Weissman, J.S. (2012). The ribosome profiling strategy for monitoring translation in vivo by deep sequencing of ribosome-protected mRNA fragments. *Nat Protoc* 7, 1534-1550.
- Ingolia NT, Brar GA, Stern-Ginossar N, Harris MS, Talhouarne GJS, Jackson SE, Wills MR & Weissman JS (2014). Ribosome Profiling Reveals Pervasive Translation Outside of Annotated Protein-Coding Genes. *Cell Reports* 8, 1365–1379.
- Ingolia, N.T., Ghaemmaghami, S., Newman, J.R., and Weissman, J.S. (2009). Genome-wide analysis in vivo of translation with nucleotide resolution using ribosome profiling. *Science* 324, 218-223.
- Ingolia N, Lareau L & Weissman J (2011). Ribosome Profiling of Mouse Embryonic Stem Cells Reveals the Complexity and Dynamics of Mammalian Proteomes. *Cell* 147, 789–802.
- Inoue, E., Mochida, S., Takagi, H., Higa, S., Deguchi-Tawarada, M., Takao-Rikitsu, E., Inoue, M., Yao, I., Takeuchi, K., Kitajima, I., et al. (2006). SAD: a presynaptic kinase associated with synaptic vesicles and

the active zone cytomatrix that regulates neurotransmitter release. *Neuron* 50, 261-275.

Jensen, L.J., Kuhn, M., Stark, M., Chaffron, S., Creevey, C., Muller, J., Doerks, T., Julien, P., Roth, A., Simonovic, M., et al. (2009). STRING 8--a global view on proteins and their functional interactions in 630 organisms. *Nucleic Acids Res* 37, D412-416.

Jiang, C.H., Tsien, J.Z., Schultz, P.G., and Hu, Y.H. (2001). The effects of aging on gene expression in the hypothalamus and cortex of mice. *Proc Natl Acad Sci U S A* 98, 1930-1934.

Kaganovich, D., Kopito, R., and Frydman, J. (2008). Misfolded proteins partition between two distinct quality control compartments. *Nature* 454, 1088-1095.

Katz, Y., Wang, E.T., Airoidi, E.M., and Burge, C.B. (2010). Analysis and design of RNA sequencing experiments for identifying isoform regulation. *Nat Methods* 7, 1009-1015.

Kevei, E., and Hoppe, T. (2014). Ubiquitin sets the timer: impacts on aging and longevity. *Nat Struct Mol Biol* 21, 290-292.

Kishi, M., Pan, Y.A., Crump, J.G., and Sanes, J.R. (2005). Mammalian SAD kinases are required for neuronal polarization. *Science* 307, 929-932.

Kong J & Lasko P (2012). Translational control in cellular and developmental processes. *Nat Rev Genet* 13, 383-394.

Kulkarni S, Muralidharan B, Panda A, Bakthavachalu B, Vindu A & Seshadri V (2011). Glucose-stimulated Translation Regulation of Insulin by the 5' UTR-binding Proteins. *J Biol Chem* 286, 14146-14156.

Laplanche M & Sabatini D (2012). mTOR Signaling in Growth Control and Disease. *Cell* 149, 274-293.

Lee, C.K., Weindruch, R., and Prolla, T.A. (2000). Gene-expression profile of the ageing brain in mice. *Nat Genet* 25, 294-297.

Lessard, J., Wu, J.I., Ranish, J.A., Wan, M., Winslow, M.M., Staahl, B.T., Wu, H., Aebersold, R., Graef, I.A., and Crabtree, G.R. (2007). An essential switch in subunit composition of a chromatin remodeling complex during neural development. *Neuron* 55, 201-215.

Loerch, P.M., Lu, T., Dakin, K.A., Vann, J.M., Isaacs, A., Geula, C., Wang, J., Pan, Y., Gabuzda, D.H., Li, C., et al. (2008). Evolution of the aging brain transcriptome and synaptic regulation. *PLoS One* 3.

- Lopez-Otin, C., Blasco, M.A., Partridge, L., Serrano, M., and Kroemer, G. (2013). The hallmarks of aging. *Cell* 153, 1194-1217.
- Love M, Huber W & Anders S (2014) Moderated estimation of fold change and dispersion for RNA-seq data with DESeq2. *Genome Biol* 15.
- Lovtrup-Rein, H., and McEwen, B.S. (1966). Isolation and fractionation of rat brain nuclei. *J Cell Biol* 30, 405-415.
- Lu, T., Pan, Y., Kao, S.Y., Li, C., Kohane, I., Chan, J., and Yankner, B.A. (2004). Gene regulation and DNA damage in the ageing human brain. *Nature* 429, 883-891.
- Lund, E., Guttinger, S., Calado, A., Dahlberg, J.E., and Kutay, U. (2004). Nuclear export of microRNA precursors. *Science* 303, 95-98.
- Ma X & Blenis J (2009). Molecular mechanisms of mTOR-mediated translational control. *Nat Rev Mol Cell Bio* 10, 307-318.
- Mair, W., Morantte, I., Rodrigues, A.P., Manning, G., Montminy, M., Shaw, R.J., and Dillin, A. (2011). Lifespan extension induced by AMPK and calcineurin is mediated by CRTCL-1 and CREB. *Nature* 470, 404-408.
- Mak, S.K., McCormack, A.L., Langston, J.W., Kordower, J.H., and Di Monte, D.A. (2009). Decreased alpha-synuclein expression in the aging mouse substantia nigra. *Exp Neurol* 220, 359-365.
- Masters PM, Bada JL & Zigler JS (1977). Aspartic acid racemisation in the human lens during ageing and in cataract formation. *Nature* 268, 71-3.
- Mura M, Hopkins T, Michael T, Abd-Latip N, Weir J, Aboagye E, Mauri F, Jameson C, Sturge J, Gabra H, Bushell M, Willis A, Curry E & Blagden S (2014). LARP1 post-transcriptionally regulates mTOR and contributes to cancer progression. *Oncogene* 34, 5025-36.
- Nagaraj, Kulak A, Cox, Neuhauser, Mayr, Hoerning, Vorm & Mann (2012). System-wide Perturbation Analysis with Nearly Complete Coverage of the Yeast Proteome by Single-shot Ultra HPLC Runs on a Bench Top Orbitrap. *Molecular & Cellular Proteomics* 11, M111.013722-M111.013722.
- Ogden CL, Carroll MD, Kit BK, Flegal KM. (2014). Prevalence of Childhood and Adult Obesity in the United States, 2011-2012. *JAMA* 311(8):806-814. doi:10.1001/jama.2014.732.
- Ori, A., Andres-Pons, A., and Beck, M. (2014). The use of targeted proteomics to determine the stoichiometry of large macromolecular assemblies. *Methods Cell Biol* 122, 117-146.

- Ori, A., Banterle, N., Iskar, M., Andres-Pons, A., Escher, C., Khanh Bui, H., Sparks, L., Solis-Mezarino, V., Rinner, O., Bork, P., et al. (2013). Cell type-specific nuclear pores: a case in point for context-dependent stoichiometry of molecular machines. *Mol Syst Biol* 9, 648.
- Ori A, Toyama B, Harris M, Bock T, Iskar M, Bork P, Ingolia N, Hetzer M & Beck M (2015). Integrated Transcriptome and Proteome Analyses Reveal Organ-Specific Proteome Deterioration in Old Rats. *Cell Syst* 1, 224–237.
- Price, Guan, Burlingame, Prusiner & Ghaemmaghami (2010). Analysis of proteome dynamics in the mouse brain. *Proceedings of the National Academy of Sciences* 107, 14508–14513.
- Rabut G, Doye V & Ellenberg J (2004). Mapping the dynamic organization of the nuclear pore complex inside single living cells. *Nat Cell Biol* 6, 1114–1121.
- Rani V, Deep G, Singh RK, Palle K & Yadav UC (2016). Oxidative stress and metabolic disorders: Pathogenesis and therapeutic strategies. *Life Sci.* 148, 183–93.
- Rhie, B.H., Song, Y.H., Ryu, H.Y., and Ahn, S.H. (2013). Cellular aging is associated with increased ubiquitylation of histone H2B in yeast telomeric heterochromatin. *Biochem Biophys Res Commun* 439, 570–575.
- Ron D & Walter P (2007). Signal integration in the endoplasmic reticulum unfolded protein response. *Nat Rev Mol Cell Bio* 8, 519–529.
- Rui L (2014). SH2B1 regulation of energy balance, body weight, and glucose metabolism. *World Journal of Diabetes* 5, 511.
- Sanz E, Yang L, Su T, Morris D, McKnight S & Amieux P (2009). Cell-type-specific isolation of ribosome-associated mRNA from complex tissues. *Proc Natl Acad Sci* 106, 13939–13944.
- Savas, J.N., Toyama, B.H., Xu, T., Yates, J.R., and Hetzer, M.W. (2012). Extremely long-lived nuclear pore proteins in the rat brain. *Science* 335, 942–942.
- Schubert U, Antón L, Gibbs J, Norbury C, Yewdell J & Bennink J (2000). Rapid degradation of a large fraction of newly synthesized proteins by proteasomes. *Nature* 404, 770–4.
- Schumacher, B., van der Pluijm, I., Moorhouse, M.J., Kosteas, T., Robinson, A.R., Suh, Y., Breit, T.M., van Steeg, H., Niedernhofer, L.J., van Ijcken, W., et al. (2008). Delayed and accelerated aging share common longevity assurance mechanisms. *PLoS Genet* 4, e1000161.

Schwartz, B.E., and Ahmad, K. (2005). Transcriptional activation triggers deposition and removal of the histone variant H3.3. *Genes Dev* 19, 804-814.

Sengupta S, Peterson T & Sabatini D (2010). Regulation of the mTOR Complex 1 Pathway by Nutrients, Growth Factors, and Stress. *Mol Cell* 40, 310–322.

Shipston, M.J. (2014). Ion channel regulation by protein S-acylation. *J Gen Physiol* 143, 659-678.

Smyth, G.K. (2005). Limma: linear models for microarray data. In *Bioinformatics and Computational Biology Solutions Using R and Bioconductor*, C.V. Gentleman R, Dudoit S, Irizarry R and Huber W (eds.), ed. (Springer, New York), pp. 397-420.

Spalding, K.L., Bhardwaj, R.D., Buchholz, B.A., Druid, H., and Frisen, J. (2005). Retrospective birth dating of cells in humans. *Cell* 122, 133-143.

Strimmer, K. (2008). *fdrtool*: a versatile R package for estimating local and tail area-based false discovery rates. *Bioinformatics* 24, 1461-1462.

Sun, D., Luo, M., Jeong, M., Rodriguez, B., Xia, Z., Hannah, R., Wang, H., Le, T., Faull, K.F., Chen, R., et al. (2014). Epigenomic profiling of young and aged HSCs reveals concerted changes during aging that reinforce self-renewal. *Cell stem cell* 14, 673-688.

Supek F, Bošnjak M, Škunca N, Šmuc T. (2011) REVIGO summarizes and visualizes long lists of Gene Ontology terms. *PLoS ONE* doi:10.1371/journal.pone.0021800.

Toyama, B.H., Savas, J.N., Park, S.K., Harris, M.S., Ingolia, N.T., Yates, J.R., 3rd, and Hetzer, M.W. (2013). Identification of long-lived proteins reveals exceptional stability of essential cellular structures. *Cell* 154, 971-982.

Vabulas R & Hartl F (2005). Protein Synthesis upon Acute Nutrient Restriction Relies on Proteasome Function. *Science* 310, 1960–1963.

Valášek L, Szamecz B, Hinnebusch A & Nielsen K (2007). In vivo stabilization of preinitiation complexes by formaldehyde cross-linking. *Methods Enzymol* 429, 163–183.

Vattem K & Wek R (2004). Reinitiation involving upstream ORFs regulates ATF4 mRNA translation in mammalian cells. *P Natl Acad Sci Usa* 101, 11269–11274.

Verzija N, DeGroot J, Thorpe S, Bank R, Shaw J, Lyons T, Bijlsma J, Lafeber F, Baynes J & TeKoppele J (2000). Effect of collagen turnover on

the accumulation of advanced glycation endproducts. *J Biol Chem* 275, 39027–39031.

Walther, D.M., and Mann, M. (2011). Accurate quantification of more than 4000 mouse tissue proteins reveals minimal proteome changes during aging. *Mol Cell Proteomics* 10, M110 004523.

Wek, Jiang & Anthony (2006). Coping with stress: eIF2 kinases and translational control. *Biochem Soc Trans* 34, 7-11.

Welsh M, Scherberg N, Gilmore R & Steiner D (1986). Translational control of insulin biosynthesis. Evidence for regulation of elongation, initiation and signal-recognition-particle-mediated translational arrest by glucose. *Biochem J* 235, 459–467.

Wethmar, K., Barbosa-Silva, A., Andrade-Navarro, M., and Leutz, A. (2014). uORFdb—a comprehensive literature database on eukaryotic uORF biology. *Nucleic Acids Res* 42, D60–D67.

Winzell M & Ahrén B (2004). The High-Fat Diet–Fed Mouse A Model for Studying Mechanisms and Treatment of Impaired Glucose Tolerance and Type 2 Diabetes. *Nestle Nutr Works Se* 53, S215–S219.

Wood, S.H., Craig, T., Li, Y., Merry, B., and de Magalhaes, J.P. (2013). Whole transcriptome sequencing of the aging rat brain reveals dynamic RNA changes in the dark matter of the genome. *Age (Dordr)* 35, 763-776.

Wu, R.S., Tsai, S., and Bonner, W.M. (1982). Patterns of histone variant synthesis can distinguish G0 from G1 cells. *Cell* 31, 367-374.

Zahn, J.M., Sonu, R., Vogel, H., Crane, E., Mazan-Mamczarz, K., Rabkin, R., Davis, R.W., Becker, K.G., Owen, A.B., and Kim, S.K. (2006). Transcriptional profiling of aging in human muscle reveals a common aging signature. *PLoS Genet* 2, e115.

Zhang P, McGrath B, Li S, Frank A, Zambito F, Reinert J, Gannon M, Ma K, McNaughton K & Cavener D (2002). The PERK eukaryotic initiation factor 2 alpha kinase is required for the development of the skeletal system, postnatal growth, and the function and viability of the pancreas. *Mol Cell Biol* 22, 3864–74.

MICHAEL S. HARRIS

Born July 17, 1987 in Buffalo, NY

EDUCATION

Johns Hopkins University, Baltimore MD

Ph.D. in Biology 2016 (expected)
Dissertation: Translational control in nutrient response and aging

Allegheny College, Meadville PA

B.S. *cum laude* in Biology 2009
Thesis: Analysis of the interaction between the genes *minidisks* and *microdisks* in *Drosophila melanogaster*

RESEARCH EXPERIENCE

University of California–Berkeley, Berkeley CA

Visiting Student Researcher Dec. 2013-present
Advisor: Nicholas Ingolia

Carnegie Institution Dept. of Embryology, Baltimore MD

Predocutorial Fellow May 2011-Nov. 2013
Advisor: Nicholas Ingolia

Allegheny College, Meadville PA

Undergraduate Researcher 2007-2009
Advisor: Glen Wurst

Worthington Biochemical Corporation, Lakewood NJ

Summer Research Assistant Summer 2008-2010
Supervisor: David Skrincosky

AWARDS

Alden Scholar, Allegheny College 2006-2009
Trustee's Scholarship, Allegheny College 2005-2009

TEACHING EXPERIENCE

Johns Hopkins University, Baltimore MD

Teaching Assistant, General Biology Spring 2013
Teaching Assistant, Cell Biology Spring 2012
Teaching Assistant, Biochemistry Fall 2011, 2012

PUBLICATIONS

- Ori A, Toyama B, **Harris MS**, Bock T, Iskar M, Bork P, Ingolia N, Hetzer M, Beck M. Integrated Transcriptome and Proteome Analyses Reveal Organ-Specific Proteome Deterioration in Old Rats. *Cell Systems* 1, 224–237. Sept 23, 2015.
- Ingolia NT, Brar GA, Stern-Ginossar N, **Harris MS**, Talhouarne GJS, Jackson SE, Wills MR, Weissman JS. Ribosome profiling reveals pervasive translation outside of annotated protein-coding genes. *Cell Reports* 8(5). Sept 11, 2014.
- Toyama BH, Savas JN, Park SK, **Harris MS**, Ingolia NT, Yates JR, Hetzer MW. Identification of long-lived proteins reveals exceptional stability of essential cellular structures. *Cell* 154(5). Aug 29 2013.